Identification of Molecular Determinants Contributing to the Function of NPH3 in Phototropic Hypocotyl Bending

Dissertation

der Mathematisch-Naturwissenschaftlichen Fakultät

der Eberhard Karls Universität Tübingen

zur Erlangung des Grades eines

Doktors der Naturwissenschaften

(Dr. rer. nat.)

vorgelegt von

Lea Reuter

aus Wiesbaden

Tübingen

2022

Gedruckt mit Genehmigung der Mathematisch-Naturwissenschaftlichen Fakultät der Eberhard Karls Universität Tübingen.

Tag der mündlichen Qualifikation:	28.02.2023
Dekan:	Prof. Dr. Thilo Stehle
1. Berichterstatter/-in:	Prof. Dr. Claudia Oecking
2. Berichterstatter/-in:	Prof. Dr. Klaus Harter
3. Berichterstatter/-in	*Prof. Dr. Ute Höcker*

Table of contents

List of abbreviations

ABCB	ATP-binding cassette B
ADR	ACTIVATED DISEASE RESISTANCE
AGC	cAMP-dependent protein kinase, cGMP-dependent protein kinase G and phospholipid-dependent protein kinase C
ARF7	AUXIN RESPONSE FACTOR 7
A. thaliana	*Arabidopsis thaliana*
A. tumefaciens	*Agrobacterium tumefaciens*
AUX1	AUXIN RESISTANT 1
BFA	Brefeldin A
BH	basic hydrophobic
BKI1	BRI1 KINASE INHIBITOR 1
BL	Blue light
BLUS1	Blue Light Signaling 1
BRI1	BRASSINOSTEROID INSENSITIVE 1
BRX	BREVIS RADIX
BTB	bric-a-brac, tramtrack, and broad complex
BZR1	BRASSINAZOLE-RESISTANT 1
CC	Coiled-coil
CCT	Cryptochrome C-terminus
CDC42	Cellular division control protein 42
CHX	Cycloheximide
CLSM	Confocal laser scanning microscopy
CPT1	COLEOPTILE PHOTOTROPISM 1
Col-0	Columbia-0
CRL3	CUL3 RING E3 UBIQUITIN LIGASE
cry	Cryptochromes
D	Dark
D6PK	D6 protein kinase
DNA	Deoxyribonucleic acid
DOT3	DEFECTIVELY ORGANIZED TRIBUTARIES 3
E. coli	*Escherichia coli*

ENP	ENHANCER OF PINOID
ER	endoplasmic reticulum
FAC	FLORIGEN ACTIVATION COMPLEX
FAD	Flavin adenine dinucleotide
FD	FLOWERING LOCUS D
FMN	Flavin mononucleotide
FRL	Far red light
FT	FLOWERING LOCUS T
GFP	Green Fluorescent Protein
h	hour
Hd3a	Heading date 3a
IAA	Indole-3-acetic acid
IDR	Intrinsically disordered region
IP	Immuno-precipitation
LAX	Like AUX1
LIP	Linear interacting peptide
LLPS	Liquid liquid phase separation
LOV	Light, oxygen or voltage
mA	milli ampere
MAB4	MACCHI-BOU 4
MAKR2	MEMBRANE ASSOCIATED KINASE REGULATOR 2
MAP	Myristoylation and palmitylation
MEL	MAB4/ENP/NPY1-LIKE
min	Minute
MS	Mass spectrometry
MTHF	5,10-methenyltetrahydrofolate
N. benthamiana	*Nicotiana benthamiana*
NCH1	NRL PROTEIN FOR CHLOROPLAST MOVEMENT 1
NLR	Nucleotide-binding leucine-rich repeat
NPH	NON PHOTOTROPIC HYPOCOTYL
NPR1	NONEXPRESSER OF PATHOGENESIS-RELATED GENES 1
NPY	NAKED PINS IN YUCCA

NRL	NPH3/RPT2-like protein family
PAO	Phenylarsine oxide
PAR	Partitioning defective
PAX	PROTEIN KINASE ASSOCIATED WITH BRX
phot	Phototropin
PHR	Photolyase homology region
Pi4P	Phosphatidylinositol-4-phosphate
PIP5K	Pi4P 5 kinase
PID	PINOID
PIN	PIN-formed
PKS	Phytochrome Kinase Substrate
PM	Plasma membrane
R-D	Retransfer to darkness
RFP	Red Fluorescent Protein
RL	Red light
RNA	Ribonucleic acid
RPT	ROOT PHOTOTROPISM
RT	Room temperature
SA	Salicylic acid
SDS-PAGE	Sodium dodecyl sulfate polyacrylamide gel electrophoresis
SLiM	Short linear motif
T-DNA	Transfer DNA
UV	Ultra violet
UVR8	UV RESISTANCE LOCUS 8
WAG	WAVY ROOT GROWTH
WT	Wild type
Y2H	Yeast two hybrid

List of figures

List of tables

List of movies

1 Introduction

1.1 Phototropism

Plants are sessile organisms and consequently, their ability to adapt to environmental changes is of utmost importance. Light is a crucial abiotic factor influencing plant development and growth. The ability of plants to adapt their growth to the direction of incoming light is known as phototropism or phototropic response. The growth towards a light source is called positive phototropism and is performed by the shoot whereas the growth away from a light source is called negative phototropism and normally takes place in the root. This directed growth is caused by a lateral gradient of the plant hormone auxin with a higher auxin concentration on the shaded side of the plant.

The positive phototropism can be separated into two responses, the first and the second positive phototropic response. During the first positive phototropic response only the coleoptile tip bends whereas the second positive phototropism occurs in lower regions of the coleoptile (Christie and Murphy, 2013; Briggs, 2014). The first positive phototropism was studied in grass coleoptiles and underlies the Bunsen-Roscoe law of reciprocity, stating that a short, bright pulse of light induces the same response in bending like a longer, less bright pulse of light (Christie and Murphy, 2013; Briggs, 2014). The second positive phototropic response is not following the law of reciprocity but is time-dependent and needs a prolonged irradiation (Christie and Murphy, 2013; Briggs, 2014). Essential for the phototropic response is the perception of the incoming light via photoreceptors.

1.2 Photoreceptors

Plants are able to recognize different light qualities with the help of photoreceptors. They enable plants to distinguish between differing wavelengths of light such as ultra violet (UV) divided into UVB and UVA, blue light (BL, 380-500 nm), red light (RL) and far red light (FRL) (Legris and Boccaccini, 2020). Phytochromes are essential for the recognition of RL and FRL, and are known to be involved in seed germination and shade avoidance (Franklin and Quail, 2010). The photoreceptor UV RESISTANCE LOCUS8 (UVR8) is required for the detection of UVB light and might be involved in UV protection and also possibly in the phototropic response induced by UV light (Jenkins, 2014; Legris and Boccaccini, 2020). The most important source of light for the phototropic response, however, is BL.

In plants, three types of BL receptors are known: Zeitlupe proteins, cryptochromes (crys) and phototropins (phots). Proteins of the Zeitlupe family contain a light, oxygen or voltage sensing domain (LOV) and are important for regulation of the circadian clock and the photoperiodic

control of flowering (Takase *et al.*, 2011; Suetsugu and Wada, 2013; Christie *et al.*, 2015). Crys contain a N-terminal photolyase homology region (PHR) and a specific cryptochrome C-terminus (CCT) (Liu *et al.*, 2011; Christie *et al.*, 2015). While the CCT is important for cry signaling the PHR is the chromophore binding region and binds a flavin adenine dinucleotide (FAD) and a 5,10-methenyltetrahydrofolate (MTHF) (Hoang, Bouly and Ahmad, 2008; Liu *et al.*, 2011; Christie *et al.*, 2015). Cry1 and cry2 localize in the nucleus and are involved in plant development and growth (Cashmore *et al.*, 1999; Chaves *et al.*, 2011; Christie *et al.*, 2015). Yet, for the phototropic response the most important BL receptors are phot1 and phot2.

1.2.1 Phototropins & Blue light perception

Phototropins are photoreceptors involved in responses involved in plant growth and optimization of photosynthetic efficiency. This includes the phototropic response, light-induced opening of stomata, chloroplast accumulation and leaf positioning and flattening (Kinoshita *et al.*, 2001; Sakai *et al.*, 2001; Sakamoto and Briggs, 2002; Inoue *et al.*, 2008a). In the phototropic response phot1 acts under low and high light intensities, whereas phot2 acts only under high light intensities (Sakai *et al.*, 2001). The two known phototropins, phot1 and phot2, are activated by light and function as serine/threonine kinases undergoing autophosphorylation in BL (Christie *et al.*, 2015). Phototropins contain a C-terminal serine/threonine kinase domain and two N-terminal LOV domains (LOV1 and LOV2) (Motchoulski and Liscum, 1999). The LOV domains function as BL sensors and are able to non-covalently bind a flavin mononucleotide (FMN) as chromophore (Christie *et al.*, 1998; Christie *et al.*, 2015). BL irradiation leads to a covalent binding between FMN and a cysteine residue (Christie, 2007; Christie *et al.*, 2015). Thus, in darkness the N-terminal LOV domains inhibit the kinase domain activity, whereas upon BL irradiation, phots undergo conformational changes resulting in activation of the kinase domain and subsequently autophosphorylation (Matsuoka and Tokutomi, 2005). Autophosphorylation seems to be essential for the phototropic response, since mutation of S851 in the activation loop causes a loss of the phototropic response (Inoue *et al.*, 2008a). BL-triggered phosphorylation of phot1 is furthermore required for the interaction with 14-3-3 proteins (Inoue *et al.*, 2008a). 14-3-3 proteins normally interact with their target proteins in a phosphorylation-dependent manner (see chapter 1.4). However, the function of 14-3-3 binding to phot1 remains elusive, since exchange of the 14-3-3 binding sites in phot1 to alanine abolished BL-induced 14-3-3 binding but did not impair the phototropic response (Inoue *et al.*, 2008a).

The conformational change leading to kinase activation is mediated by the LOV2 domain (Inoue *et al.*, 2008a). Although structurally similar, LOV1 and LOV2 exhibit different functions. While LOV2 is involved in phot autophosphorylation and regulation of the activity, LOV1 is important for dimerization and regulation of photosensitivity (Matsuoka and Tokutomi, 2005; Christie, 2007; Inoue *et al.*, 2008a; Kimura *et al.*, 2020). The process of autophosphorylation of phototropins is reversible in darkness and also referred to as photocycling (Kaiserli *et al.*, 2009; Hart *et al.*, 2019). The photocycling of phots can be engineered by mutating the phot LOV2 domain. This can affect the lifetime of photocycling, thus resulting in altered phototropic responses (Hart *et al.*, 2019).

Besides its own autophosphorylation, only few candidates are known to be phosphorylated by phots directly. The kinase Blue Light Signaling 1 (BLUS1) is phosphorylated by both phot1 and phot2 and is essential for the activation of the H^+-ATPase and subsequently stomata opening (Takemiya *et al.*, 2013; Christie *et al.*, 2015). Phytochrome Kinase Substrate 4 (PKS4) is another substrate of phot1 and functions as a positive regulator of the phototropic response under low light conditions and as a negative regulator under high light intensities. This switch from a positive to a negative regulator is due to a phosphorylation of PKS4 by phot1 in a light-dependent manner (Demarsy *et al.*, 2012; Christie *et al.*, 2015; Schumacher *et al.*, 2018).

Both phot1 and phot2 mainly localize to the PM in darkness (Sakamoto and Briggs, 2002; Kong *et al.*, 2006), yet the molecular mechanism underlying their PM association is unclear. Upon BL irradiation phot1 is partially internalized via endocytosis (Kaiserli *et al.*, 2009), while phot2 is translocated to the Golgi apparatus (Kong *et al.*, 2006). Permanent attachment of phot1 to the PM via myristoylation and farnesylation prevented internalization of phot1, however both phot1 variants were still able to restore the phototropic response in the *phot1phot2* mutant background (Preuten *et al.*, 2015). Hence, the function of phot1 internalization upon BL remains elusive.

Phototropins belong to the cAMP-dependent protein kinase, cGMP-dependent protein kinase G and phospholipid-dependent protein kinase C VIII (AGC VIII) kinase family (Lanassa Bassukas, Xiao and Schwechheimer, 2022). It is worth mentioning that other members of this AGC VIII kinase family, namely PINOID (PID) and D6 protein kinase (D6PK), phosphorylate PIN proteins (Ding *et al.*, 2011; Lanassa Bassukas, Xiao and Schwechheimer, 2022). Phot1, however, is not able to phosphorylate the hydrophilic loop of PIN3 *in vitro* (Ding *et al.*, 2011). PIN proteins are also involved in the phototropic response by redistributing auxin in the hypocotyl of irradiated plants (Lanassa Bassukas, Xiao and Schwechheimer, 2022).

1.3 Auxin transport & PIN proteins

The ability of plants to align their growth with an incoming light stimulus was first observed in the tips of grass coleoptiles by Darwin in the 19th century (Darwin and Darwin, 1880). Darwin and his son proved that perception of the light stimulus occurs in the tip of grass coleoptiles and suggested that “some influence” is transferred to lower plant parts (Darwin and Darwin, 1880; Christie and Murphy, 2013). Later, the plant hormone auxin was identified to be responsible for transmission of this stimulus and the Cholodny-Went hypothesis was established to explain how perception of the light stimulus and auxin are involved in the phototropic response of plants (Christie and Murphy, 2013). The Cholodny-Went hypothesis states that perception of a unilateral light stimulus leads to a redistribution of auxin in the tip resulting in an asymmetric distribution with a higher auxin concentration on the shaded side of the plant. Subsequently, auxin translocates to the lower parts of the plant and the auxin gradient promotes differential elongation of cells resulting in bending towards the light (Went and Thimann, 1937).

The plant hormone auxin is responsible for the regulation of numerous developmental and physiological processes. Indole-3-acetic acid (IAA) is the most abundant form of auxin and exists in its protonated form IAAH in the apoplast (pH ~5). From here, it can enter the cell via passive diffusion through the plasma membrane (PM) or via auxin influx carrier like AUXIN RESISTANT 1 (AUX1) from the AUX1/LAX (Like AUX1) protein family if present in the deprotonated form IAA^- (Péret *et al.*, 2012). Once IAA enters the cell it is deprotonated due to a higher pH in the cytosol and no longer able to diffuse passively across the PM. The transport from the cell to the apoplast is carried out by auxin efflux carrier including ATP-binding cassette B (ABCB) proteins and PIN-formed (PIN) proteins (Geisler *et al.*, 2005; Blakeslee *et al.*, 2007). Localization of these auxin efflux carrier in the PM defines the direction of auxin transport, resulting in the polar auxin transport from the shoot to the root, but also the establishment of local auxin minima, maxima and auxin gradients (Grunewald and Friml, 2010).

PIN proteins function as auxin efflux carrier and are named after the *pin1* mutant phenotype, which is characterized by a not fully developed, pin-like inflorescence (Okada *et al.*, 1991). There are eight characterized PIN proteins that can be divided into canonical and non-canonical PIN proteins (Krecek *et al.*, 2009; Sauer and Kleine-Vehn, 2019). PIN1-4 and 7 are canonical PINs, whereas PIN5, 6 and 8 are classified as non-canonical PIN proteins (Sauer and Kleine-Vehn, 2019). PIN proteins contain a central cytosolic and hydrophilic loop accompanied by several transmembrane domains on each side of the loop (Krecek *et al.*, 2009; Sauer and Kleine-Vehn, 2019). Canonical and non-canonical PIN proteins differ mainly in the length of the cytosolic loop and their localization. While non-canonical PIN proteins have

a shorter cytosolic loop and primarily localize to the endoplasmic reticulum (ER), canonical PINs have a longer hydrophilic loop and show a polar localization at the PM. Therefore, non-canonical PINs are not involved in the polar auxin transport, but are important for intracellular auxin transport and homeostasis (Sauer and Kleine-Vehn, 2019).

The canonical PIN proteins, however, are essential for the polar auxin transport. PIN1-4 and 7 are expressed in a tissue-specific manner with different polarity, determining the auxin transport in the plant. PIN1 for example is basally localized in cells of the vasculature mediating the auxin flow from the shoot tip to the root tip. PIN2, on the other hand, shows an apical localization in root epidermal cells and is required for auxin transport to the root tip (Grunewald and Friml, 2010; Christie and Murphy, 2013). PIN3 is displaying an apolar localization in endodermis cells in the hypocotyl in darkness, but relocalizes to the inner side of the endodermal cells showing a lateral localization upon irradiation (Ding *et al.*, 2011; Rakusová, Fendrych and Friml, 2015). Furthermore, PIN3 is involved in the gravitropic response (Grunewald and Friml, 2010; Christie and Murphy, 2013; Rakusová, Fendrych and Friml, 2015). PIN4 shows a polar localization in the root meristem and PIN7 in the embryonic meristem (Grunewald and Friml, 2010).

PIN 3, 4 and 7 are thought to be involved in the phototropic response, where they might act redundantly since single mutants did not show an impaired phototropic response but only the *pin3 pin4 pin7* triple mutant (Willige *et al.*, 2013). PIN proteins are known to cycle continuously between the PM and endosomes via clathrin-dependent endocytosis (Dhonukshe *et al.*, 2007). To guarantee a fast response to a light stimulus, the polar localization of PIN proteins has to be modified as a result of light perception as shown for PIN3 (Ding *et al.*, 2011). However, the exact molecular mechanism behind the reallocation remains yet to be determined.

The regulation of PIN protein activity occurs mainly via phosphorylation. This takes place in the hydrophilic and cytosolic loop of the proteins (Zourelidou *et al.*, 2014; Lanassa Bassukas, Xiao and Schwechheimer, 2022). The phosphorylation sites in the hydrophilic loop are named S1, S2 and S3 and are mainly phosphorylated by the AGC VIII kinases D6PK and PID (Sauer and Kleine-Vehn, 2019; Lanassa Bassukas, Xiao and Schwechheimer, 2022). *d6pk* triple mutants are reported to exhibit an impaired auxin transport (Zourelidou *et al.*, 2014), while PID and the two close related kinases WAVY ROOT GROWTH 1 (WAG1) and WAG2 influence the polarity of PIN proteins (Sauer and Kleine-Vehn, 2019).

PIN polarity is maintained by several aspects like clustering of PIN proteins that reduces lateral diffusion and endocytosis (Kleine-Vehn *et al.*, 2011). Moreover, the polarity of PIN proteins is maintained by other proteins, such as members of the NPH3/RPT2-like protein family (NRL). Here it was shown that proteins from the MACCHI-BOU 4 (MAB4) subfamily display the same polar localization as PIN proteins and could contribute to the maintenance of PIN polarity (Furutani *et al.*, 2011) (see chapter 1.5).

Additionally, 14-3-3 proteins contribute to PIN polarity (Keicher *et al.*, 2017). To examine the effect of members of the 14-3-3 epsilon group on plant growth and development, expression of three ubiquitously expressed members (epsilon, mu and omicron) was repressed via RNA interference or artificial microRNA (Keicher *et al.*, 2017). This repression caused phenotypes related to auxin transport like agravitropism and altered auxin distribution patterns (Keicher *et al.*, 2017). Furthermore, the polar localization of PIN proteins was affected, suggesting 14-3-3 proteins to contribute to PIN polarity. However, direct interaction between PIN proteins and 14-3-3 proteins could not be shown (Keicher *et al.*, 2017). These findings suggest that reduced 14-3-3 expression impairs auxin transport by affecting PIN recycling at the PM (Keicher *et al.*, 2017).

1.4 14-3-3 proteins

14-3-3 proteins belong to a highly conserved protein family that is present in every eukaryotic organism (Ferl, 1996; van Heusden, 2005). In general, the number of 14-3-3 isoforms depend on the complexity of the organism, higher eukaryotic organisms contain multiple isoforms. *Arabidopsis thaliana* for example comprises 13 isoforms and mammalian cells comprise seven isoforms (Yaffe *et al.*, 1997; DeLille, Sehnke and Ferl, 2001). 14-3-3 proteins can be divided into two groups, the epsilon and the non-epsilon group (DeLille, Sehnke and Ferl, 2001). The ancestral epsilon group contains five isoforms, while the non-epsilon group comprises eight isoforms (DeLille, Sehnke and Ferl, 2001; Rosenquist *et al.*, 2001). It is assumed that the ancestral epsilon group is involved in fundamental regulatory processes, while the non-epsilon group contributes to organism-specific processes (Ferl, Manak and Reyes, 2002; Jaspert, Throm and Oecking, 2011).

14-3-3 proteins normally interact in a sequence-specific and phosphorylation-dependent manner with their target proteins. 14-3-3 proteins form a W-like dimer with two binding grooves (Yaffe, 2002; Mackintosh, 2004; Chi *et al.*, 2015). They form complexes with their target proteins and can change for example localization, activity or the conformation (Mackintosh, 2004). So far, three binding motifs containing a serine or threonine are known, including mode

I and II that are located internally and mode III which is located C-terminally (Yaffe *et al.*, 1997; Coblitz *et al.*, 2005; Coblitz *et al.*, 2006).

14-3-3 proteins are involved in numerous cellular processes and several interaction partners of plant 14-3-3 proteins are well characterized. The activity of the H^+-ATPase is needed for secondary active transport process and transport of ions across the PM. The H^+-ATPase is kept at a low activity state by its C-terminal autoinhibitory domain and becomes activated upon phosphorylation-dependent 14-3-3 association (Jahn *et al.*, 1997; Oecking *et al.*, 1997; Kinoshita and Shimazaki, 1999). The 14-3-3 proteins bind via a C-terminal mode III motif (Oecking *et al.*, 1997; Kinoshita and Shimazaki, 1999). Phosphorylation of the C-terminal 14-3-3 binding motif and subsequent binding of 14-3-3s causes a conformational change, abolishing the autoinhibitory effect leading to increased activity of the H^+-ATPase (Jahn *et al.*, 1997; Jaspert, Throm and Oecking, 2011). In stomatal guard cells the H^+-ATPase is activated in BL by a phosphorylation - mediated by phototropins - and subsequent 14-3-3 association leading to K^+ accumulation and subsequent stomata opening (Kinoshita and Shimazaki, 1999; Ueno *et al.*, 2005).

Furthermore, 14-3-3 proteins contribute to the formation of the FLORIGEN ACTIVATION COMPLEX (FAC) with the FLOWERING LOCUS T (FT) and the transcription factor FLOWERING LOCUS D (FD) in rice (Jaspert, Throm and Oecking, 2011; Taoka *et al.*, 2011). This complex promotes flowering by activating the transcription of genes involved in floral development (Jaspert, Throm and Oecking, 2011). The FD homolog in rice OsFD1 and 14-3-3 were identified as interaction partners of the FT homolog in rice Heading date 3a (Hd3a) in a Y2H screen (Jaspert, Throm and Oecking, 2011; Taoka *et al.*, 2011).

Another 14-3-3 target protein is the nitrate reductase that mediates the reduction of nitrate to nitrite. Here, association of 14-3-3 leads to an inactivation of the target protein (Bachmann *et al.*, 1996). Furthermore, the transcription factor BRASSINAZOLE-RESISTANT 1 (BZR1) is an interaction partner of 14-3-3 proteins. BZR1 is involved in the brassinosteroid signaling pathway. Binding to 14-3-3 proteins causes a retention of BZR1 in the cytoplasm and prevents relocalization to the nucleus (Gampala *et al.*, 2007). Recognition of brassinosteroids at the PM leads to a dissociation of 14-3-3 proteins from BZR1 and a relocalization of BZR1 to the nucleus (Gampala *et al.*, 2007; Oecking and Jaspert, 2009; Wang *et al.*, 2011).

As already mentioned in chapter 1.2.1 phot1 and phot2 were identified as target proteins for 14-3-3s, which can only bind to phot autophosphorylated at S849 and S851 (Inoue *et al.*, 2008a; Kinoshita *et al.*, 2003). Interestingly, a former member from our group was able to identify 14-3-3 proteins as a putative interaction partner of proteins belonging to the NON PHOTOTRPIC HYPOCOTYL 3 (NPH3) / ROOT PHOTOTROPISM 2 (RPT2)-like (NRL)

protein family, among those NPH3 and RPT2 (Throm, 2017). A *nph3 A. thaliana* mutant displays an impaired phototropic response upon BL irradiation and a rpt2 mutant shows an impaired hypocotyl bending under high light intensities (Inada *et al.*, 2004). Hence, RPT2 and NPH3 are involved in hypocotyl phototropism.

1.5 NPH3/RPT2-like (NRL) protein family

The NRL protein family is named after two members of the protein family: NON PHOTOTROPIC HYPOCOTYL 3 (NPH3) and ROOT PHOTOTROPISM 2 (RPT2). In addition, the NRL protein family comprises 31 proteins that are characterized by a NPH3 domain with unknown function (Pedmale, Celaya and Liscum, 2010; Christie *et al.*, 2018). Furthermore, most NRL family members contain a N-terminal bric-a-brac, tramtrack, and broad complex (BTB) domain and/or a C-terminal coiled-coil (CC) domain (Pedmale, Celaya and Liscum, 2010). Members of the NRL protein family can be grouped into six subclades in *Arabidopsis thaliana*. The best characterized proteins are members of the three subclades RTP2/ NRL PROTEIN FOR CHLOROPLAST MOVEMENT 1 (NCH1), NPH3 or NAKED PINS IN YUCCA (NPY) (Christie *et al.*, 2018).

Besides NPH3, the proteins NRL12, NRL4 and NRL23/ DEFECTIVELY ORGANIZED TRIBUTARIES 3 (DOT3) belong to the NPH3 subclade. NRL4 and NRL12 are not characterized in detail so far, however, DOT3 is known to contribute to leaf vein patterning and vasculature development (Petricka, Clay and Nelson, 2008; Christie *et al.*, 2018).

Members of the NPY subclade are involved in auxin trafficking and contribute to PIN polarity. MAB4/ ENHANCER OF PINOID (ENP)/ NPY1 and the homologous proteins MAB/ENP/NPY1-LIKE (MEL) 1-4 contribute to PIN polarity and are thought to control auxin transport (Furutani *et al.*, 2011). PM associated MAB4 displays a similar polarity to that of PIN1 during embryogenesis and MEL proteins seem to contribute to PIN polarity thereby regulating auxin transport (Furutani *et al.*, 2011). Single mutant backgrounds of MEL1-4 did not display any phenotypes, *mab4* single mutants however, show mild defects in organ formation (Furutani *et al.*, 2007; Furutani *et al.*, 2011). Combination of the *mab4* mutant background with *mel1* or *mel2* caused severe defects in the development of cotyledons and floral organs (Furutani *et al.*, 2011). A *mab4 mel1 mel2* triple mutant even displayed a pin-like inflorescences, suggesting that proteins from the NPY subclade act redundantly (Furutani *et al.*, 2011).

NCH1 and RPT2 are the best characterized proteins from the RPT2/NCH1 subclade. NCH1 is important for the phototropin mediated chloroplast accumulation response and is able to directly interact with phot1 *in vitro* (Suetsugu *et al.*, 2016). RPT2 was identified in a screen for *Arabidopsis* mutants being impaired in the phototropic response in the hypocotyl and the root

(Sakai *et al.*, 2000). *rpt2* mutants display a normal phototropic response under low light conditions (up to 0.1 µmol/m^2/s), but show an impaired hypocotyl bending under higher light intensities (Sakai *et al.*, 2000; Inada *et al.*, 2004; Haga *et al.*, 2015). Moreover, RPT2 is required for leaf positioning, leaf flattening and chloroplast accumulation (Inada *et al.*, 2004; Christie *et al.*, 2018). BL induces transcription of RPT2 in a phot1-independent manner, however stabilization of the RPT2 protein under BL is phot1-dependent (Kimura *et al.*, 2020). Moreover, RPT2 is degraded by the ubiquitin-proteasome pathway when phot1 is inactive (Kimura *et al.*, 2020). RPT2 and phot1 are able to interact via the N-terminal region of RPT2 – containing the BTB domain - and the LOV domains of phot1 in a Y2H assay (Inada *et al.*, 2004). More specifically, RPT2 binds to the LOV1 domain of phot1 (Kimura *et al.*, 2020). Therefore, RPT2 might inhibit the autophosphorylation of phot1 and thereby suppresses the photosensitivity and/or kinase activity of phot1 (Kimura *et al.*, 2020). Besides phot1, RPT2 is also able to interact with NPH3 via the N-terminal regions of both proteins in a Y2H assay (Inada *et al.*, 2004). The exact function of this interaction is unknown so far, but in a *rpt2* mutant the subcellular localization of NPH3 is altered after prolonged BL irradiation (Haga *et al.*, 2015).

1.5.1 NPH3

In 1995 a genetic screen identified four loci to be affected in the phototropic response, including NPH1, NPH3 and NPH4 (Liscum and Briggs, 1995). NPH1 was later on identified as phot1 and NPH4 was identified as AUXIN RESPONSE FACTOR 7 (ARF7) (Christie *et al.*, 1999; Harper *et al.*, 2000). In 1999 NPH3 was shown to be a phot1 interacting protein essential for phototropism (Motchoulski and Liscum, 1999).

Besides the phototropic response, NPH3 is also involved in leaf positioning and leaf expansion, but not in chloroplast accumulation, avoidance movement and stomatal opening (Inoue *et al.*, 2008b; Suetsugu *et al.*, 2016; Christie *et al.*, 2018). Since the autophosphorylation of phot1 is not affected in a *nph3* mutant, it seems to function downstream of phot1 (Liscum and Briggs, 1995). In rice the NPH3 ortholog COLEOPTILE PHOTOTROPISM 1 (CPT1) was identified (Haga *et al.*, 2005). The establishment of an asymmetric, lateral auxin gradient in the *cpt1* mutant failed after application of ^{3}H-IAA (Haga *et al.*, 2005). Therefore, the establishment of the lateral auxin gradient during phototropic response in rice is thought to occur downstream of CPT1 (Haga *et al.*, 2005).

Subcellular fractionation demonstrated that NPH3 localizes like phot1 to the PM in darkness although it is hydrophilic (Motchoulski and Liscum, 1999) and is internalized into particle-like structures in the cytosol upon BL irradiation (Haga *et al.*, 2015; Sullivan *et al.*, 2019).

Interestingly, the formation of these particles is reversible after prolonged irradiation or when irradiated seedlings are returned to darkness (Haga *et al.*, 2015). The mechanism behind PM association in darkness and dissociation upon BL is unknown so far, but it has been postulated that the C-terminal region including the CC domain could be involved in PM association (Inoue *et al.*, 2008b), since a C-terminally truncated - including a part of the CC domain - NPH3 variant displayed localization to particles after transient expression in *Vicia faba* guard cells (Inoue *et al.*, 2008b). For PM dissociation in BL, phot1 seems to be essential, since the PM dissociation of NPH3 is impaired in a *phot1* mutant background (Haga *et al.*, 2015). Subcellular fractionation studies revealed that NPH3 partially shifts from the microsomal to the soluble fraction upon BL irradiation (Haga *et al.*, 2015).

Furthermore, NPH3 is present in a phosphorylated state in darkness and becomes rapidly dephosphorylated upon BL irradiation evident by an increased electrophoretic mobility (Pedmale and Liscum, 2007; Haga *et al.*, 2015). In addition, treatment with phosphatase inhibitors showed that NPH3 actually is dephosphorylated upon BL treatment, since the treatment with okadaic acid, cantharidin or endothall prevented the increased electrophoretic mobility in BL (Pedmale and Liscum, 2007). Vice versa treatment with a phosphatase caused an increased electrophoretic mobility for NPH3 independent of BL irradiation (Pedmale and Liscum, 2007). The phosphorylation in darkness apparently is phot1-independent, while the dephosphorylation upon BL treatment turned out to be phot1-dependent (Pedmale and Liscum, 2007). Similar to the subcellular localization of NPH3 the phosphorylation status is reversible after prolonged irradiation or when irradiated seedlings are transferred back to darkness (Pedmale and Liscum, 2007; Haga *et al.*, 2015). In darkness, several amino acid residues - S213, S223, S233, S237 - were shown to contribute to the phosphorylation of NPH3, since mutation of this residues led to an increased electrophoretic mobility in darkness (Tsuchida-Mayama *et al.*, 2008). Mass spectrometric analysis of dark or light treated seedlings recently revealed seven phosphorylation sites in NPH3 including S213, S223 and S237 (Kimura *et al.*, 2021). However, the kinase responsible for phosphorylation in darkness and the phosphatase responsible for dephosphorylation in BL remain yet to be identified.

Since the alteration of the phosphorylation status und change in the subcellular localization seem to correlate, it was hypothesized that dephosphorylation could be a prerequisite for or a consequence of particle-like structure formation in BL (Haga *et al.*, 2015; Sullivan *et al.*, 2019; Legris and Boccaccini, 2020). Furthermore, it was stated that NPH3 present in particles and in a dephosphorylated state represents the inactive form, while association to the PM in the phosphorylated state would promote the phototropic response (Haga *et al.*, 2015; Sullivan *et al.*, 2019).

As already mentioned, almost all NRL proteins including NPH3 comprise three domains: an N-terminal BTB domain, a central NPH3 domain and a C-terminal CC domain. The function of the central NPH3 domain is not known so far. The BTB domain and the CC domain are known to mediate in protein-protein interactions. NPH3 is for example able to interact with the LOV domains of phot1 via its C-terminal region as shown with a Y2H assay and *in vivo* with Co-Immunoprecipitation (Motchoulski and Liscum, 1999; de Carbonnel *et al.*, 2010). Moreover, studies have also reported that NPH3 interacts with PHYTOCHROME KINASE SUBSTRATE 1 (PKS1) and PKS2, two phytochrome signaling elements (Lariguet *et al.*, 2006; de Carbonnel *et al.*, 2010). PKS1 and PKS2 were shown to be important for the phototropic response under low light intensities (Lariguet *et al.*, 2006). *In vitro* and *in vivo* experiments demonstrate that NPH3 interacts with PKS1 and PKS2 (Lariguet *et al.*, 2006; de Carbonnel *et al.*, 2010). In addition, NPH3 is thought to be part of the CUL3 RING E3 UBIQUITIN LIGASE (CRL3) complex ($CRL3^{NPH3}$) where it functions as a substrate adapter (Roberts *et al.*, 2011). Under low BL intensities this complex could mediate mono/multiubiquitination of phot1, whereas under high BL intensities phot1 mono/multi- and polyubiquitination is mediated by $CRL3^{NPH3}$ (Roberts *et al.*, 2011).

Furthermore, Christian Throm from our group identified 14-3-3 proteins as putative interaction partners of NPH3. The 14-3-3 binding motif seems to be located in the NPH3 C-terminal region (Throm, 2017). This interaction and the 14-3-3 binding site were later confirmed with *in vivo* experiments performed by Tanja Schmidt (Reuter *et al.*, 2021; Schmidt, 2022).

1.6 Aim of the work

NPH3 is essential for the phototropic response and acts downstream of the blue light receptor phot1 (Motchoulski and Liscum, 1999). However, little is known of how exactly NPH3 contributes to the phototropic response. Christian Throm identified 14-3-3 proteins as putative interaction partners of NPH3 and, in addition, the 14-3-3 binding motif in the C-terminal region of NPH3 (Throm, 2017). Tanja Schmidt confirmed this interaction later by performing *in vivo* experiments (Reuter *et al.*, 2021; Schmidt, 2022). 14-3-3 interaction was also shown for phot1 (Kinoshita *et al.*, 2003; Inoue *et al.*, 2008a) and furthermore 14-3-3 proteins contribute to the polarity of PIN proteins (Keicher *et al.*, 2017) – two other important components for the phototropic response. Therefore, it is of great interest to elucidate the impact of 14-3-3 interaction on the subcellular localization and the phosphorylation status of NPH3 under dark and BL conditions.

NPH3 associates to the PM in darkness although it is a hydrophilic protein (Motchoulski and Liscum, 1999). Since the mechanism underlying PM association remains elusive so far, this work aims at investigating the molecular mechanism causing PM localization of NPH3 in darkness. Furthermore, NPH3 detaches from the PM upon BL irradiation and is internalized into particle-like structures in the cytosol (Haga *et al.*, 2015). A detailed characterization of the particle-like structures, including a biochemical examination of their nature, is still missing. Therefore, this thesis aims at examining the nature of the particle-like structures. Based on structural dissection of NPH3, this thesis moreover aims to determine the motifs required for particle formation under differing light conditions.

Besides the changes in subcellular localization, also the phosphorylation status of NPH3 is altered upon BL irradiation. NPH3 is present in a phosphorylated state in darkness, but is rapidly dephosphorylated upon BL treatment, as evident by an increased electrophoretic mobility (Pedmale and Liscum, 2007; Haga *et al.*, 2015). Remarkable results in our lab revealed that 14-3-3 proteins and NPH3 interact in a strictly BL-dependent manner (Reuter *et al.*, 2021; Schmidt, 2022). This is contradictory to the dephosphorylation upon BL treatment, since 14-3-3 proteins are known to interact in a phosphorylation-dependent manner with their target proteins. Therefore, we are interested in examining the phosphorylation status of NPH3 upon BL treatment.

2 Material and Methods

2.1 Material

Various consumables used for this work like reaction tubes and tips were purchased from Eppendorf (Hamburg, Germany) or Greiner Bio-One GmbH (Frickenhausen, Germany).

2.1.1 Plasmids

Plasmids containing constructs under 35S promoter were generated by Andrea Bock, Jutta Keicher and Tanja Schmidt using Gateway Cloning system (Tab 2.1).

Table 2. 1: Plasmids used in this study generated using Gateway Cloning system

Construct	Vector	Resistance
35S::GFP:NPH3	pH7WGF2*	Spectinomycin
35S::RFP:NPH3	pB7WGR2*	Spectinomycin
35S::GFP:NPH3-S744A	pH7WGF2*	Spectinomycin
35S::RFP:NPH3-S744A	pB7WGR2*	Spectinomycin
35S::GFP:NPH3ΔC51	pH7WGF2*	Spectinomycin
35S::RFP:NPH3ΔC51	pB7WGR2*	Spectinomycin
35S::GFP:NPH3ΔN54	pH7WGF2*	Spectinomycin
35S::RFP:NPH3ΔN54	pB7WGR2*	Spectinomycin
35S::RFP:NPH3-5KR/A	pB7WGR2*	Spectinomycin
35S::GFP:NPH3ΔC28	pH7WGF2*	Spectinomycin
35S::RFP:NPH3ΔC28	pB7WGR2*	Spectinomycin
35S::GFP:NPH3-4K/A	pH7WGF2*	Spectinomycin
35S::RFP:NPH3-4K/A	pB7WGR2*	Spectinomycin
35S::RFP:NPH3-4WLM/A	pB7WGR2*	Spectinomycin
35S::RFP:NPH3-C51	pB7WGR2*	Spectinomycin
35S::RFP:NPH3-C164	pB7WGR2*	Spectinomycin
35S::GFP:NPH3ΔN155	pH7WGF2*	Spectinomycin
35S::RFP:NPH3ΔN155	pB7WGR2*	Spectinomycin
35S::RFP:NPH3ΔC93	pB7WGR2*	Spectinomycin
35S::RFP:NPH3ΔC121	pB7WGR2*	Spectinomycin
35S::RFP:NPH3ΔC164	pB7WGR2*	Spectinomycin
35S::RFP:NPH3-LIP	pB7WGR2*	Spectinomycin
35S::RFP:NPH3-CON	pB7WGR2*	Spectinomycin
35S::RFP:NPH3-RR/A	pB7WGR2*	Spectinomycin
35S::RFP:NPH3ΔC51-CON	pB7WGR2*	Spectinomycin
35S::RFP:NPH3ΔC51-LYRA	pB7WGR2*	Spectinomycin
35S::GFP:NPH3-S744D	pH7WGF2*	Spectinomycin
35S::RFP:NPH3-S744D	pB7WGR2*	Spectinomycin
35S::GFP:NPH3-S746A	pH7WGF2*	Spectinomycin
35S::RFP:NPH3-S746A	pB7WGR2*	Spectinomycin
35S::GFP:NPH3-S746D	pH7WGF2*	Spectinomycin
35S::RFP:NPH3-S746D	pB7WGR2*	Spectinomycin
35S::mCherry:NPH3 II 35S::14-3-3:mEGFP	pFRETgc-2in1-CN*[2]	Spectinomycin
35S::mCherry:NPH3-S744A II 35S::14-3-3:mEGFP	pFRETgc-2in1-CN*[2]	Spectinomycin

*(Karimi, Depicker and Hilson, 2007) *[2] (Hecker *et al.*, 2015)

Plasmids containing constructs under the endogenous promoter of NPH3 were generated by Andrea Bock and Jutta Keicher using Golden Gate Cloning system (Tab 2.2).

Table 2. 2: Plasmids used in this study generated using Golden Gate Cloning system

Construct	Vector backbone	Resistance
pNPH3::GFP:NPH3	BB10 Plus	Spectinomycin
pNPH3::GFP:NPH3-S744A	BB10 Plus	Spectinomycin
pNPH3::GFP:NPH3ΔC51	BB10 Plus	Spectinomycin
pNPH3::GFP:NPH3ΔN54	BB10 Plus	Spectinomycin
pNPH3::GFP:NPH3-5KR/A	BB10 Plus	Spectinomycin
pNPH3::GFP:NPH3ΔC28	BB10 Plus	Spectinomycin
pNPH3::GFP:NPH3-4K/A	BB10 Plus	Spectinomycin
pNPH3::GFP:NPH3-4WLM/A	BB10 Plus	Spectinomycin
pNPH3::GFP:NPH3ΔN155	BB10 Plus	Spectinomycin

Modification of the phospholipid composition of the plant plasma membrane was achieved by using a genetic tool that specifically depletes the pool of phosphatidylinositol-4-phosphate (Pi4P) from the plasma membrane. The tool was published in 2016 by Simon et al. (Simon *et al.*, 2016), wherein the active catalytic domain of the yeast SAC1 protein was fused with a MAP (myristoylation and palmitoylation) sequence for permanent plasma membrane attachment (MAP:mCherry:SAC1). As a control the catalytically inactive version of SAC1 (MAP:mCherry:$SAC1_{DEAD}$) was used (Simon *et al.*, 2016).

2.1.2 Plants

In this work *Arabidopsis thaliana*, ecotype Columbia-0 (Col-0) was used. Seeds from a T-DNA induced loss-of-function mutant of NPH3 *A.thaliana nph3-7* (SALK_110039, Col-0 background) were obtained from NASC (Nottingham Arabidopsis Stock Centre) and used for the generation of transgenic lines. Stable transformation and identification of homozygous lines was done by Jutta Keicher and Tanja Schmidt (Tab 2.3).

Table 2. 3: Transgenic lines used in this study

Construct	Background	Independent lines
35S::GFP:NPH3	*nph3-7*	35S::GFP:NPH3 #8 , #17
35S::GFP:NPH3-S744A	*nph3-7*	35S::GFP:NPH3-S744A #19 , #28
35S::GFP:NPH3-4K/A	*nph3-7*	35S::GFP:NPH3-4K/A #1 , #19
35S::GFP:NPH3ΔC28	*nph3-7*	35S::GFP:NPH3ΔC28 #6 , #10
35S::GFP:NPH3ΔN54	*nph3-7*	35S::GFP:NPH3ΔN54 #15 , #22
pNPH3::GFP:NPH3	*nph3-7*	pNPH3::GFP:NPH3 #1 , #4
pNPH3::GFP:NPH3-S744A	*nph3-7*	pNPH3::GFP:NPH3-S744A #7, #13

For transient expression *Nicotiana benthamiana* was used. The tobacco plants were cultivated and propagated by the central greenhouse of the ZMBP at the Eberhard Karls University Tübingen.

2.1.3 Bacteria

Transient transformation was performed by using the bacterial strain *Agrobacterium tumefaciens* GV3101 (Koncz and Schell, 1986) and heterologous protein expression in bacteria was performed by using the bacterial strain *Escherichia coli* M15 (Qiagen, Hilden). To propagate plasmids the *E. coli* strain One Shot™ TOP10 (Thermo Fisher Scientific GmbH, Dreieich) was used.

For a better expression after transient transformation the silencing suppressor strain p19 (Win and Kamoun, 2004) was used (indicated in figure legends when co-infiltrated).

2.1.4 Chemicals & Kits

Following chemicals and kits were used during this work.

Table 2. 4: Utilized chemicals and kits

Chemical / Kit	Manufacturer
2-(N-morpholino)ethanesulfonic acid (MES)	Carl Roth GmbH + Co. KG, Karlsruhe
3-(N-morpholino)propanesulfonic acid (MOPS)	Carl Roth GmbH + Co. KG, Karlsruhe
3,5-Dimethoxy-4-hydroxyacetophenone (Acetosyringone)	Sigma-Aldrich Chemie GmbH, Taufkirchen
4-(2-hydroxyethyl)-1-piperazineethanesulfonic acid (HEPES)	Carl Roth GmbH + Co. KG, Karlsruhe
Acetic acid	Carl Roth GmbH + Co. KG, Karlsruhe
Albumin bovine Fraction V (BSA)	SERVA Electrophoresis GmbH, Heidelberg
Ammoniumperoxodisulfate (APS)	Carl Roth GmbH + Co. KG, Karlsruhe
Ampicillin	Sigma-Aldrich Chemie GmbH, Taufkirchen
Bromophenol blue	Carl Roth GmbH + Co. KG, Karlsruhe
cOmplete™ (Protease Inhibitor Cocktail)	Roche Holding, Basel (CH)
Coomassie® Brilliant Blue R 250	SERVA Electrophoresis GmbH, Heidelberg
Cycloheximide	Sigma-Aldrich Chemie GmbH, Taufkirchen
Dimethylsulfoxide (DMSO)	Carl Roth GmbH + Co. KG, Karlsruhe
Dithiotreitol (DTT)	Carl Roth GmbH + Co. KG, Karlsruhe
ECL™ Prime Western Blotting Detection Reagent	Cytiva Europe GmbH, Freiburg
Ethanol (EtOH)	Sigma-Aldrich Chemie GmbH, Taufkirchen
Ethylenediaminetetraacetic acid (EDTA)	Carl Roth GmbH + Co. KG, Karlsruhe
GeneJET Plasmid Miniprep Kit	Thermo Fisher Scientific GmbH, Dreieich
Gentamicin	SERVA Electrophoresis GmbH, Heidelberg
Glycerol	Carl Roth GmbH + Co. KG, Karlsruhe
Glycine	Carl Roth GmbH + Co. KG, Karlsruhe
Hydrochloric acid (HCl)	Sigma-Aldrich Chemie GmbH, Taufkirchen
Imidazole	Carl Roth GmbH + Co. KG, Karlsruhe
Isopropyl β-d-1-thiogalactopyranoside (IPTG)	PEQLAB Biotechnologie GmbH, Erlangen

Kanamycin	Duchefa Biochemie, Haarlem (NL)
LB-Agar (Luria/Miller)	Carl Roth GmbH + Co. KG, Karlsruhe
LB-Medium (Luria/Miller)	Carl Roth GmbH + Co. KG, Karlsruhe
Magnesium chloride ($MgCl_2$) hexahydrate	Carl Roth GmbH + Co. KG, Karlsruhe
Methanol (MeOH)	Sigma-Aldrich Chemie GmbH, Taufkirchen
Milk powder	Carl Roth GmbH + Co. KG, Karlsruhe
Monosodium phosphate (NaH_2PO_4)	Carl Roth GmbH + Co. KG, Karlsruhe
Murashige and Skoog Medium „Basal Salt Mixture“ (MS medium)	Duchefa Biochemie, Haarlem (NL)
Nondidet P40 (NP-40)	Sigma-Aldrich Chemie GmbH, Taufkirchen
Phosphatase Inhibitor Mix I (PIM I)	SERVA Electrophoresis GmbH, Heidelberg
PHYTO AGAR	Duchefa Biochemie, Haarlem (NL)
Polyvinylpyrrolidone (PVP)	Sigma-Aldrich Chemie GmbH, Taufkirchen
Ponceau S	SERVA Electrophoresis GmbH, Heidelberg
Potassium hydroxide (KOH)	Carl Roth GmbH + Co. KG, Karlsruhe
Rifampicin	Duchefa Biochemie, Haarlem (NL)
ROTIPHORESE®Gel 30 (37,5:1)	Carl Roth GmbH + Co. KG, Karlsruhe
ROTI®Nanoquant	Carl Roth GmbH + Co. KG, Karlsruhe
Sodium chloride (NaCl)	Carl Roth GmbH + Co. KG, Karlsruhe
Sodium deoxycholate (DOC)	Carl Roth GmbH + Co. KG, Karlsruhe
Sodium dodecyl sulfate (SDS)	Carl Roth GmbH + Co. KG, Karlsruhe
Sodium hydroxide (NaOH)	Merck Chemicals GmbH, Darmstadt
Spectinomycin	Duchefa Biochemie, Haarlem (NL)
Sucrose	Carl Roth GmbH + Co. KG, Karlsruhe
Tetramethylethylenediamine (TEMED)	Honeywell Fluka®, Seelze
TNT® Quick Coupled Transcription/Translation System	Promega GmbH, Walldorf
TRIS	Carl Roth GmbH + Co. KG, Karlsruhe
Triton X-100	Sigma-Aldrich Chemie GmbH, Taufkirchen
TWEEN® 20	Carl Roth GmbH + Co. KG, Karlsruhe

2.1.5 Buffers and solutions

The following buffers and solutions were used for this work. If not stated differently buffers and solutions were prepared by using double-distilled water (ddH_2O).

Table 2. 5: Utilized buffers and solutions

Buffer/Solution	Composition
½ MS medium	2.2 g MS „Basal Salt Mixture“ / L pH adjusted to 5,7 with KOH 1 % PHYTO AGAR autoclaved
2x SDS sample buffer	125 mM TRIS/HCl (pH 6,8) 4 % SDS 20 % Glycerol 0.01 % Bromophenol blue 1 tablet cOmplete™ per 50 ml 10 % DTT **added fresh**

10x SDS Running buffer	250 mM TRIS 1.92 M Glycine 1 % SDS
10x TBS buffer	500 mM TRIS 1.5 M NaCl 10 mM $MgCl_2$ pH adjusted to 7,8 with HCl
10x Transfer buffer	200 mM TRIS 1.5 M Glycine 0.1 % SDS 20 % EtOH **added freshly** to 1xTransfer buffer
AS medium (Infiltration tobacco)	10 mM $MgCl_2$ 150 µM Acetosyringone 10 mM MES/NaOH (pH 5,6)
Blocking solution	4 % milk powder Dissolved in 1xTBS buffer
Coomassie destaining solution	40 % MeOH 10 % Acetic acid
Coomassie staining solution	40 % MeOH 10 % Acetic acid 0.1 % Coomassie® Brilliant Blue R 250
Elution buffer (Protein purification)	50 mM NaH_2PO_4 300 mM NaCl 125 mM Imidazole pH adjusted to 8 with NaOH
Extraction buffer (Co-Immunoprecipitation)	50 mM TRIS/HCl (pH 7,5) 150 mM NaCl 1 mM EDTA 0.75 % Triton X-100 1 x cOmplete™ & PIM I
Extraction buffer (Raw extract)	20 mM TRIS/HCl (pH 7) 150 mM NaCl 1 mM EDTA 1 % Triton X-100 0.1 % SDS 5 mM DTT 1 x cOmplete™ & PIM I
Homogenisation buffer (Microsomal preparation)	50 mM HEPES (pH 7,8) 500 mM Sucrose 3 mM DTT 3 mM EDTA 1 % PVP 1 x cOmplete™ & PIM I
Incubation buffer (Far Western)	50 mM MOPS/KOH (pH6,5) 20 % Glycerol 1 mM DTT 5 mM $MgCl_2$
LB-Agar (Luria/Miller)	40 g LB-Agar / L autoclaved

LB-Medium (Luria/Miller)	25 g LB-Medium / L autoclaved
Lysis buffer (Protein purification)	50 mM NaH_2PO_4 300 mM NaCl 10 mM Imidazole pH adjusted to 8 with NaOH
Ponceau S	0.1 % Ponceau S 2 % Acetic acid
Solubilization buffer (Immunoprecipitation)	25 mM TRIS/HCl (pH 8) 150 mM NaCl 1 % NP40 2 mM DTT 0.5 % DOC 1 x cOmplete™ & PIM I
Stripping buffer	0.2 M Glycine 0.1 % SDS 1 % TWEEN® 20 pH adjusted to 2,2 with HCl
TBS-T	1 x TBS buffer 0.2 % TWEEN® 20
TMS buffer (Microsomal preparation)	5 mM MES/TRIS (pH 6,5) 330 mM Sucrose 2 mM DTT 1 x cOmplete™ & PIM I
Washing buffer (Protein purification)	50 mM NaH_2PO_4 300 mM NaCl 20 mM Imidazole pH adjusted to 8 with NaOH
Washing buffer (Immunoprecipitation)	25 mM TRIS/HCl (pH 8) 150 mM NaCl
Washing buffer I (Co-Immunoprecipitation)	50 mM TRIS/HCl (pH 7,5) 150 mM NaCl 1 mM EDTA 0.1 % Triton X-100
Washing buffer II (Co-Immunoprecipitation)	50 mM TRIS/HCl (pH 7,5) 150 mM NaCl

2.1.6 Antibodies

Following antibodies were used in this work.

Table 2. 6: Utilized antibodies

Antibody	Manufacturer	Dilution
α-GFP	Thermo Fisher Scientific, Sindelfingen	1:1000
α-RGS-His	Qiagen, Hilden	1:2000
α-RFP 5F8	Chromotek GmbH, Planegg	1:1000
α-NPH3	Eurogentec, Liege (BEL)	1:1000
α-NPH3 pS744	Eurogentec, Liege (BEL)	1:500
α-HA high affinity	Roche Holding, Basel (CH)	1:2000
α-Rabbit	Promega, Walldorf	1:10,000
α-Rat	Sigma-Aldrich Chemie GmbH, Taufkirchen	1:10,000
α-Mouse	Promega, Walldorf	1:10,000

The rabbit α-NPH3 and α-NPH3 pS744 antibodies were generated by using the synthetic peptide NH_2-PPRKPRRWRN-S(PO_3H_2)-IS-COOH followed by affinity purification against the non-phosphorylated and phosphorylated peptide (Eurogentec, Liege, BEL).

2.2 Methods

2.2.1 Cloning procedure

Cloning procedures followed standard techniques of the Gateway Cloning system (Thermo Fisher Scientific GmbH, Dreieich) or the Golden Gate Cloning system (Binder *et al.*, 2014). Cloning was jointly performed by Andrea Bock, Jutta Keicher, and Tanja Schmidt along with me.

2.2.1.1 Transformation of *Escherichia coli*

For propagation of plasmids the plasmid was transformed into One Shot™ TOP10 *E. coli* cells via heat shock. 100 µL of the competent cells were thawed on ice and the plasmid was added. The cells were then kept on ice for 5 min followed by 45 seconds (sec) heat shock at 42 °C. Afterwards 900 µL LB-Medium were added to the transformed cells and the cells were incubated at 37 °C (overhead rotor) for 1 h. 100 µL of the bacteria were then plated on LB-Agar plates containing spectinomycin (100 µg/mL). The plates were stored for 1 day at 37 °C.

2.2.1.2 Plasmid isolation

Plasmid isolation was done by using the GeneJET Plasmid Miniprep Kit (Tab 2.4) according to the manufacturers' protocol. Concentration and quality of the purified plasmid DNA were measured using the NanoDrop® ND-1000 Spectrophotometer (Thermo Fisher Scientific GmbH, Dreieich).

2.2.2 Sterilization of seeds and cultivation of etiolated seedlings

For surface sterilization, either seeds of transgenic lines (Tab 2.3) or Col-0 were incubated in 70 % ethanol (EtOH) containing 0.05 % Triton X-100 for 10 minutes (min) with overhead rotation. Afterwards the solution was removed and seeds were incubated in 100 % EtOH for another 5 min with overhead rotation. The seeds were subsequently dried on sterile filter paper. Surface sterilized seeds were sown on plates with ½ MS medium.

For cultivation of etiolated seedlings, seeds were stratified at least two nights at 4 °C and afterwards incubated in fluorescent white light for 4 hours. Seedlings were grown in darkness for 2-3 days at room temperature (RT).

Subsequently etiolated seedlings were either used for analysis at the microscope or harvested as plant material for further experiments. Therefore, the material was directly harvested under red safety light (dark control) or treated with overhead blue light (BL) (1 µmol/m^2/s) for up to 30 min and immediately frozen in liquid nitrogen. A part of the etiolated seedlings was retransferred to darkness after BL irradiation.

To examine whether inhibition of protein synthesis alters the subcellular localization of NPH3, etiolated seedlings were transferred to plates containing cycloheximide (100 µM) for 1 hour (h) by Tanja Schmidt before further analysis at the microscope.

2.2.3 Transient transformation of *Nicotiana benthamiana*

2.2.3.1 Transformation of *Agrobacterium tumfaciens*

Transformation of competent *A. tumefaciens* was performed via heat shock. 100 µL of competent bacteria (*A. tumefaciens* GV3101) were thawed on ice and the appropriate binary vector was added. Afterwards the bacterial cells were kept on ice for 5 min followed by 5 min snap freezing in liquid nitrogen and a subsequent heat shock at 37 °C for 5 min. The transformed cells were recovered in 500 µL LB-Medium and were incubated at RT (overhead rotor) for 3-4 h. 100 µL of the bacterial suspension were plated on LB-Agar plates containing the antibiotics rifampicin, gentamycin and spectinomycin, except for p19 (rifampicin, gentamicin, kanamycin) (Tab 2.7). The plates were stored for 2 days at 28 °C.

Table 2. 7: Used antibiotics

Antibiotics	Concentration
Gentamicin	15 µg/mL
Rifampicin	50 µg/mL
Spectinomycin	100 µg/mL
Kanamycin	10 µg/mL

2.2.3.2 Transient transformation of *N. benthamiana* leaves

Transient transformation was performed as described in Grefen et al. 2010 (Grefen *et al.*, 2010). Therefore a preculture of transformed *A.tumefaciens* (see chapter 2.2.3.1) was incubated over night at 28 °C under constant shaking. The next morning 500 µL of this culture were added to 4.5 mL fresh LB-Medium with the respective antibiotics (see chapter 2.2.3.1) and incubated at 28 °C for another 3-4 h. Following, 4 mL of the bacterial suspension were centrifuged at 2000 xg for 5 min. The bacteria pellet was washed with ddH_2O and centrifuged again at 2000 xg for 5 min. Subsequently the pellet was resuspended in 1 mL AS medium (Tab 2.5) and the OD at 600 nm was measured. OD was adjusted to 0.1-0.3 and afterwards the bacterial suspension was incubated on ice for 30 min. For coinfiltration the bacteria were mixed 1:1, except for p19 which was always coinfiltrated with an OD of 0.1. For infiltration, 3-4 weeks old *N. benthamiana* plants were used and the abaxial side of the leaves was infiltrated with a syringe without needle. After infiltration the plants were kept in light for 24 h and subsequently transferred to darkness for approximately 17 h.

The plants were further used for analysis at the microscope or harvested as plant material for further experiments. Therefore, the material was directly harvested under red safety light (dark control) or treated with overhead BL (10 µmol/m^2/s) for up to 40 min and immediately frozen in liquid nitrogen. For several experiments, a part of the leaves was retransferred to darkness after BL irradiation.

2.2.4 Cell free protein expression

In vitro transcription and translation were performed with the TNT® T7 Quick Coupled Transcription/Translation System (Tab 2.4). The binary vectors for the cell free protein expression were cloned by Andrea Bock (NPH3 variants in pGADT7 AD, Takara Bio Europe, Saint-Germain-en-Laye, FRA). 1 µg of plasmid DNA was mixed with 40 µL TNT® Quick Master Mix, 1 µL of 1 mM Methionine and 2 µL of nuclease-free water. The reaction was incubated at 30 °C for 90 min. The *in vitro* transcription and translation was verified with an immunodetection against hemagglutinin (HA).

2.2.5 Protein expression and purification

Arabidopsis 14-3-3 proteins (omega isoform) tagged with an RGS-His_6-Tag were expressed in *E. coli* M15. For this the expression vector pQE-30 (Qiagen, Hilden) was used. The bacteria were grown in LB-medium containing ampicillin (100 µg/mL) and kanamycin (25 µg/mL). Protein expression was induced by isopropyl β-d-1-thiogalactopyranoside (IPTG, end concentration: 0.5 mM) and bacteria were grown over night at 16 °C. The bacteria were pelleted and stored an -20 °C. After thawing on ice, the pellet was resuspended in lysis buffer (Tab 2.5) containing lysozyme (2 mg/mL buffer). The cells were lysed by sonication and

centrifuged at 10,000 xg for 30 min and 4 °C. The lysate was filtered through Miracloth (Merck Chemicals GmbH, Darmstadt) and transferred to HisTrap™ FF crude (Cytiva Europe GmbH, Freiburg) equilibrated with lysis buffer (Tab 2.5). Afterwards the column was washed with washing buffer (Tab 2.5) five times. For elution of the purified protein 3 mL elution buffer (Tab 2.5) were added to the column. The eluate was saved, mixed with glycerol (30 % end concentration) and stored at -20 °C.

Protein concentration was determined photometrically by using Roti®Nanoquant (Tab 2.4) according to the manufacturer's protocol. In addition, a standard curve with albumin bovine fraction V (BSA) was determined to calculate the protein concentration. The efficiency of the protein purification was verified with a sodium dodecyl sulfate polyacrylamide gel electrophoresis (SDS-PAGE) (see chapter 2.2.10) stained with Coomassie® Brilliant Blue (Tab 2.5).

2.2.6 Preparation of microsomal membranes

For preparation of microsomal membranes transiently transformed *N. benthamiana* leaves were used. The plant material was crushed in liquid nitrogen and homogenized with homogenization buffer (Tab 2.5) in a ratio of 3:1 (buffer: plant material). The homogenate was centrifuged at 10,000 xg and 4 °C for 20 min followed by a filtration through Miracloth (Merck Chemicals GmbH, Darmstadt). Afterwards the filtrate was centrifuged again at 100,000 xg and 4 °C for 45 min. The supernatant was aliquoted, snap frozen and stored as "soluble protein fraction". The microsomal pellet was resuspended in TMS buffer (Tab 2.5) and subsequently aliquoted, snap frozen and stored as "microsomal protein fraction". Measurement of the protein concentration was again done photometrically by using Roti®Nanoquant (Tab 2.4) (see chapter 2.2.5). 7.5 µg protein of the "soluble" and the "microsomal protein fraction" were loaded to SDS gels (see chapter 2.2.10) for further immunodetection. Samples were mixed 1:1 with 2x SDS sample buffer (Tab 2.5) and heated to 70 °C for 4 min.

2.2.7 Co-Immunoprecipitation

Co-Immunoprecipitation (CoIP) was performed after protocol modified from Park et al. 2012 (Park *et al.*, 2012) with plant material from transiently transformed *N. benthamiana* leaves. Dark treated samples were processed under red safety light. 500 mg crushed plant material were mixed with 1.5 mL extraction buffer (Tab 2.5) and solubilized with over-head-rotation for 1 h at 4 °C. In the meantime, 20 µL GFP-Trap® Agarose (Chromotek, Planegg) were equilibrated in extraction buffer. After solubilization the extract was centrifuged for 40 min at maximum speed and 4 °C followed by another centrifugation of the supernatant for 10 min with the same settings. 100 µL of the supernatant were frozen as "Input" whereas the remaining supernatant was given to the agarose beads. The beads were now incubated with

the supernatant by over-head-rotation at 4 °C for 1.5 h. Afterwards the beads were washed 3 times with washing buffer I (Tab 2.5). After the third washing the reaction tubes were changed and the beads were washed once with washing buffer II (Tab 2.5). Subsequently the washing buffer was removed completely and the beads were stored at -20 °C. Before performing SDS- PAGE 40 µL of 2x SDS sample buffer (Tab 2.5) were added to the beads and the beads were then heated to 95 °C for 5 min. The Input was mixed 1:1 with 2x SDS sample buffer and also heated to 95 °C for 5min. The successful CoIP was verified via immunodetection.

2.2.8 Immunoprecipitation

For immunoprecipitation either transiently transformed *N. benthamiana* leaves (300-500 mg) or etiolated transgenic *A. thaliana* seedlings (50 mg) were used. Experiments were performed according to a modified protocol from Albert et al. 2015 (Albert *et al.*, 2015). Dark treated samples were processed under red safety light. The plant material was ground in liquid nitrogen and mixed with either 1.7 mL (*N. benthamiana*) or 200 µL (*A. thaliana*) solubilization buffer (Tab 2.5). Afterwards the homogenate was incubated with over-head-rotation at 4 °C for 1 h followed by centrifugation for 1 h with maximum speed at 4 °C. In the meantime, equilibration of 20 µL GFP-Trap® Agarose (Chromotek, Planegg) in solubilization buffer was done. After centrifugation the supernatant was transferred to the agarose beads and incubated with over-head-rotation for 1 h at 4 °C. The beads were then washed two times in solubilization buffer and reaction tubes were changed after the second washing step. In the end the beads were washed twice with washing buffer (Tab 2.5), supernatant was completely removed and the beads were stored at -20 °C. Before performing SDS- PAGE 40 µL of 2x SDS sample buffer (Tab 2.5) were added to the beads and the beads were then denatured at 70 °C for 10 min (*A. thaliana*) or at 95 °C for 5 min (*N. benthamiana*). The successful immunoprecipitation was verified via immunodetection.

2.2.9 Preparation of crude extract

Preparation of crude extract was done by grinding either 2 snap-frozen leaf disks (15 mg) of transiently transformed *N. benthamiana* or approximately 50 snap-frozen, 3-day old, etiolated seedlings (11 mg) of transgenic *A. thaliana* directly in 100 µL 2x SDS sample buffer (Tab 2.5). This was followed by incubation on ice for 5-10 min and subsequent denaturation at 95 °C for 5 min (*N. benthamiana*) or 70 °C for 10 min (*A. thaliana*). For dark treated samples the processing of the plant material was performed under red safety light. Before sample loading the samples were centrifuged at maximum speed for 5 min (*N.benthamiana*) or 5000 xg for 5 min (*A. thaliana*).

For an alternative preparation of crude extract for *N. benthamiana*, the 2 snap-frozen leaf disks were ground using the TissueLyser II (Qiagen, Hilden). Ground plant material was mixed with 60 µL extraction buffer (Tab 2.5) per leaf disk. Extracts were then kept on ice for 5 min followed by centrifugation at 13,000 rpm and 4 °C for 15 min. The supernatant was transferred to a new reaction tube and stored at -20 °C. For SDS-PAGE, 10 µL extract were mixed with 10 µL 2x SDS sample buffer (Tab 2.5) and heated to 95 °C for 5 min. For dark treated samples the processing of the plant material was performed under red safety light.

2.2.10 SDS-PAGE, Western Blotting & Immunodetection

For separation of the proteins of interest, SDS-PAGEs were performed followed by western Blotting and immunodetection. SDS gels were cast using the ROTIPHORESE®Gel 30 (Tab 2.4). For SDS-PAGEs of purified protein from bacteria (see chapter 2.2.5) a 12 % resolving gel was used, for all other SDS-PAGEs a 7.5 % resolving gel was used. After denaturing, the samples were loaded to the gels followed by separation of the denatured proteins via gel electrophoresis at constant 15-20 mA at RT. As a standard the “PageRuler™ Prestained Protein Ladder, 10 to 180 kDa” (Thermo Fisher Scientific, Sindelfingen) was used.

After gel electrophoresis, separated proteins were transferred to a nitrocellulose membrane (Amersham™ Protran™ 0.45 µm NC 300 mm x 4 m, Cytiva Europe GmbH, Freiburg). Protein transfer was performed by using the “TE 22 Mini Tank Transfer Unit” (Cytiva Europe GmbH, Freiburg) and the method published by Towbin et al. 1979 (Towbin, Staehelin and Gordon, 1979) (buffer see Tab 2.5). Transfer settings were as follows: 200 mA for 1.5 h at RT or 64 mA overnight at 4 °C. To check the successful transfer, the membrane was incubated in Ponceau S (Tab 2.5) for 5-10 min.

Afterwards membranes were blocked in blocking solution (Tab 2.5) for at least 1 h at RT followed by incubation in the appropriate first antibody (Tab 2.6) for 1.5 h at RT or overnight at 4 °C. After incubation in the first antibody the membranes were washed three times with TBS-T (Tab 2.5) followed by incubation in the secondary antibody (Tab 2.6) for 1 h. Subsequently the membranes were washed two times with TBS-T and once with 1xTBS. Detection was carried out using the ECL™ Prime Western Blotting Detection Reagent (Cytiva Europe GmbH, Freiburg) and the Amersham ImageQuant 800 (Cytiva Europe GmbH, Freiburg) imaging system.

2.2.11 Far Western

Far Western analysis was performed after western blotting of immunoprecipitated samples from either transgenic *A. thaliana* lines or transiently transformed *N. benthamiana* leaves. After transfer to nitrocellulose the membrane was blocked (see chapter 2.2.10) for minimum 1 h. Then the membrane was incubated in incubation buffer (Tab 2.5) containing purified His-

tagged 14-3-3 proteins (20 µg protein/ mL buffer) over night at 4 °C followed by 1 h incubation at RT. Subsequently the immunodetection (see chapter 2.2.10) was performed using the RGS-His-antibody (Tab 2.6).

2.2.12 Confocal laser scanning microscopy

Confocal laser scanning mircoscopy (CLSM) was done at the upright Leica TCS SP8 (Leica Microsystems GmbH, Wetzlar). Imaging was performed on leaves of *N. benthamiana* or hypocotyls of etiolated *A. thaliana* seedlings. For imaging the "HC PL APO CS2 63x/1.20 WATER" objective was used, the settings for detecting fluorophores were as follows: GFP excitation 488 nm, emission 505-530 nm; RFP excitation 552 nm, emission 600-630 nm. When two fluorophores were detected simultaneously the line sequential mode was used to reduce "crosstalk" between the signals. Images in one experiment were taken with the same settings and processed with the "Leica Application Suite X 3.5.7.23225" (Leica Microsystems GmbH, Wetzlar).

For recording movies, the dissociation from the PM was initiated with the GFP-laser (488 nm) at 20 % power. Afterwards 50 images of a single cell were taken immediately after each other creating a time lapse movie.

Single-cell time-lapse imaging was performed with transiently transformed *N. benthamiana* leaves expressing RFP:NPH3 under 35S promoter. Therefore z-stacks of an epidermal cell were taken with 30 consecutive planes along the Z axis covering the whole cell. The "dark state" of the cell was imaged (just excitation of RFP) followed by initiation of PM dissociation by means of the GFP-laser (488 nm). Imaging was done over a time of 32 min with intervals for each z-stack of 3.5 min. The experiment was repeated 5 times.

2.2.13 Data Analysis

Analysis of all single-cell time-lapse experiments was performed with randomly sampled, unsaturated confocal images (1024x1024 pixels). Quantification was done with an image analysis protocol implemented in ImageJ (Schindelin *et al.*, 2012) as described by Zavaliev and Epel 2015 (Zavaliev and Epel, 2015). Parameters such as local threshold, object size, background noise and shape were determined from one randomly selected image from the data set. The resulting parameters were used for the whole set of data. Graphs show data from one single experiment.

3 Results

NPH3 was identified as putative 14-3-3 interaction partner in a Y2H screen (Jaspert, Throm and Oecking, 2011) along with other members of the NRL protein family such as RPT2 and ENP (Throm, 2017). Here, 14-3-3 isoforms from the epsilon as well as the non-epsilon group were found to putatively interact with NPH3 (Throm, 2017). Christian Throm confirmed in an Y2H assay that the full-length version of NPH3 is able to interact with isoforms of both 14-3-3 subgroups. Furthermore, he was able to identify the putative 14-3-3 binding motif within the C-terminal region of NPH3 by screening serial deletion constructs (Throm, 2017). Deletion of the C-terminal 51 amino acids but not the N-terminal 54 amino acids abolished interaction between NPH3 and 14-3-3 in yeast (Throm, 2017; Reuter *et al.*, 2021). Later, our group was able to show that other NRLs namely RPT2, ENP and DOT3 are also able to interact with 14-3-3 (epsilon, omega) (Reuter *et al.*, 2021).

In search for the specific 14-3-3 binding site in the C-terminal region of NPH3, residues that were found to be phosphorylated *in planta* (Mergner *et al.*, 2020; Wang *et al.*, 2020) were exchanged for alanine. Indeed, exclusively the exchange of the serine in position 744 in NPH3 abolished interaction with 14-3-3 proteins in yeast (NPH3-S744A) (Throm, 2017; Reuter *et al.*, 2021). Additionally, Tanja Schmidt was able to confirm via CoIP that NPH3-S744A is incapable of 14-3-3 binding *in vivo* (Reuter *et al.*, 2021; Schmidt, 2022). The serine corresponds to the third last position in NPH3 and was found to be conserved in RPT2, DOT3 and ENP, suggesting a C-terminal binding motif (Coblitz *et al.*, 2006) for 14-3-3 proteins (p(S/T)$X_{1\text{-}2}$-COOH) (Reuter *et al.*, 2021).

Interestingly, Tanja Schmidt demonstrated that interaction of NPH3 and 14-3-3 proteins is strictly BL-dependent. For that, transgenic Arabidopsis lines stably expressing 14-3-3:GFP (epsilon) were used. Etiolated seedlings were either kept in darkness for three days or treated with BL (1 µmol/m^2/s) for 30 min after three days of etiolation. Immuno-precipitation (IP) followed by mass spectrometry (MS) led to the finding that 14-3-3 association to NPH3 takes place after BL treatment but not under dark conditions (Reuter *et al.*, 2021; Schmidt, 2022). Prabha Manishankar later confirmed these findings with CoIP experiments using transiently transformed *N. benthamiana* leaves, showing that NPH3 and 14-3-3 proteins are not interacting in darkness but upon BL irradiation (Reuter *et al.*, 2021).

3.1 14-3-3 interaction with NPH3 alters the subcellular localization of NPH3 in a blue light-dependent manner

To examine whether the interaction between 14-3-3 proteins and NPH3 has any effect on the subcellular localization of NPH3, the N-terminally RFP-tagged wild type (WT) protein and NPH3-S744A were transiently and ectopically expressed in *N. benthamiana*. Dark-adapted plants (~19 h) were used for analysis at the confocal laser scanning microscope (CLSM). RFP-tagged protein versions were used because excitation with the RFP laser at 552 nm does not activate the BL photoreceptor phot1 and the following signaling cascade. Consequently, RFP-tagged NPH3 allows monitoring the “Dark” state of the protein and with turning on the GFP laser (488 nm) phot1 becomes activated. For monitoring the BL-irradiated state of NPH3, the sample was either treated with 20 % GFP laser for ~11 min or irradiated with BL from above (10 µmol/m^2/s) for 40 min.

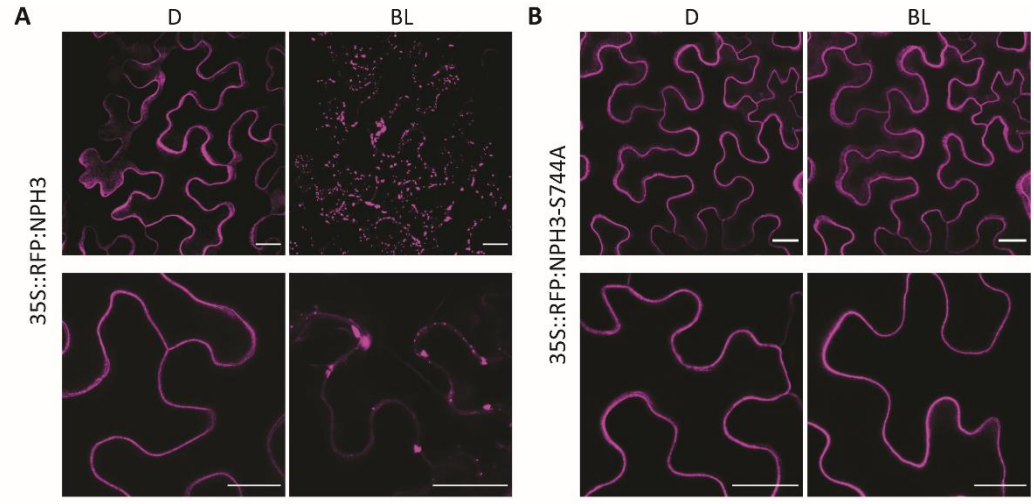

Figure 3. 1: 14-3-3 interaction with NPH3 is required for blue light-induced plasma membrane dissociation of NPH3. A Representative confocal images of epidermal cells from *N. benthamiana* leaves transiently expressing 35S::RFP:NPH3. Plants were dark adapted (D) and treated with 20 % GFP-Laser for ~11 min (upper panel BL) or irradiated with blue light (10 µmol/m2/s) for 40 min (lower panel BL). The upper panel shows the maximum projection of a z-stack. Scale bar 25 µm. **B** Representative confocal images of epidermal cells from *N. benthamiana* leaves transiently expressing 35S::RFP:NPH3-S744A. Plants were dark adapted (D) and treated with 20 % GFP-Laser for ~11 min (upper panel BL) or irradiated with blue light (10 µmol/m2/s) for 40 min (lower panel BL). The upper panel shows the maximum projection of a z-stack. Scale bar 25 µm. Experiments were repeated at least three times.

As shown in Fig 3.1A NPH3 is associated to the PM in darkness although it is hydrophilic. This was already shown in 1999 by Motchoulski and Liscum via subcellular fractionation experiments (Motchoulski and Liscum, 1999). Upon BL irradiation (Fig 3.1A lower panel) or GFP laser treatment (Fig 3.1A upper panel) NPH3 detaches from the PM and forms particle-like structures in the cytosol, confirming the findings of other groups (Haga *et al.*, 2015;

Sullivan *et al.*, 2019). However, Supplementary Movie 1 shows that NPH3 detaches from the PM first, behaving like a soluble protein localizing to cytoplasmic strands followed by particle formation after 4-5 min of GFP laser treatment (Supplementary Movie 1). The BL induced shift in subcellular localization of NPH3 was shown to be phot1 dependent (Haga *et al.*, 2015), yet detachment from the PM and formation of particle-like structures seem to be separate and consecutive processes (Reuter *et al.*, 2021).

In contrast to NPH3, NPH3-S744A is not able to dissociate from the PM and is permanently attached to the PM upon BL treatment (Fig 3.1B, Supplementary Movie 2). This clearly indicates that 14-3-3 association with NPH3 is required for BL-induced detachment of NPH3 from the PM. The findings in our lab suggest that NPH3 is phosphorylated at S744 upon BL treatment enabling 14-3-3 binding (Reuter *et al.*, 2021). Presumable phosphorylation might, however, *per se* interfere with PM association. In this regard, Prabha Manishankar was able to demonstrate that a phosphomimic version of NPH3 (exchange of serine 744 to aspartate) is not affected in PM attachment (Reuter *et al.*, 2021).

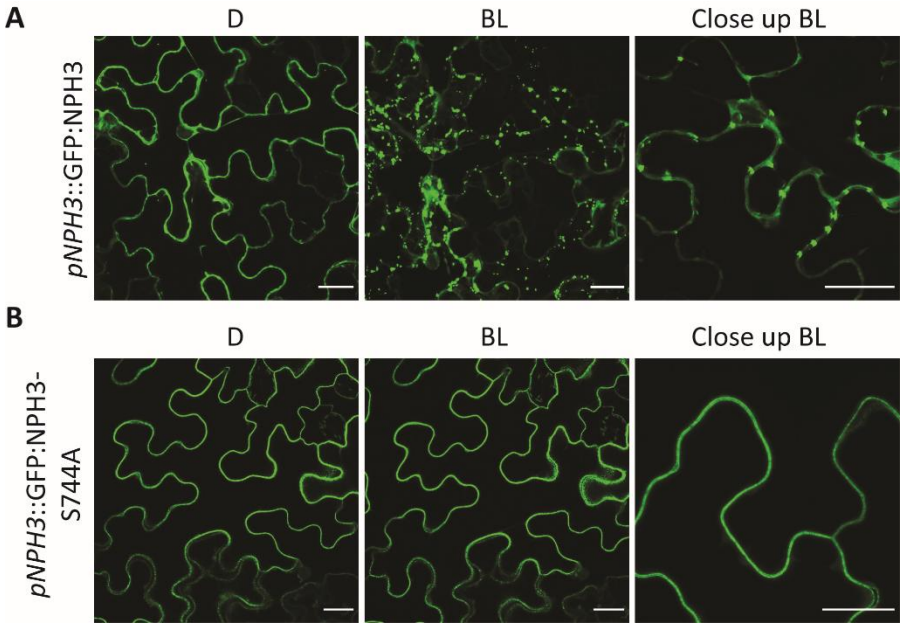

Figure 3. 2: Binding of 14-3-3 is required for blue light-induced plasma membrane dissociation of NPH3. A Representative confocal images of epidermal cells from *N. benthamiana* leaves transiently expressing *pNPH3*::GFP:NPH3. Plants were dark adapted (D) and treated with 20 % GFP-Laser for ~11 min (BL) or irradiated with blue light (10 µmol/m^2/s) for 40 min (Close up BL). BL shows maximum projection of a z-stack. Scale bar 25 µm. **B** Representative confocal images of epidermal cells from *N. benthamiana* leaves transiently expressing *pNPH3*::GFP:NPH3-S744A. Plants were dark adapted (D) and treated with 20 % GFP-Laser for ~11 min (BL) or irradiated with blue light (10 µmol/m^2/s) for 40 min (Close up BL). Scale bar 25 µm. Experiments were repeated at least three times.

To ensure that the subcellular localization of the NPH3 variants is not a consequence of overexpression, N-terminally GFP-tagged NPH3 and NPH3-S744A were in addition expressed under the control of the NPH3 endogenous promoter. Transiently transformed *N. benthamiana* plants were again dark adapted and treated with BL (10 µmol/m^2/s for 40 min) or GFP laser (20 % for ~ 11 min).

In this case, too, the WT protein is attached to the PM in darkness and forms particle-like structures after BL treatment (Fig 3.2A), while NPH3-S744A is still showing a permanent plasma membrane association (Fig 3.2B). These data confirm that formation of discrete bodies in the cytosol is not due to overexpression.

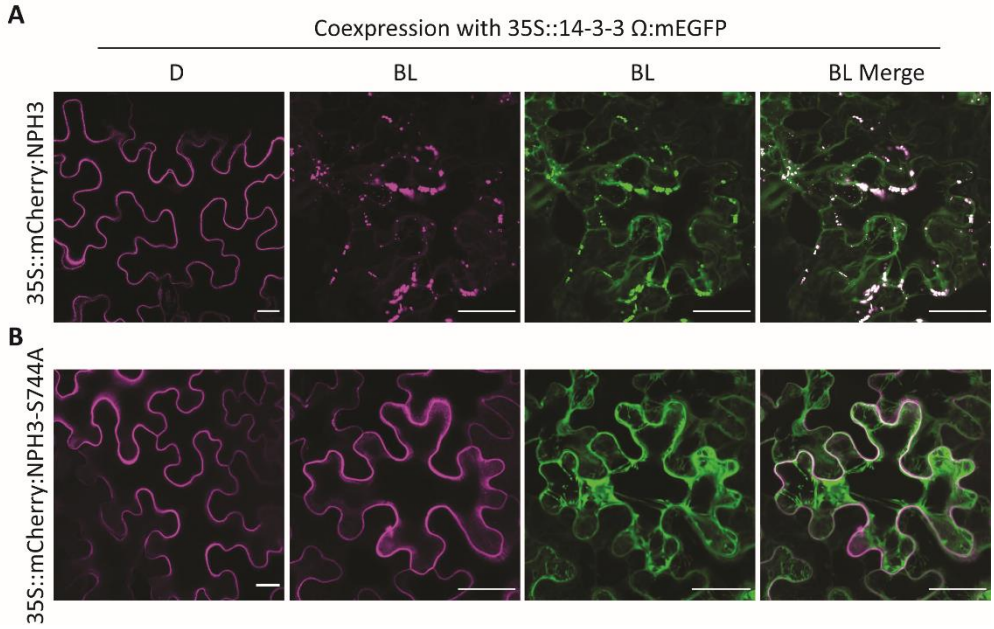

Figure 3. 3: 14-3-3 proteins colocalize with NPH3 but not NPH3-S744A in particles upon blue light irradiation. A Representative confocal images of epidermal cells from *N. benthamiana* leaves transiently co-expressing 35S::mCherry:NPH3 with 35S::14-3-3omega:mEGFP. Plants were dark adapted (D) and irradiated with blue light (10 µmol/m^2/s) for 40 min (BL). Maximum projection of a z-stack is shown for samples treated with BL. Scale bar 25 µm. **B** Representative confocal images of epidermal cells from *N. benthamiana* leaves transiently co-expressing 35S::mCherry:NPH3-S744A with 35S::14-3-3 omega:mEGFP. Plants were dark adapted (D) and irradiated with blue light (10 µmol/m^2/s) for 40 min (BL). Maximum projection of a z-stack is shown for samples treated with BL. Scale bar 25 µm. Experiments were repeated at least three times.

Transient co-expression of mEGFP tagged 14-3-3 omega with either NPH3 or NPH3-S744A in *N. benthamiana* fused to mCherry revealed that 14-3-3 proteins colocalize with the WT protein in discrete bodies in the cytosol after BL irradiation but not with NPH3-S744A (Fig 3.3). Here, 2in1 vectors allowing for 35S promoter driven expression were used. As mentioned previously, the plants were dark adapted and treated with 40 min BL from above (10 µmol/m^2/s).

NPH3 is forming particle-like structures upon BL irradiation and it becomes evident that 14-3-3 omega colocalizes with the WT protein in these particles (Fig 3.3A). On the other hand, the NPH3 mutant incapable of 14-3-3 interaction is showing permanent PM localization and no colocalization in particle-like structures with 14-3-3 proteins after BL treatment (Fig 3.3B). These findings support the results obtained by Tanja Schmidt and Prabha Manishankar demonstrating NPH3 to interact with 14-3-3 in a blue light dependent manner (Reuter *et al.*, 2021).

To investigate the consequences of 14-3-3 interaction with NPH3 on a physiological level GFP-tagged NPH3 or NPH3-S744A were stably expressed in the *Arabidopsis thaliana nph3-7* loss-of-function mutant background (Kansup *et al.*, 2014). All constructs were expressed under control of a 35S promoter. Tanja Schmidt and Jutta Keicher showed that NPH3 is able to restore the phototropic response while phototropic hypocotyl bending is still significantly reduced when NPH3-S744A was expressed (Reuter *et al.*, 2021; Schmidt, 2022). These data prove that 14-3-3 interaction with NPH3 is of functional significance during hypocotyl phototropism.

In addition to the transient localization studies in *N. benthamiana*, the subcellular localization of NPH3 and NPH3-S744A was also analyzed in transgenic Arabidopsis *nph3-7* lines. For this, three day-old etiolated seedlings were either kept in darkness, treated with 20 % GFP laser for ~ 6 min or irradiated with BL from above for 30 min (1 µmol/m^2/s). In addition, a part of the BL-irradiated seedlings was retransferred to darkness for 1 h.

In etiolated seedlings, NPH3 localizes to the PM in darkness and forms particle-like structures after GFP laser treatment or BL irradiation (Fig 3.4A). As already mentioned, NPH3 first becomes soluble before formation of these particles (Supplementary Movie 3). This corroborates the results of transient expression studies depicted in Fig 3.1 and Fig 3.2. Furthermore, the mutant incapable of 14-3-3 interaction displays a permanent PM localization (Fig 3.4B, Supplementary Movie 4) being consistent with the transient expression studies (Fig 3.1 and Fig 3.2). Interestingly, the WT protein reassociates to the PM when seedlings were transferred back to darkness after BL irradiation (Fig 3.4A). These data suggest that NPH3 cycles between the PM and particles in cytosol in a blue light-dependent manner.

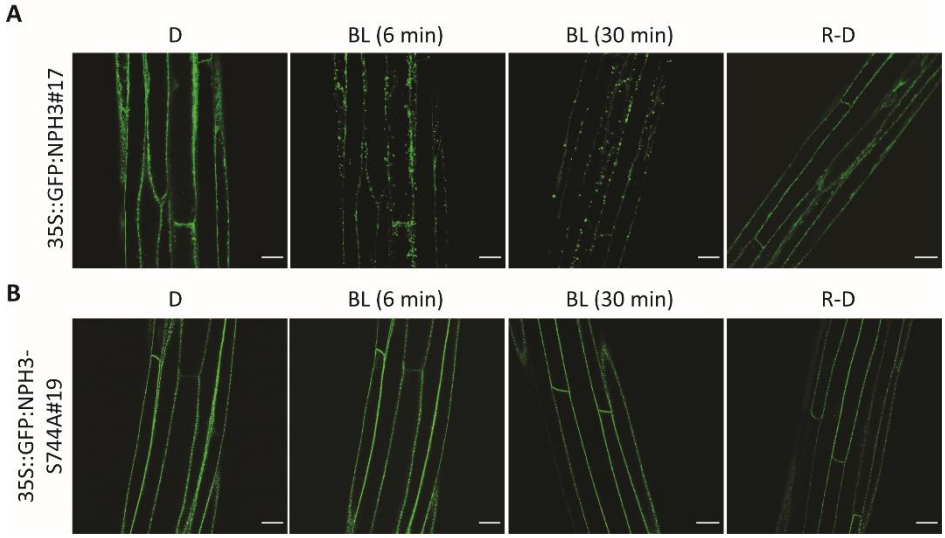

Figure 3. 4: 14-3-3 association with NPH3 is essential for light-triggered plasma membrane detachment of NPH3. A Representative confocal images of hypocotyl cells from etiolated *A. thaliana nph3-7* seedlings (3 days old) expressing 35S::GFP:NPH3. Seedlings were kept in darkness (D), treated with 20 % GFP-Laser for ~6 min, irradiated with blue light (1 µmol/m^2/s) for 30 min (BL) or transferred back to darkness after 30 min of blue light irradiation (R-D). Scale bar 25 µm. **B** Representative confocal images of hypocotyl cells from etiolated *A. thaliana nph3-7* seedlings (3 days old) expressing 35S::GFP:NPH3-S744A. Seedlings were kept in darkness (D), treated with 20 % GFP-Laser for ~6 min, irradiated with blue light (1 µmol/m^2/s) for 30 min (BL) or transferred back to darkness after 30 min of blue light irradiation (R-D). Scale bar 25 µm. Experiments were repeated at least three times. Experiments performed together with Tanja Schmidt.

Subcellular localization and ability to restore the phototropic response in transgenic lines were also analyzed for GFP:NPH3 and GFP:NPH3-S744A expressed under the endogenous promoter. Tanja Schmidt and Jutta Keicher showed that also *pNPH3*::GFP:NPH3 is able to restore the phototropic response whereas NPH3-S744A displayed a reduced capability of hypocotyl bending (Reuter *et al.*, 2021).

To examine the subcellular localization of NPH3 and NPH3-S744A expressed under the endogenous promoter, 3 day-old etiolated seedlings were kept in darkness or irradiated with BL from above (1 µmol/m^2/s) for 40 min. The protein versions display the same localization pattern as the ones expressed under the control of the 35S promoter (Fig 3.5). NPH3 localizes to the PM in darkness and forms discrete bodies in the cytosol after BL treatment (Fig 3.5A), while NPH3-S744A permanently localizes to the PM (Fig 3.5B).

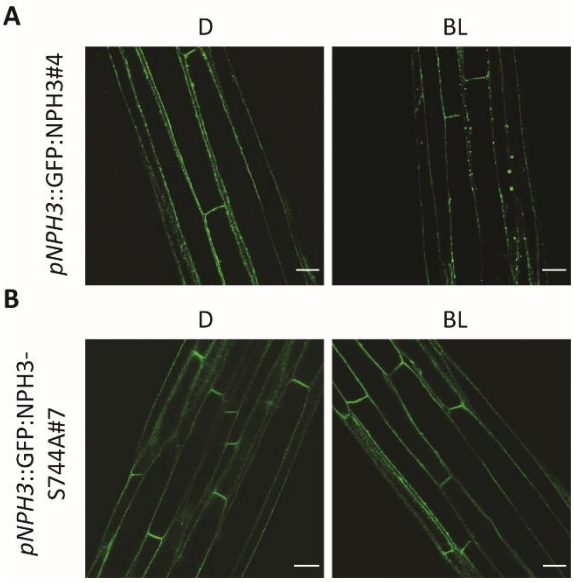

Figure 3. 5: 14-3-3 interaction with NPH3 is required for plasma membrane dissociation of NPH3. **A** Representative confocal images of hypocotyl cells from etiolated *A. thaliana nph3-7* seedlings (3 days old) expressing *pNPH3*::GFP:NPH3. Seedlings were kept in darkness (D) or irradiated with blue light (1 µmol/m^2/s) for 40 min (BL). Scale bar 25 µm. **B** Representative confocal images of hypocotyl cells from etiolated *A. thaliana nph3-7* seedlings (3 days old) expressing *pNPH3*::GFP:NPH3-S744A. Seedlings were kept in darkness (D) or irradiated with blue light (1 µmol/m^2/s) for 40 min (BL). Scale bar 25 µm. Experiments were repeated at least three times.

To verify that relocalization of NPH3 to the PM is not due to *de-novo* synthesized protein, etiolated seedlings ectopically expressing the GFP-tagged WT protein were transferred to medium containing cycloheximide (CHX) 1 h before analysis at the CLSM. Untreated etiolated seedlings served as control. CHX is an antibiotic that interrupts protein biosynthesis by inhibiting translation at the ribosomes (ENNIS and LUBIN, 1964). In etiolated seedlings, NPH3 displays a similar localization pattern when treated or not treated with CHX (Fig 3.6).

In darkness, the protein localizes to the PM. Upon BL irradiation, it forms particle-like structures in the cytosol that are still visible after 1 h of BL irradiation. Independent of CHX treatment NPH3 relocalizes to the PM when retransferred to darkness after 30 min BL treatment (Fig 3.6), demonstrating that the observed effect is not due to *de-novo* synthesis. Therefore, the subcellular localization of NPH3 at the PM and in the discrete bodies in the cytosol are reversible processes driven by the light conditions.

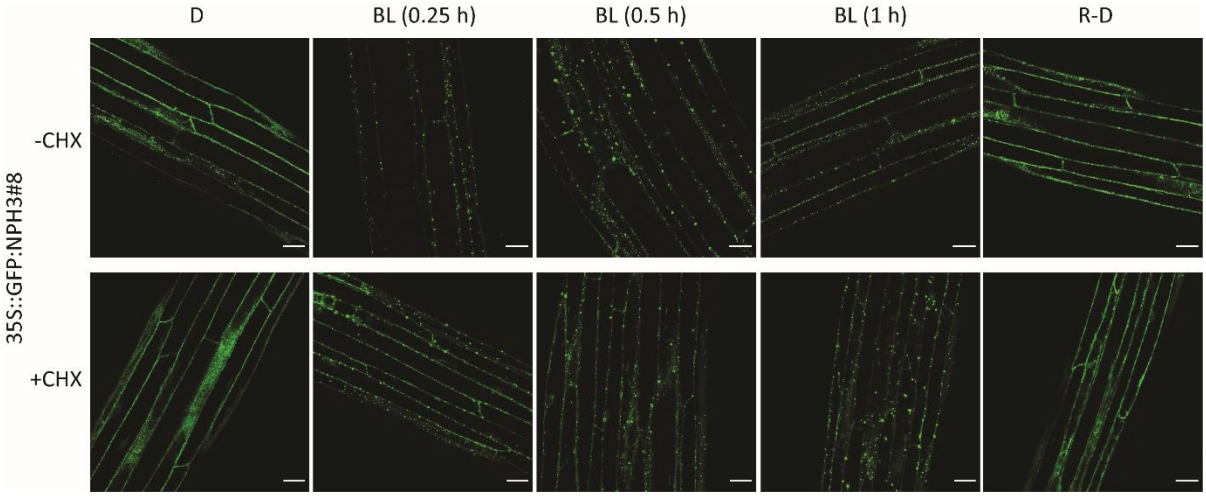

Figure 3. 6: Blue light and dark-driven cycling of NPH3 between the plasma membrane and particle-like structures in the cytosol. Representative confocal images of hypocotyl cells from etiolated *A. thaliana nph3-7* seedlings (3 days old) expressing 35S::GFP:NPH3. Seedlings were kept in darkness (D), irradiated with blue light (1 µmol/m^2/s) for indicated time points or transferred back to darkness after 30 min of blue light irradiation (R-D). Seedlings were treated with (+CHX) or without (-CHX) cycloheximide (100 µM) for 1 h. Scale bar 25 µm. Experiments were repeated at least three times. Experiments performed together with Tanja Schmidt.

To summarize, the subcellular localization of NPH3 is altered by BL from PM association to particle-like structures present in the cytosol. Furthermore, NPH3 is cycling between the PM and the cytosol and this process is reversible under differing light conditions. For the process of NPH3 PM detachment 14-3-3 proteins are required since NPH3-S744A, which is not able to associate to 14-3-3 proteins, is also incapable of PM dissociation.

3.2 NPH3 attaches to the plasma membrane via a C-terminal amphipathic helix

It is known since 1999 that NPH3 associates to the PM in darkness, although, it is hydrophilic (Motchoulski and Liscum, 1999), yet the mechanism of PM association has not been identified. PM association can for example be caused by protein-protein interaction as shown for another NRL member - MAB4 - that is recruited to the PM by PIN proteins and the phot1-homologous AGCVIII kinase PINOID (Glanc *et al.*, 2021). However, PM attachment can also be caused by protein-lipid interactions or hydrophobic interactions. Remorins for example associate to the PM via a C-terminal anchor that is embedded into the inner leaflet of the PM via hydrophobic and electrostatic interactions (Perraki *et al.*, 2012; Gronnier *et al.*, 2017). Besides Remorins, several AGCVIII kinases localize to the PM containing a basic and hydrophobic (BH) motif (Barbosa *et al.*, 2016). The AGCVIII kinases D6PK and PINOID interact with phospholipids at the PM via the BH motif (Barbosa *et al.*, 2016; Simon *et al.*, 2016). Furthermore, it was shown that alterations of the phospholipid composition and electronegativity of the PM modify the subcellular localization of D6PK (Barbosa *et al.*, 2016).

To examine whether NPH3 is also associated to the PM through interaction with phospholipids or electronegativity of the PM, NPH3 was co-expressed with SAC1. SAC1 is a genetic tool developed for plants that consists of the catalytic domain of the yeast phosphatase SAC1 fused to mCherry and localizes to the PM via a myristoylation and palmitoylation sequence (MAP). This genetic system was established by Simon et al. in 2016 and was used to specifically deplete the pool of phosphatidylinositol-4-phosphate (Pi4P) at the PM (Fig 3.7A), thereby resulting in alterations of the phospholipid composition, and hence electronegativity of the PM (Simon *et al.*, 2016; Platre *et al.*, 2018).

We made use of this system and transiently coexpressed 35S::GFP:NPH3 with SAC1 or the catalytically inactive version $SAC1_{DEAD}$ in *N. benthamiana*. The plants were dark adapted for microscopic analysis. Co-expression of NPH3 with SAC1, but not $SAC1_{DEAD}$ causes particle-like structure formation of NPH3 already in darkness (Fig 3.7B). Lipid binding assays (PIP Strips) and liposome binding assays performed by Tanja Schmidt demonstrated NPH3 to interact with polyacidic phospholipids *in vitro* (Reuter *et al.*, 2021; Schmidt, 2022). Taken together, this indicates that the PM association of NPH3 depends either on phospholipid interaction at the PM or on the electronegativity of the PM.

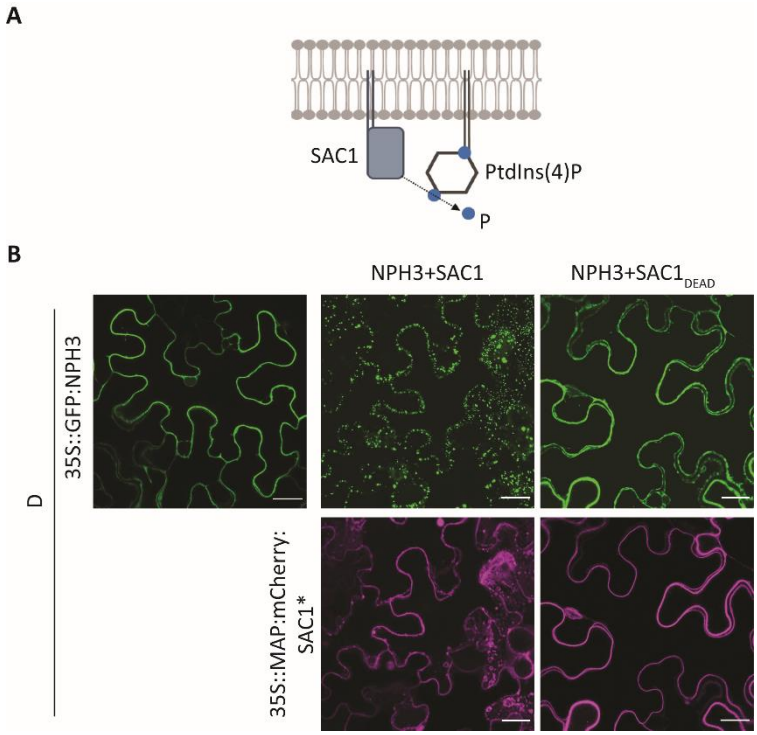

Figure 3. 7: Association of NPH3 to the plasma membrane depends on phospholipid interaction or electronegativity of the plasma membrane. A Modified schematic illustration of the genetic tool SAC1 used to specifically deplete PtdIns(4)P at the plasma membrane (adapted from Simon *et al.*, 2016) **B** Representative confocal images of epidermal cells from *N. benthamiana* leaves co-expressing 35S::GFP:NPH3 with 35S::MAP:mCherry:SAC1 or 35S::MAP:mCherry:SAC1$_{DEAD}$. Plants were dark adapted. Maximum projection of a z-stack is shown for NPH3+SAC1. Single expression of 35S::GFP:NPH3 is shown as a control. Scale bar 25 µm. Experiments were repeated at least three times**.**

To identify which region of NPH3 mediates PM association, the subcellular localization of N-terminally or C-terminally deleted versions of NPH3 were analyzed transiently in *N. benthamiana*. The plants were dark adapted and treated with 20 % GFP laser for ~ 11 min.

Deletion of the N-terminal 54 amino acid residues (35S::RFP:NPH3ΔN54) did not affect the subcellular localization of NPH3 (Fig 3.8A). However, NPH3 truncated by its C-terminal 51 amino acid residues (35S::RFP:NPH3ΔC51, Fig 3.8A) is incapable of PM association in the dark, as evident by particle formation in the cytosol (Fig 3.8B). Subcellular localization of the NPH3 variants was also examined under control of the endogenous promoter, depicting a comparable pattern to the ectopically expressed variants (Fig 3.8C).

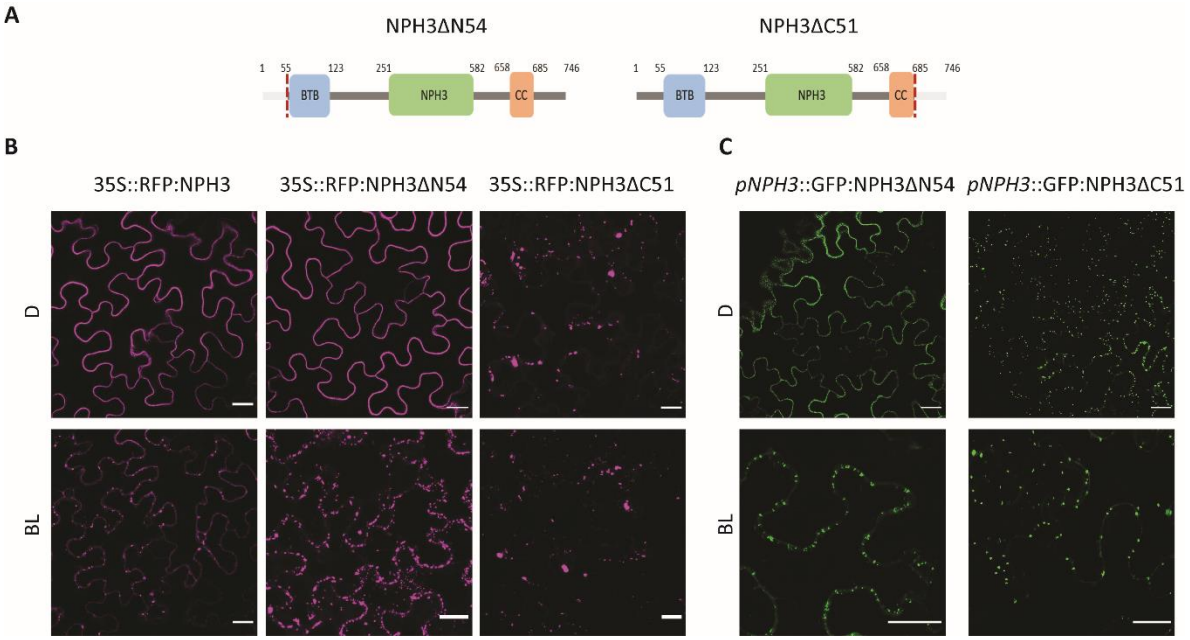

Figure 3. 8: The C-terminal region of NPH3 is required for plasma membrane association. **A** Schematic illustration of N-terminally or C-terminally deleted versions of NPH3 **B** Representative confocal images of epidermal cells from *N. benthamiana* leaves expressing 35S::RFP:NPH3 variants. Plants were dark adapted (D) and treated with 20 % GFP-Laser for ~11 min (BL). Maximum projection of a z-stack is shown for 35S::RFP:NPH3ΔN54 (BL) and 35S::RFP:NPH3ΔC51 (D + BL). **C** Representative confocal images of epidermal cells from *N. benthamiana* leaves expressing *pNPH3*::GFP:NPH3 variants. Plants were dark adapted (D) and irradiated with blue light (10 µmol/m^2/s) for 40 min (BL). Scale bar 25 µm. Experiments were repeated at least three times.

This is in accordance with previous findings from Inoue et al. showing particle formation of a NPH3 version truncated by its C-terminal region (Inoue *et al.*, 2008b). In addition, *in vitro* lipid binding assays and liposome binding assays performed by Tanja Schmidt showed that NPH3ΔC51 was incapable to bind to polyacidic phospholipids while the C-terminal 51 amino acid residues were sufficient. Altogether, these data suggest that the C-terminal region encompassing the last 51 amino acid residues is required for the PM association of NPH3 (Reuter *et al.*, 2021; Schmidt, 2022).

It is known that at least two AGCVIII kinases, namely PINOID and D6PK, associate to the PM via a BH motif (Barbosa *et al.*, 2016; Simon *et al.*, 2016). In search of a BH motif enriched in basic and hydrophobic amino acid residues, Claudia Oecking performed a BH score prediction (Brzeska *et al.*, 2010). Two BH motifs with a critical threshold value above 0.6 were identified within the C-terminal region of NPH3 (Reuter *et al.*, 2021; Schmidt, 2022). One motif enriched in arginine residues close to the 14-3-3 binding site and the second one predicted to form an amphipathic helix further upstream of the R-rich motif (Fig 3.9A). To reduce the BH score five arginine's in the first motif were exchanged for alanine (NPH3-5KR/A), this modification resulted in a reduced binding to phospholipids *in vitro* (PIP Strip assay, performed by Tanja Schmidt) (Reuter *et al.*, 2021; Schmidt, 2022). Surprisingly, RFP:NPH3-5KR/A transiently overexpressed in *N. benthamiana* remains PM associated in the dark and after BL treatment (Fig 3.9B). To confirm that this R-rich motif is dispensable for PM recruitment, the C-terminal 28 amino acid residues were deleted (RFP:NPH3ΔC28) and indeed, PM anchoring is also unaffected here (Fig 3.9B).

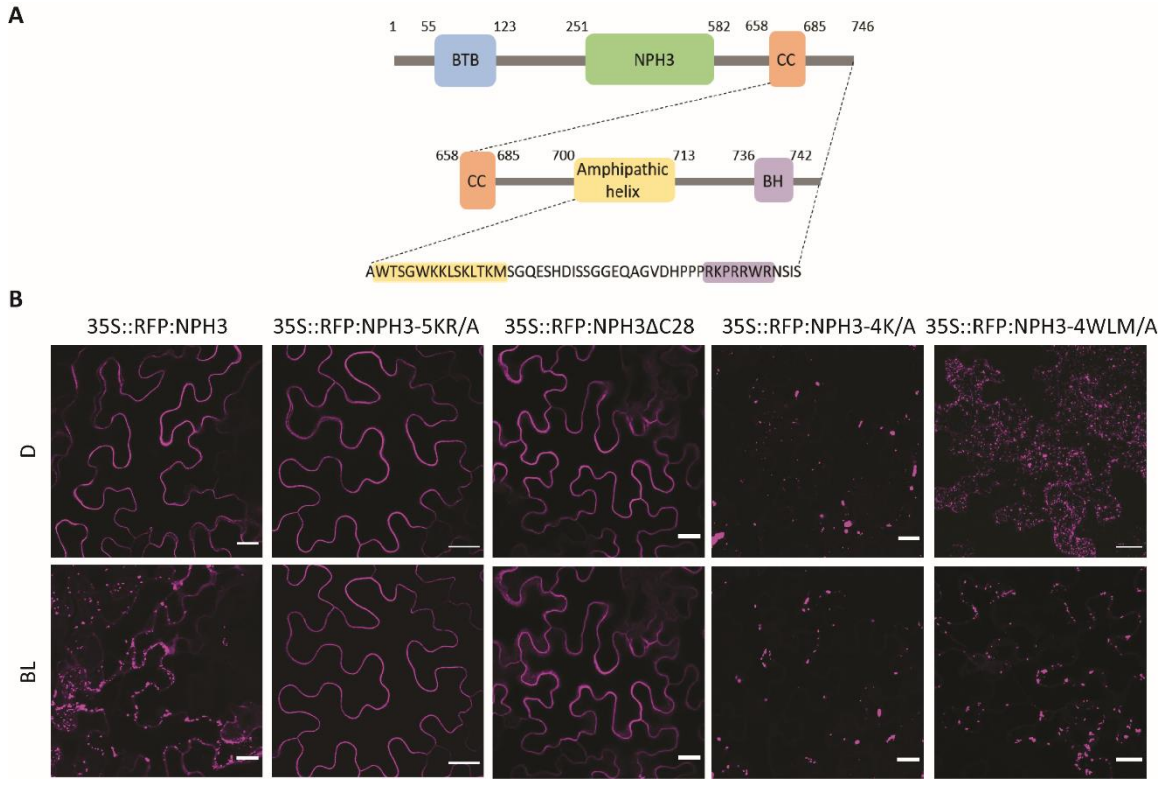

Figure 3. 9: An amphipathic helix in the C-terminal region of NPH3 is essential for plasma membrane association. A Schematic illustration of the C-terminal region of NPH3 including the amphipathic helix **B** Representative confocal images of epidermal cells from *N. benthamiana* leaves expressing 35S::RFP:NPH3 variants. Plants were dark adapted (D) and treated with 20 % GFP-Laser for ~11 min (BL). Maximum projection of a z-stack is shown for 35S::RFP:NPH3ΔC28 (D, BL), 35S::RFP:NPH3-4K/A (D, BL), 35S::RFP:NPH3-4WLM/A (D, BL) and 35S::RFP:NPH3 (BL). Scale bar 25 µm. Experiments were repeated at least three times.

The surprisingly permanent PM association of NPH3-5KR/A could be due to conformational changes caused by the exchanges of arginine to alanine or destruction of a motif required for a possible phosphorylation of the 14-3-3 binding site. On the one hand, destruction of this consensus sequence could abolish potential phosphorylation of the 14-3-3 binding site and with that 14-3-3 interaction (Sullivan *et al.*, 2021), while, on the other hand, conformational changes could cause an inhibition of 14-3-3 binding *per se*. Y2H assays performed by Andrea Bock in our lab showed no interaction between 14-3-3 proteins and NPH3-5KR/A (Andrea Bock, unpublished), however we cannot differentiate between these two scenarios.

The second BH motif (Fig 3.9A) located further upstream is characterized by a charged and a hydrophobic side, respectively - predicted to form an amphipathic helix (Reuter *et al.*, 2021). This means the basic amino acid residues are located on one side of the helix and the hydrophobic amino acid residues are located on the other side of the helix. To reduce the amphiphilicity, four lysine residues were exchanged for alanine (RFP:NPH3-4K/A) while the substitution of four hydrophobic amino acids by alanine served to decrease the hydrophobicity (RFP:NPH3-4WLM/A). Indeed, both of these NPH3 variants turned out to be unable to bind phospholipids *in vitro* (PIP Strip, liposome binding assays) (Reuter *et al.*, 2021; Schmidt, 2022). Transient overexpression of both variants in *N. benthamiana* results in cytosolic particle-like structures in darkness (Fig 3.9B). GFP laser treatment has no further effect (Fig 3.9B).

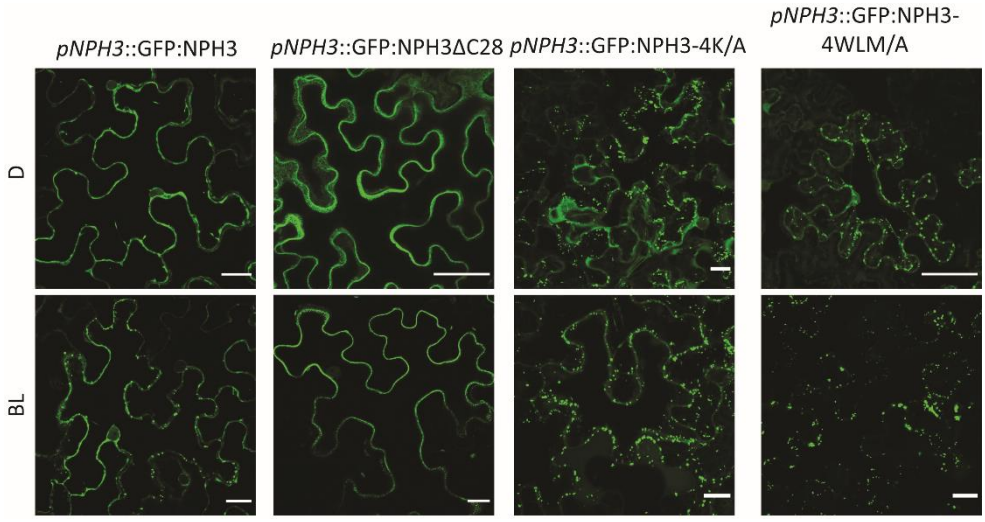

Figure 3. 10: An amphipathic helix in the C-terminal region of NPH3 is required for plasma membrane association. Representative confocal images of epidermal cells from *N. benthamiana* leaves expressing *pNPH3*::GFP:NPH3 variants. Plants were dark adapted (D) and irradiated with blue light (10 µmol/m²/s) for 40 min (BL). Maximum projection of a z-stack is shown for 35S::RFP:NPH3-4K/A, 35S::RFP:NPH3-4WLM/A (D + BL) and 35S::GFP:NPH3ΔC28 (BL). Scale bar 25 µm. Experiments were repeated at least three times.

The NPH3 mutant variants were also analyzed under control of the endogenous promoter showing a comparable subcellular localization as the ectopically expressed variants (Fig 3.10). This indicates that the amphipathic helix in the C-terminal region of NPH3 is required for PM association *in vivo*.

Altogether, we hypothesize that the amphipathic helix of NPH3 is embedded in the inner leaflet of the PM with partial membrane penetration as shown for Remorins (Gronnier *et al.*, 2017). The hydrophobic side of the helix would interact with the hydrocarbon region of the bilayer whereas the basic amino acid residues of the amphipathic helix interact through electrostatic interaction with negatively charged head groups of the phospholipids resulting in PM association of NPH3. 14-3-3 binding upon BL irradiation could induce a conformational change, triggering “extraction” of the helix out of the bilayer.

3.3 The C-terminal 164 amino acids are sufficient for plasma membrane association of NPH3

In vitro experiments performed by Tanja Schmidt showed that the C-terminal 51 amino acid residues downstream of the CC domain of NPH3 are capable to bind to polyacidic phospholipids (Reuter *et al.*, 2021; Schmidt, 2022). To examine whether these C-terminal 51 amino acids (NPH3-C51, Fig 3.11A) are sufficient for PM association *in vivo*, RFP:NPH3-C51 was transiently overexpressed in *N. benthamiana*.

Subcellular localization studies reveal that NPH3-C51 is cytosolic and localizes to the nucleus already in darkness (Fig 3.11B) and thus, is not sufficient for PM association in darkness. A second NPH3 variant was generated containing the C-terminal 164 amino acid residues - downstream the NPH3 domain and comprising the CC domain - (RFP:NPH3-C164, Fig 3.11A) and transiently overexpressed in *N. benthamiana*. In contrast to NPH3-C51, this NPH3 variant is able to associate to the PM in darkness, indicating that the 164 C-terminal amino acid residues are sufficient for PM attachment (Fig 3.11B). These findings suggest that, in addition to the amphipathic helix that is responsible for phospholipid interaction there has to be another characteristic additionally required for PM association in darkness.

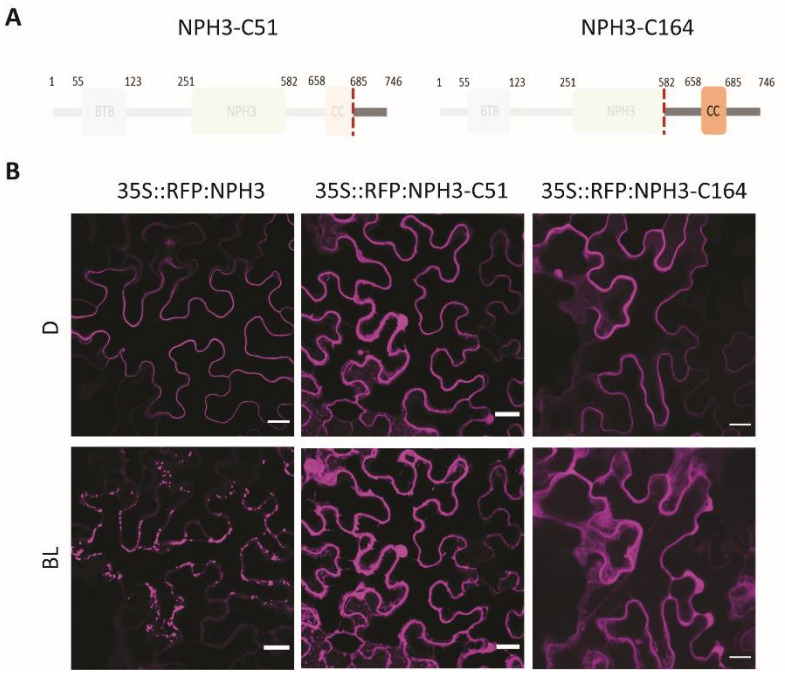

Figure 3. 11: The C-terminal 164 amino acids are sufficient for plasma membrane association in darkness. A Schematic illustration of the C-terminal fragment versions of NPH3 **B** Representative confocal images of epidermal cells from *N. benthamiana* leaves expressing 35S::RFP:NPH3 variants. 35S::RFP:NPH3-C51 and 35S::RFP:NPH3-C164 were co-infiltrated with p19. Plants were dark adapted (D) and treated with 20 % GFP-Laser for ~11min (BL). Maximum projection of a z-stack is shown for 35S::RFP:NPH3-C51 (D, BL), 35S::RFP:NPH3-C164 (D , BL) and 35S::GFP:NPH3 (BL). Scale bar 25 µm. Experiments were repeated at least three times.

NPH3-C51 also displays cytosolic and nuclear localization after treatment with 20 % GFP laser for ~ 11 min, thus BL treatment is not altering the subcellular localization of NPH3-C51 (Fig 3.11B). Different to NPH3-C51, NPH3-C164 associates to the PM in darkness and becomes soluble after GFP laser treatment but does not form particle-like structures (Fig 3.11B), suggesting that the C-terminal 164 amino acid residues are not sufficient for particle-like structure formation in BL.

3.4 NPH3 shows characteristics of biomolecular, membraneless condensates in a light-dependent manner

PM detachment and particle-like structure formation of NPH3 are separate and consecutive processes (see Supplementary Movie 1). After transient expression in *N. benthamiana,* NPH3 first detaches from the PM upon BL and becomes cytosolic, visible as cytoplasmic strands followed by particle formation. Internalization of proteins localizing to the PM can be mediated by endocytosis, this is the case for example for phot1 (Kaiserli *et al.*, 2009). However, NPH3 is insensitive to Brefeldin A (BFA) treatment, suggesting it is not internalized via endocytosis (Haga *et al.*, 2015).

One possibility would be the involvement of 14-3-3 proteins in the particle formation. Since NPH3 and 14-3-3 interact in a strictly BL-dependent manner (Reuter *et al.*, 2021; Sullivan *et al.*, 2021; Schmidt, 2022), it could be highly likely that association of 14-3-3 proteins is responsible for particle formation. However, the particle formation of the NPH3 variant NPH3ΔC51 that lacks the 14-3-3 binding site (Fig 3.8, 3.15) indicates that 14-3-3 proteins are not required for particle formation.

To confirm these findings, we again made use of the genetic tool SAC1 that depletes Pi4P at the PM, (see chapter 3.2) co-expressed transiently in *N.benthamiana* with 35S::GFP:NPH3-S744A, the NPH3 variant incapable of 14-3-3 interaction. The plants were dark adapted and it becomes evident that comparable to the WT protein (Fig 3.7B) NPH3-S744A localizes to particles following co-expression of SAC1 but not the catalytically inactive version $SAC1_{DEAD}$ (Fig 3.12A). These data clearly show that particles form as a consequence of PM detachment and 14-3-3 proteins are not required for particle formation but for detachment from the PM. However, the identity of the particle-like structures has been not clearly determined.

To address this, a subcellular fractionation was performed to determine the subcellular localization of the membrane- and non-membrane-associated state of different NPH3 variants in darkness. For this, the different GFP:NPH3 versions were transiently overexpressed in *N. benthamiana*. As expected, NPH3, NPH3-S744A and NPH3ΔN54 which localize to the PM in darkness, are exclusively detected in the microsomal fractions (Fig 3.12B). Interestingly, NPH3ΔC51 that permanently localizes to discrete bodies is mainly present in the soluble fraction (Fig 3.12B), suggesting that NPH3 may be present in membraneless particles upon BL irradiation.

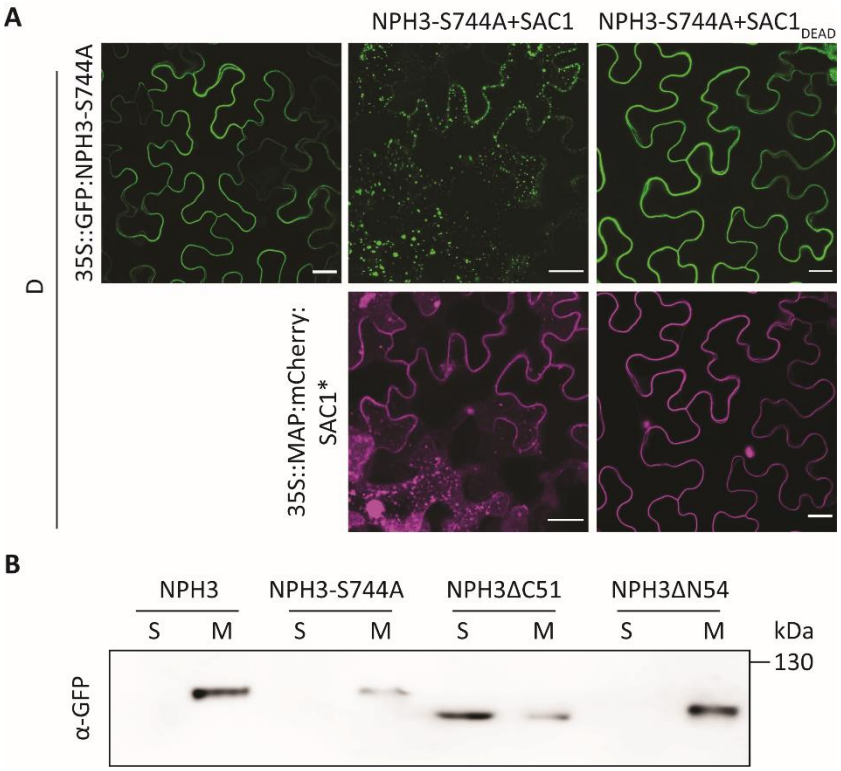

Figure 3. 12: Particle formation is independent of 14-3-3 interaction and deletion of the C-terminal region shifts NPH3 to membraneless condensates. A Representative confocal images of epidermal cells from *N. benthamiana* leaves co-expressing 35S::GFP:NPH3-S744A with 35S::MAP:mCherry:SAC1 or 35S::MAP:mCherry:SAC1$_{DEAD}$. Plants were dark adapted. Maximum projection of a z-stack is shown for NPH3-S744A+SAC1. Single expression of 35S::GFP:NPH3-S744A is shown as a control. Scale bar 25 µm. **B** anti-GFP immunoblot after subcellular fractionation of dark adapted *N. benthamiana* leaf samples transiently expressing 35S::GFP:NPH3 variants. 7.5 µg protein of each fraction were separated on a 7.5 % SDS-PAGE gel. It is noteworthy that the total amount of soluble proteins (S) is ~15 times higher as compared to the total amount of microsomal proteins (M) obtained after 100,000 × g centrifugation. Experiments were repeated at least three times.

A process that could be responsible for the formation of biomolecular, membraneless condensates is liquid liquid phase separation (LLPS) (Cuevas-Velazquez and Dinneny, 2018; Jaillais and Ott, 2020). LLPS is a process where two liquids unmix into two separate phases as soon as at least one of the liquids reaches a certain critical concentration threshold (Alberti, 2017; Banani *et al.*, 2017). The process of LLPS can be positively influenced by different parameters like temperature or post-translational modifications (Alberti, 2017). These membraneless droplets can for example function as compartments in the cell and favor interactions between proteins or other macromolecules that are present in a high concentration (Alberti, 2017; Cuevas-Velazquez and Dinneny, 2018). Other characteristics of these biomolecular condensates are that they are like spheres with a fluid content, furthermore can fuse upon contact and rearrange their contents within seconds (Cuevas-Velazquez and Dinneny, 2018; Jaillais and Ott, 2020). An example for LLPS in plants are processing bodies (P-bodies) known to store or degrade RNA (Alberti, 2017). Also, proteins such as the

phosphoprotein of a rhabdovirus are able to perform LLPS in the host plant (Fang *et al.*, 2022), which allows for replication of the rhabdovirus. Proteins that undergo LLPS often contain intrinsically disordered regions (IDRs) and modular interaction domains (Alberti, 2017; Banani *et al.*, 2017; Cuevas-Velazquez and Dinneny, 2018). IDRs are probably involved in LLPS because they display a high degree of conformational flexibility (Cuevas-Velazquez and Dinneny, 2018) and indeed NPH3 contains IDRs (Reuter *et al.*, 2021).

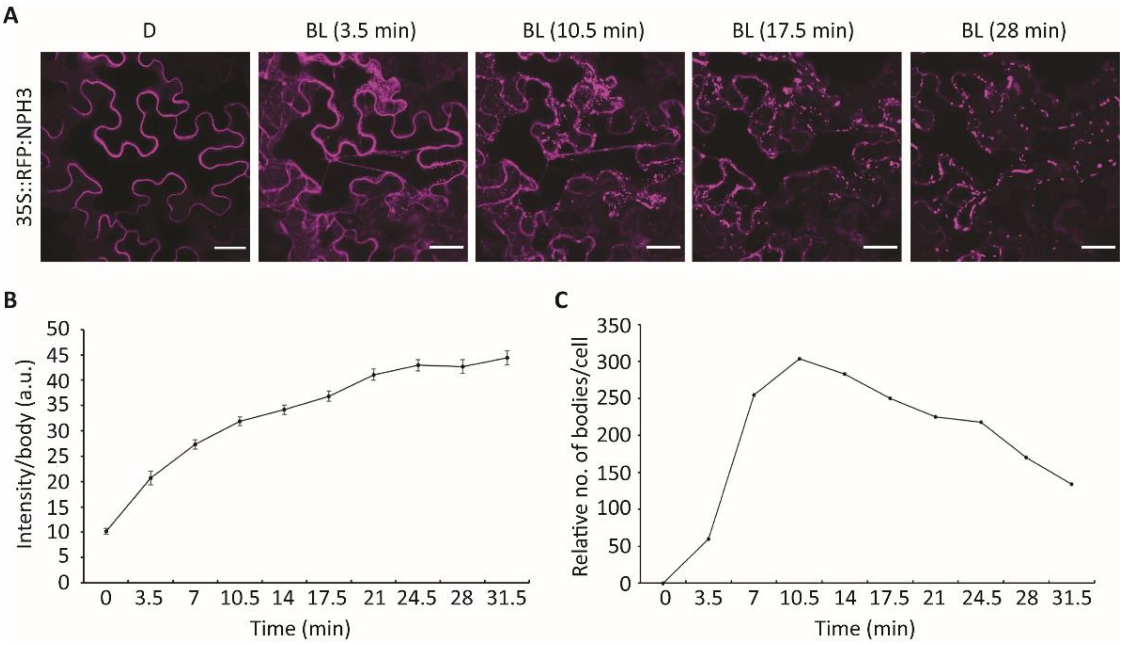

Figure 3. 13: NPH3 shows characteristics of biomolecular condensates upon blue light irradiation. A Single-cell time-lapse imaging of 35S::RFP:NPH3 transiently expressed in *N. benthamiana* leaf epidermal cells. Plants were dark adapted (D) and condensate formation was induced by using the GFP-Laser at 20 % (BL). Maximum projection of a z-stack is shown for all time points, selected time points are shown. Scale bar 25 µm. **B** fluorescence intensity per body over time (mean ± SEM) from A. **C** Relative number of bodies per cell over time from A. One representative of five replicates is shown.

A method to examine whether the protein of interest shows characteristics of LLPS is single-cell time-lapse imaging (Zavaliev *et al.*, 2020). Here a single leaf epidermal cell from *N. benthamiana* transiently expressing 35S::RFP:NPH3 was monitored, first in darkness and then upon GFP laser treatment (20 %). In darkness, a z-stack was taken scanning 30 consecutive planes along the Z axis covering the entire thickness of an epidermal cell, followed by GFP-laser treatment that initiated condensate formation and consecutive z-stacks were taken over a time period of ~ 32 min.

In darkness, NPH3 is associated to the PM as expected (Fig 3.13A) and after inducing PM detachment via irradiation with the GFP-laser, the protein first becomes soluble and localizes to cytoplasmic strands (Fig 3.13A: 3.5min). Over time, condensates are forming, the size of which increases with prolonged irradiation (Fig 3.13A). Condensate formation was also quantified using an image analysis protocol implemented in ImageJ (Zavaliev and Epel, 2015). As expected, the intensity per condensate increases over time (Fig 3.13B). The relative number of bodies, however, increases within the first 10-15 min of BL treatment and decreases afterwards (Fig 3.13C). This seems to be due to fusion of smaller condensates. It is worth mentioning that these features are characteristics of biomolecular, membraneless condensates that undergo LLPS.

3.5 The N-terminal BTB domain and an additional region upstream the CC domain are required for condensate formation of NPH3 after blue light irradiation

To investigate which domains or regions are involved in the formation of condensates upon blue light irradiation, we had a closer look at the domain structure of NPH3. NPH3 contains two domains that are known to be involved in protein-protein interaction, namely a N-terminal BTB domain and a C-terminal CC domain (Fig 3.14A) (Motchoulski and Liscum, 1999). BTB/POZ domains are characterized by a minimum of five conserved α-helices and three β-sheets and proteins containing a BTB/POZ domain can mediate aggregate formation *in vivo* (Albagli *et al.*, 1995; Stogios *et al.*, 2005). It is already known that the BTB domain of NPH3 can bind to the BTB domain of another NRL protein (RPT2) in yeast (Inada *et al.*, 2004) as well as to a CUL3a ubiquitin ligase (Roberts *et al.*, 2011).

To analyze involvement of the BTB domain in formation of condensates upon BL irradiation, the subcellular localization of NPH3 lacking the BTB domain (NPH3ΔN155, Fig 3.14A) was compared to NPH3 and NPH3ΔN54. Transient expression of RFP-tagged variants in *N. benthamiana* was driven by a 35S promoter. The plants were dark adapted and treated with 20 % GFP laser for ~ 11 min. In addition, GFP:NPH3ΔN155 was expressed under the endogenous promoter of NPH3.

Similar to the WT and NPH3ΔN54, the NPH3ΔN155 localizes to the PM in darkness but seems to detach from PM extremely rapid upon BL irradiation (Fig 3.14B). In contrast to WT and NPH3ΔN54, NPH3ΔN155 remains cytoplasmic after dissociation and is thus unable to form condensates (Fig 3.14B), indicating that the BTB domain is required for condensate formation.

A time-lapse movie was taken which shows that dissociation from the PM occurs immediately following BL treatment (20 % GFP laser) (Supplementary Movie 5).

However, GFP-tagged NPH3ΔN155 expressed under the endogenous promoter localizes to the cytosol already in “darkness” (Fig 3.14C). This is due to the fact that NPH3ΔN155 under the endogenous promoter is tagged with GFP. Since the GFP laser activates the signaling cascade leading to PM detachment of NPH3, we cannot monitor the “Dark” state of this NPH3 variant properly. Nevertheless, NPH3ΔN155 under the endogenous promoter is not able to form condensates upon BL treatment and remains cytoplasmic, supporting that the BTB domain is required for condensate formation.

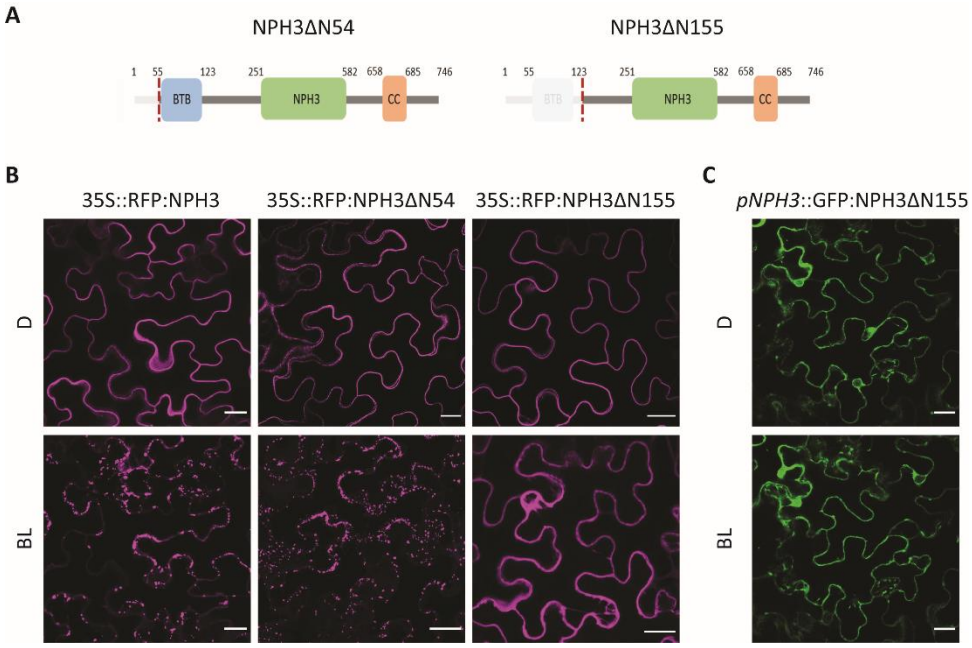

Figure 3. 14: Deletion of the N-terminal region of NPH3 prevents formation of condensates in the cytosol upon blue light irradiation. A Schematic illustration of N-terminally deleted versions of NPH3 **B** Representative confocal images of epidermal cells from *N. benthamiana* leaves expressing 35S::RFP:NPH3 variants. 35S::RFP:NPH3ΔN155 was co-infiltrated with p19. Plants were dark adapted (D) and treated with 20 % GFP-Laser for ~11 min (BL). Maximum projection of a z-stack is shown for 35S::RFP:NPH3 (D, BL), 35S::RFP:NPH3ΔN54 (BL) and 35S::RFP:NPH3ΔN155 (BL). Scale bar 25 µm. **C** Representative confocal images of epidermal cells from *N. benthamiana* leaves expressing *pNPH3*::GFP:NPH3ΔN155. Plants were dark adapted (D) and treated with 20 % GFP-Laser for ~11min (BL). Scale bar 25 µm. Experiments were repeated at least three times.

Besides the BTB domain NPH3 contains a C-terminal CC domain (Motchoulski and Liscum, 1999) which, in addition to the BTB domain, is known to promote protein-protein interaction (Lupas, 1996). Indeed, the C-terminal region of NPH3 including the CC domain was shown to interact with the N-terminal region of phot1 in a Y2H assay (Motchoulski and Liscum, 1999). Besides the CC domain the C-terminal region of NPH3 comprises up to two IDRs (Reuter *et*

al., 2021). IDRs are known to play an important role in condensate formation (Banani *et al.*, 2017). We therefore examined several serial deletions of the C-terminal region of NPH3 for their capability to form condensates in darkness: (i) deletion of the CC domain (NPH3ΔC93), (ii) deletion of the C-terminal 121 amino acid residues (NPH3ΔC121), and (iii) deletion of the entire C-terminal region downstream of NPH3 domain (NPH3ΔC164) (Fig 3.15A). These NPH3 variants were N-terminally tagged with RFP and transiently overexpressed in *N. benthamiana* and the subcellular localization was compared to the one of the WT protein and NPH3ΔC51 (Fig 3.15B). The plants were dark adapted and furthermore BL treated (20 % GFP laser for ~11 min).

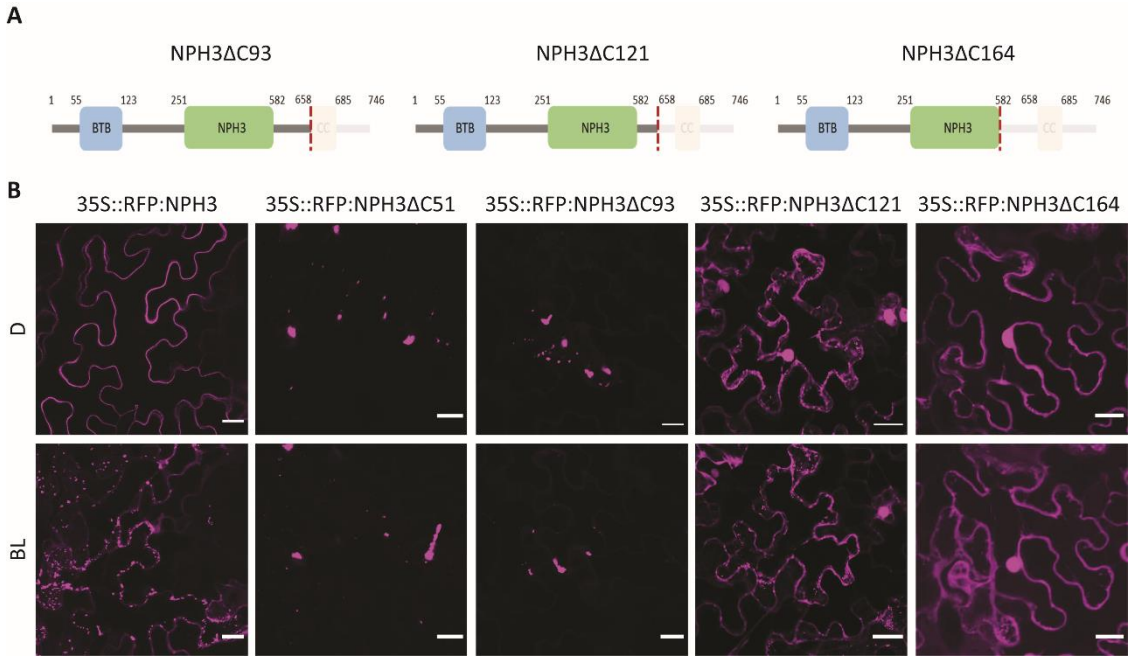

Figure 3. 15: In addition to the BTB domain a region downstream the NPH3 domain is involved in condensate formation. A Schematic illustration of C-terminally deleted versions of NPH3 **B** Representative confocal images of epidermal cells from *N. benthamiana* leaves expressing 35S::RFP:NPH3 variants. 35S::RFP:NPH3ΔC93 was co-infiltrated with p19. Plants were dark adapted (D) and treated with 20 % GFP-Laser for ~11 min (BL). Maximum projection of a z-stack shown except for 35S::RFP:NPH3 (D). Scale bar 25 µm. Experiments were repeated at least three times.

Deletion of the C-terminal 51 amino acid residues (NPH3ΔC51) results in permanent particle formation (Fig 3.8B, 3.15B), NPH3ΔC93 as well localizes to discrete bodies under dark and BL conditions (Fig 3.15B). Deletion of the CC domain does therefore not modify the capability of NPH3 to form condensates, indicating that the CC domain is not required for this process. Deletion of the C-terminal 121 amino acid residues, however, impacts condensate formation, as shown in partial localization to the cytosol and the nucleus (Fig 3.15B). Yet, we do not observe exclusively cytoplasmic localization. NPH3ΔC164 eventually shows permanent

localization to the cytosol and nucleus (Fig 3.15B), indicating that a region between the CC domain and the central NPH3 domain is required for formation of condensates.

A structure prediction of NPH3 was performed with AlphaFold (Jumper *et al.*, 2021; Varadi *et al.*, 2022). This is an artificial intelligence (AI) that provides a protein structure prediction database developed by DeepMind. AlphaFold is capable of predicting protein structures with an accuracy comparable to experiments (Jumper *et al.*, 2021; Varadi *et al.*, 2022). In Fig 3.16A the predicted structure of NPH3 is presented, residues that are colored in dark blue have a very high model confidence (named pLDDT), residues that are colored in light blue have a confident pLDDT, residues colored in yellow have a low pLDDT and residues in orange have a very low pLDDT. This means regions in blue are expected to be modelled highly accurate (dark blue) or respectively well (light blue), while regions in yellow and orange should be treated with caution (yellow) or not be interpreted (orange) (https://alphafold.ebi.ac.uk/entry/Q9FMF5, last checked: 2022-08-08, 12:56). Further Fig 3.16B displays the C-terminal region of NPH3 with marks of the serial deletions from Fig 3.15. As only deletion of the 164 C-terminal amino acid residues abolished condensate formation but not deletion of the C-terminal 121 amino acids, the region between these two serial deletions is highlighted in Fig 3.16C. Here, one of two highly conserved regions among the NRL proteins (^{583}HAAQNERLPL^{592}) (Motchoulski and Liscum, 1999) as well as a linear interacting peptide (LIP), also called short linear motif (SLiM) (^{594}VVVQVLF^{600}) is present (Fig 3.16D). LIPs often locate within IDRs (van der Lee *et al.*, 2014) and only form their three-dimensional structure upon binding to another molecule.

To examine whether this conserved region or the LIP are involved in particle formation, three mutant variants of NPH3 were generated - exchanged amino acid residues highlighted in grey: (i) mutation of the conserved region II by exchanging the highly conserved amino acid residues QNE to alanine (^{583}HAAQNERLPL^{592}) (NPH3-CON), (ii) mutation of the LIP by exchanging three valines for alanine (^{594}VVVQVLF^{600}) (NPH3-LIP), (iii) mutation of two arginine within and between the conserved region II and the LIP (^{583}HAAQNERLPLRVVVQVLF^{600}) (NPH3-RR/A).

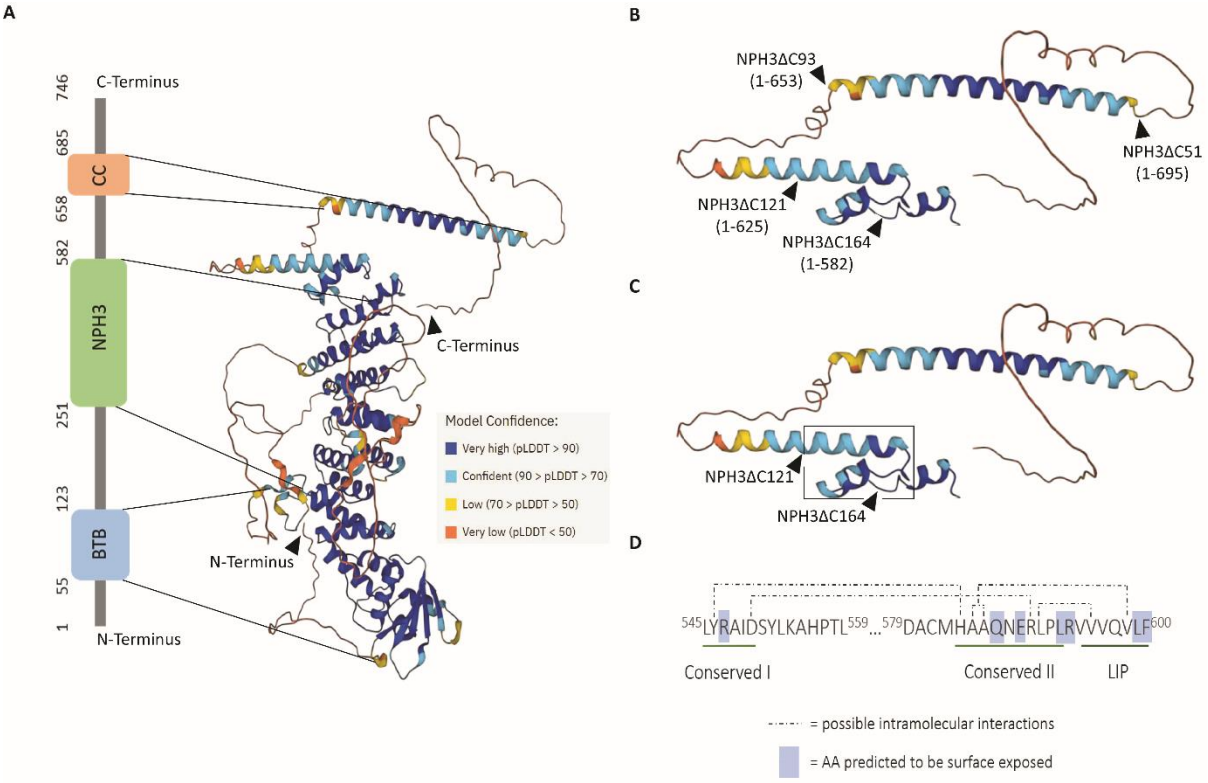

Figure 3. 16: Protein structure prediction of NPH3 by AlphaFold. A Predicted protein structure of NPH3 by AlphaFold (https://alphafold.ebi.ac.uk/entry/Q9FMF5, last checked: 2022-08-08, 12:56). Schematic illustration of NPH3 on the left. Respective domains connected between the schematic illustration and the predicted protein structure of AlphaFold. **B** Predicted protein structure of the C-terminal region of NPH3 by AlphaFold (https://alphafold.ebi.ac.uk/entry/Q9FMF5, last checked: 2022-08-08, 12:56). Serial C-terminal deletions from Fig 3.15 marked with arrowheads. **C** Predicted protein structure of the C-terminal region of NPH3 by AlphaFold (https://alphafold.ebi.ac.uk/entry/Q9FMF5, last checked: 2022-08-08, 12:56). Region possibly contributing to condensate formation highlighted. **D** Amino acid sequence of the conserved region I and II and the LIP.

All these mutations aim to disrupt inter- or intramolecular interactions. Q586, E588 and R593 for example might be surface exposed and with that could contribute to intermolecular interactions (Fig 3.16D, Suppl. Fig 1F,H+J). Furthermore, exchange of N587, R589, V595, V596 and V598 to alanine could disrupt intramolecular interactions (Fig 3.16D, Suppl. Fig 1G,I,K-M). All constructs were RFP-tagged and transiently overexpressed in *N. benthamiana*. Plants were dark adapted and treated with 20 % GFP laser for ~ 11 min. All three NPH3 variants show a similar localization, in darkness they are associated to the PM and upon BL irradiation they detach from the PM and localize exclusively to the cytosol (Fig 3.17A). These results suggest that at least two or all three of the identified regions might contribute to condensate formation. To test this, higher order mutant variants were generated. First, mutation of the conserved region II (NPH3-CON) was combined with the deletion of the C-terminal 51 amino acid residues (NPH3ΔC51-CON). This mutant as expected is not able to

associate to the PM anymore due to deletion of the C-terminal 51 amino acid residues (Fig 3.17B). However, NPH3ΔC51-CON is still able to generate condensates, although they are smaller compared to NPH3ΔC51 condensates (Fig 3.17B). Hence, mutation of the conserved region II is not sufficient to abolish formation of condensates.

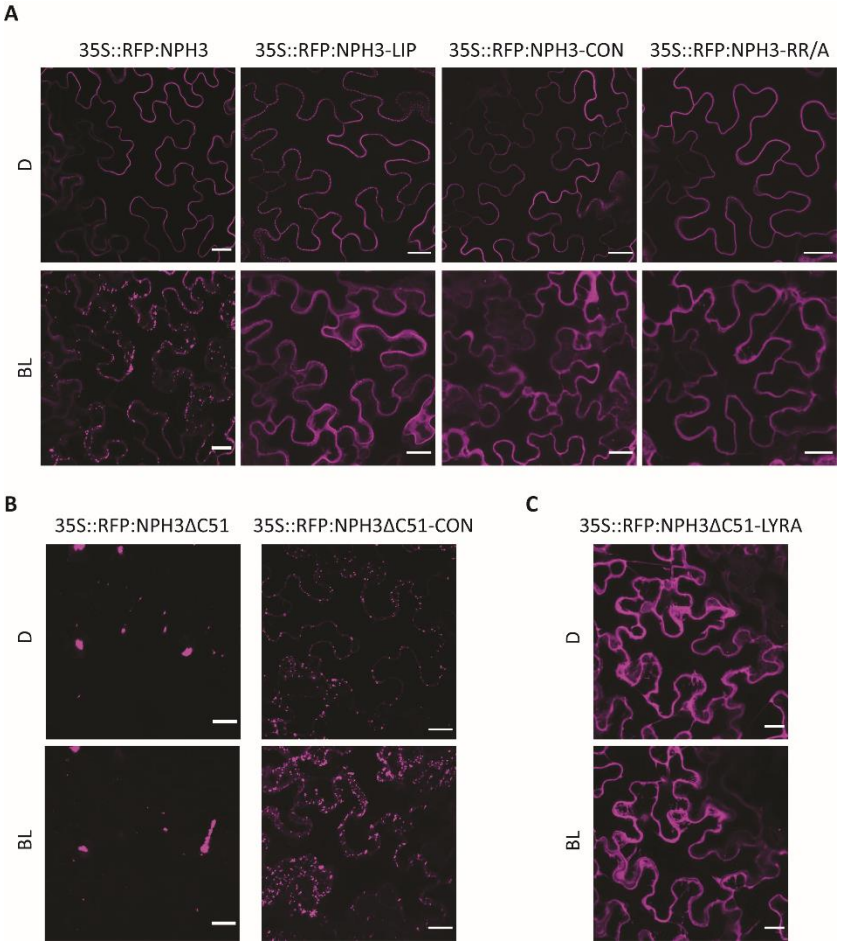

Figure 3. 17: Conserved motifs in the C-terminal region might be involved in condensate formation. A Representative confocal images of epidermal cells from *N. benthamiana* leaves expressing 35S::RFP:NPH3 variants. All constructs except of 35S::RFP:NPH3 were co-infiltrated with p19. Plants were dark adapted (D) and treated with 20 % GFP-Laser for ~11 min (BL). Maximum projections of a z-stack are shown for BL. Scale bar 25 µm. **B** Representative confocal images of epidermal cells from *N. benthamiana* leaves expressing 35S::RFP:NPH3ΔC51 (images already shown in Fig 3.15B) or 35S::RFP:NPH3ΔC51-CON. 35S::RFP:NPH3ΔC51-CON was co-infiltrated with p19. Plants were dark adapted (D) and treated with 20 % GFP-Laser for ~11min (BL). Maximum projection of a z-stack shown except for 35S::RFP:NPH3ΔC51-CON (D). Scale bar 25 µm. **C** Representative confocal images of epidermal cells from *N. benthamiana* leaves expressing 35S::RFP:NPH3ΔC51-LYRA. Construct was co-infiltrated with p19. Plants were dark adapted (D) and treated with 20 % GFP-Laser for ~11min (BL). Maximum projection of a z-stack is shown. Scale bar 25 µm. Experiments were repeated at least three times, except for C which was repeated two times.

In addition to the conserved region II, a conserved region I is located upstream in the NPH3 domain (^{545}LYRAID^{550}) (Motchoulski and Liscum, 1999) (Fig 3.16D). These two conserved regions were identified together in 1999. In order to examine whether this conserved region I might also be involved in condensate formation, the tyrosine and arginine were exchanged to alanine (^{545}LYRAID^{550}). Y546 could contribute to intramolecular interactions, while R547 might be surface exposed and could be involved in intermolecular interactions (Fig 3.16D, Suppl. Fig 1D+E). These mutations were introduced in NPH3ΔC51 (NPH3ΔC51-LYRA) to study the subcellular localization in a mutant incapable of PM association. Subcellular localization revealed that this variant permanently localizes in the cytosol (Fig 3.17C). However, it should be noted here that this experiment was only performed twice and investigation of the GFP-tagged NPH3 variant by Prabha Manishankar showed localization to particle-like structures.

These data suggest that none of the conserved regions described here when mutated alone or mutated in combination with NPH3ΔC51 is sufficient to abolish generation of condensates. Moreover, these results also indicate that at least two or more of these conserved regions jointly contribute to condensate formation. Therefore, higher order mutant variants should be analyzed in future.

All in all, the BTB domain in the N-terminal region of NPH3 is required but not sufficient for condensate formation. In addition, a region or several motifs located between the NPH3 domain and the CC domain are involved in generation of condensates in the cytosol. With respect to the latter, additional experiments with multiple mutations have to be performed to identify essential motifs.

3.6 NPH3 shows alternating modifications of its phosphorylation status under differing light conditions

Several studies in the past have described that NPH3 is phosphorylated in darkness when associated to the PM. Notably, phosphorylation of NPH3 in darkness turned out to be phot1-independent. Upon BL irradiation and in a phot1-dependent manner, NPH3 becomes dephosphorylated resulting in a slightly increased electrophoretic mobility during SDS-PAGE (Pedmale and Liscum, 2007; Haga *et al.*, 2015; Sullivan *et al.*, 2019). This BL-dependent modification of its electrophoretic mobility will be referred to as “general” (de)phosphorylation of NPH3 in the following chapters.

IP-MS performed by Tanja Schmidt revealed that NPH3 and 14-3-3 proteins interact in a strictly BL-dependent manner (Reuter *et al.*, 2021; Schmidt, 2022). It is very well-known that 14-3-3 proteins mostly interact with their target proteins in a phosphorylation dependent manner (Mackintosh, 2004) suggesting phosphorylation of the 14-3-3 binding site (S744) in NPH3 upon BL irradiation. Phosphorylation of this 14-3-3 binding site would be in contrast to the BL-induced “general” dephosphorylation of NPH3.

To test this, a phosphosite-specific peptide antibody was generated that was assumed to specifically recognize the phosphorylated serine at position 744 (α-pS744) and, in addition, an antibody against the unmodified peptide served as control (α-NPH3). The specificity of α-pS744 was examined by comparing GFP:NPH3 and GFP:NPH3-S744A – the mutant incapable of 14-3-3 interaction - in regard of their phosphorylation status (Fig 3.18A+B). The NPH3 variants were either transiently overexpressed in *N. benthamiana* or ectopically expressed in transgenic *A. thaliana nph3-7* lines (see chapter 3.1). The plants were dark adapted (D) and treated with BL (Fig 3.18A+B) followed by GFP-IP. Indeed, NPH3 shows an increased electrophoretic mobility upon BL irradiation, indicating the “general” dephosphorylation. Whereas the electrophoretic mobility of NPH3-S744A is not altered under differing light conditions (Fig 3.18A+B), hence does not become “generally” dephosphorylated upon BL. Furthermore, the phosphosite-specific peptide antibody specifically recognizes NPH3 upon BL irradiation but not NPH3-S744A (Fig 3.18A+B) confirming the specificity of the antibody. Taken together the phosphorylation and dephosphorylation events of NPH3 are highly complex. BL triggers two posttranslational modifications: (i) the phosphorylation of the 14-3-3 binding site (S744) and (ii) a “general” dephosphorylation (Fig 3.18).

To confirm the CoIP data obtained by Tanja Schmidt, the IP of NPH3 and NPH3-S744A was combined with a far western analysis. Here, binding of purified recombinant 14-3-3 proteins to IP samples separated by SDS-PAGE and transferred to nitrocellulose membrane shows that 14-3-3 proteins are exclusively able to bind to the BL treated WT protein but not to NPH3-S744A (Fig 3.18A+B) (Reuter *et al.*, 2021; Schmidt, 2022). Altogether, phosphorylation of S744 mediates 14-3-3 association and seems to be required for the BL-induced “general” dephosphorylation of NPH3.

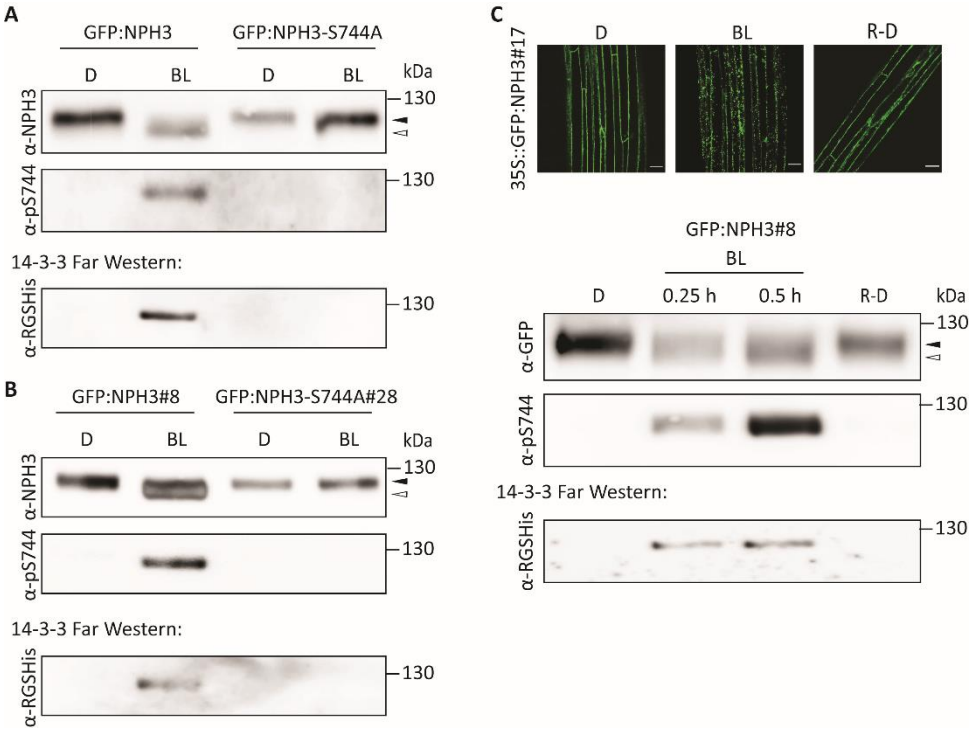

Figure 3. 18: For NPH3 two alternating phosphorylation events are occurring under differing light conditions. A Immunoblot analysis and 14-3-3 far western of immunoprecipitated proteins (IP α-GFP) from transiently transformed *N. benthamiana* expressing 35S::GFP:NPH3 variants separated on a 7.5 % SDS-PAGE gel. Plants were dark adapted (D) and irradiated with blue light (10 µmol/m^2/s) for 40 min (BL). **B** Immunoblot analysis and 14-3-3 far western of immunoprecipitated proteins (IP α-GFP) from etiolated *A. thaliana nph3-7* seedlings expressing 35S::GFP:NPH3 variants (3 days old) separated on a 7.5 % SDS-PAGE gel. Seedlings were kept in darkness (D) or irradiated with blue light (1 µmol/m^2/s) for 1 h (BL). **C** Upper panel: Representative confocal images of hypocotyl cells from etiolated *A. thaliana nph3-7* seedlings (3 days old) expressing 35S::GFP:NPH3. Seedlings were kept in darkness (D), treated with 20 % GFP-Laser for ~6 min (BL) or transferred back to darkness after 30 min of blue light irradiation (R-D), R-D already shown in Fig 3.4. Scale bar 25 µm. Lower panel: Immunoblot analysis and 14-3-3 far western of immunoprecipitated proteins (IP α-GFP) from etiolated *A. thaliana nph3-7* seedlings expressing 35S::GFP:NPH3 (3 days old) separated on a 7.5 % SDS-PAGE gel. Seedlings were kept in darkness (D), irradiated with blue light (1 µmol/m^2/s) for indicated time points or transferred back to darkness for 1 h after 30 min blue light irradiation (R-D). Experiments were repeated at least three times. Black arrowheads indicate the phosphorylated state of NPH3 whereas white arrowheads indicate the dephosphorylated state of NPH3.

Representative confocal images of NPH3 display the cycling of the protein between the PM and the cytosolic condensates under differing light treatments (see chapter 3.1) (Fig 3.18C). NPH3 is attached to the PM in darkness, forms cytosolic condensates upon BL irradiation and reassociates to the PM when retransferred to darkness (Fig 3.18C). An GFP-IP was performed with transgenic lines expressing 35S::GFP:NPH3 in the *nph3-7* background. The etiolated seedlings were either dark treated (D), irradiated with BL from above for the indicated time points (BL) (Fig 3.18C) or retransferred to darkness after 30 min of BL treatment (R-D). Immunological detection of NPH3 indicates a phosphorylated state in darkness visible by a decreased electrophoretic mobility (Fig 3.18C), while upon BL irradiation NPH3 displays a higher electrophoretic mobility (Fig 3.18C). This “general” dephosphorylation of NPH3 is clearly reversible since the protein shifts upwards as consequence of retransfer to darkness (R-D). This confirms the findings of Pedmale and Liscum in 2007 who demonstrated that transfer to darkness after BL treatment causes a “general” rephosphorylation of NPH3 (Pedmale and Liscum, 2007). Furthermore, phosphorylation of S744 takes place exclusively upon BL but is neither detectable in darkness nor R-D (Fig 3.18C). Far western analysis further confirms that phosphorylation of S744 determines 14-3-3 association with NPH3 (Fig 3.18C). All in all, the two posttranslational modifications of NPH3 triggered by BL are reversible after retransfer to darkness, meaning after R-D NPH3 is “generally” rephosphorylated and S744 becomes dephosphorylated.

A time course experiment was performed by irradiating etiolated seedlings (35S::GFP:NPH3 in *nph3-7*) with BL for different time points. Phosphorylation of S744 is already detectable after 0.5 min of BL irradiation, whereas the electrophoretic shift indicative of a “general” dephosphorylation becomes visible after 6 min and is completed after 30 min (Fig 3.19A). Thus, phosphorylation of S744 precedes the “general” dephosphorylation of NPH3 upon BL treatment. Again, these processes of posttranslational modifications are reversible upon retransfer of seedlings to darkness (Fig 3.19A). Far western analysis performed after GFP-IP indicates that 14-3-3 binding correlates positively with phosphorylation of S744 and is detectable after 0.5 min (Fig 3.19B).

In addition, we examined whether these reversible changes in the electrophoretic mobility of NPH3 occur in *A. thaliana* wild-type Col-0 seedlings. Indeed, the dephosphorylation of NPH3 is also visible here after 4 min of BL irradiation and the dephosphorylation is already complete after 15 min (Fig 3.19C). Unfortunately, the sensitivity of the phosphosite-specific peptide antibody was not high enough to detect phosphorylation of S744 in these samples.

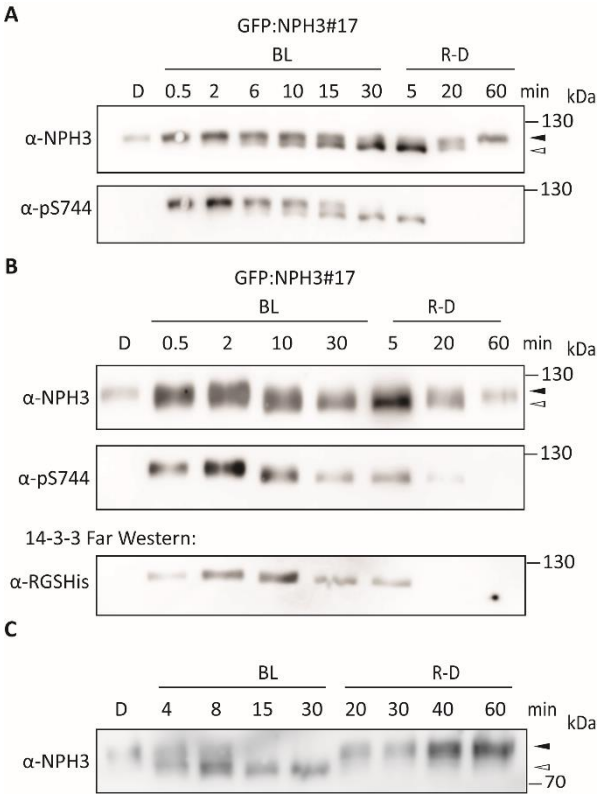

Figure 3. 19: The phosphorylation of S744 precedes the "general" dephosphorylation of NPH3 upon blue light irradiation. A Immunoblot analysis of crude extracts from etiolated *A. thaliana nph3-7* seedlings expressing 35S::GFP:NPH3 (3 days old) separated on a 7.5 % SDS-PAGE gel. Seedlings were kept in darkness (D), irradiated with blue light (1 µmol/m^2/s) for the indicated time or transferred back to darkness after 30 min blue light irradiation. **B** Immunoblot analysis and 14-3-3 far western of immunoprecipitated proteins (IP α-GFP) from etiolated *A. thaliana nph3-7* seedlings expressing 35S::GFP:NPH3 (3 days old) separated on a 7.5 % SDS-PAGE gel. Seedlings were kept in darkness (D), irradiated with blue light (1 µmol/m^2/s) for the indicated time or transferred back to darkness after 30 min blue light irradiation. **C** Immunoblot analysis of crude extracts from etiolated *A. thaliana* Col-0 seedlings (3 days old) separated on a 7.5 % SDS-PAGE gel. Seedlings were kept in darkness (D), irradiated with blue light (1 µmol/m^2/s) for the indicated time or transferred back to darkness after 30 min blue light irradiation. Experiments were repeated at least three times. Black arrowheads indicate the phosphorylated state of NPH3 whereas white arrowheads indicate the dephosphorylated state of NPH3.

Taken together, BL triggers two posttranslational modifications in NPH3: a BL induced phosphorylation of S744 followed by a "general" dephosphorylation of NPH3, the latter detectable via an electrophoretic mobility shift in an SDS-PAGE. These two posttranslational modifications are reversible when irradiated seedlings are retransferred to darkness. "General" dephosphorylation of NPH3 is, however, abolished in NPH3-S744A that is incapable of 14-3-3 interaction and PM dissociation.

3.7 Subcellular localization and phosphorylation status of NPH3 variants in transgenic Arabidopsis lines

Haga et al. proposed in 2015 that the “generally” dephosphorylated NPH3 being present in cytosolic particles represents the inactive form of NPH3 (Haga *et al.*, 2015). In line with this, Sullivan et al. considered the “generally” phosphorylated, PM-localized version of NPH3 to promote hypocotyl bending (Sullivan *et al.*, 2019). However, the results obtained by Tanja Schmidt and Jutta Keicher indicate NPH3-S744A to exhibit a significantly reduced capability for hypocotyl bending (Reuter *et al.*, 2021; Schmidt, 2022). This mutant, however, permanently localizes to the PM and exists in a constitutively “generally” phosphorylated state, indicating PM localization and “general” phosphorylation of NPH3 to be insufficient to trigger the phototropic response.

To address functional significance of both the subcellular localization and the phosphorylation status of NPH3, transgenic *nph3-7* lines ectopically expressing different variants of NPH3 N-terminally fused to GFP were generated by Tanja Schmidt and Jutta Keicher. Here, either (i) the permanently condensate forming version NPH3-4K/A (see Fig 3.9B), (ii) the permanently PM localizing version NPH3ΔC28 (see Fig 3.9B) or (iii) NPH3ΔN54, that - comparable to NPH3 - detaches from the PM upon BL irradiation followed by condensate formation (see Fig 3.8B) were used.

First, the subcellular localization of all these versions was analyzed and the WT protein served as control. Etiolated seedlings were kept in darkness, treated with 20 % GFP laser for ~ 6 min or transferred back to darkness after 30 min of BL irradiation (1µmol/m^2/s). NPH3-4K/A displays the subcellular localization already observed in transiently transformed *N. benthamiana* leaves (Fig 3.9B). It permanently localizes to condensates both under dark and light conditions (Fig 3.20A). In addition, NPH3ΔC28 localizes permanently to the PM (Fig 3.20A) reflecting the results obtained in transiently transformed *N. benthamiana* leaves (Fig 3.9B). The same holds true for GFP:NPH3ΔN54 (Fig 3.8B) which localizes to the PM in darkness, but forms condensates in the cytosol upon BL treatment (Fig 3.20A). Furthermore, it is able to reassociate to the PM when retransferred to darkness (Fig 3.20A). Worth mentioning, in phototropic response assays performed by Tanja Schmidt and Jutta Keicher, exclusively NPH3ΔN54 could be shown to functionally restore the phototropic response while NPH3-4K/A and NPH3ΔC28 turned out to be incapable (Reuter *et al.*, 2021; Schmidt, 2022). In addition, Prabha Manishankar confirmed that transgenic *nph3-7* lines ectopically expressing GFP:NPH3ΔC51 are not restoring the phototropic response (Reuter *et al.*, 2021).

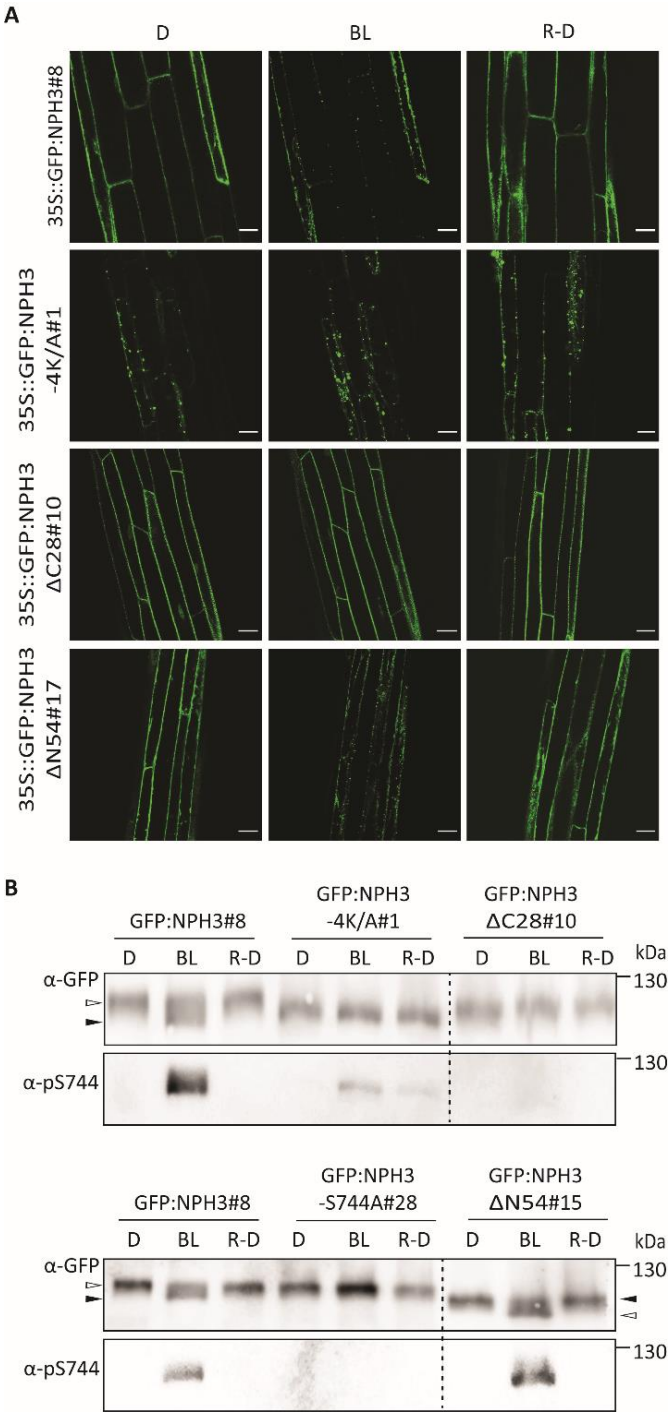

Figure 3. 20: Subcellular localization and phosphorylation status of NPH3 variants in transgenic lines. A Representative confocal images of hypocotyl cells from etiolated *A. thaliana nph3-7* seedlings (3 days old) expressing 35S::GFP:NPH3 variants. Seedlings were kept in darkness (D), treated with 20 % GFP laser for ~ 6 min or transferred back to darkness after 30 min of blue light irradiation (R-D). Scale bar 25 µm. Experiments were repeated at least three times. Experiment performed together with Tanja Schmidt. **B** Immunoblot analysis of crude extracts from etiolated *A. thaliana nph3-7* seedlings (3 days old) expressing 35S::GFP:NPH3 variants separated on a 7.5 % SDS-PAGE gel. Seedlings were kept in darkness (D), irradiated with blue light (1 µmol/m^2/s) for 30 min or transferred back to darkness after 30 min of blue light irradiation (R-D). Experiments were repeated at least three times. Black arrowheads indicate the phosphorylated state of NPH3 whereas white arrowheads indicate the dephosphorylated state of NPH3. Experiment performed together with Tanja Schmidt.

Secondly, the phosphorylation status of the different mutant versions of NPH3 in the transgenic lines was investigated. The WT protein served as control and BL-induced S744 phosphorylation and the “general” dephosphorylation as well as S744 dephosphorylation, and the coinciding “general” rephosphorylation after retransfer to darkness are observable (Fig 3.20B). Surprisingly, NPH3-4K/A exists in a constitutive “generally” dephosphorylated state and becomes slightly phosphorylated at S744 upon BL irradiation (Fig 3.20B). NPH3ΔC28, on the other hand, is characterized by a permanent “generally” phosphorylated state comparable to NPH3-S744A (Fig 3.20B). Both variants are not phosphorylated at S744 due to absence of the motif (Fig 3.20B). The phosphorylation status of NPH3ΔN54, reflects exactly NPH3 in that BL induces phosphorylation of S744 followed by “general” dephosphorylation, while retransfer to darkness reverses these posttranslational modifications (Fig 3.20B).

Taken together, neither NPH3 variants constitutively localizing to condensates or to the PM are functional. Cycling between the PM and the cytosolic condensates seems to be required for the function of NPH3. NPH3 is attached to the PM in darkness, upon BL irradiation the serine at position 744 becomes phosphorylated followed by 14-3-3 binding (Reuter *et al.*, 2021; Sullivan *et al.*, 2021). This results in localization to the cytosol subsequently leading to the formation of membraneless condensates. Transfer back to darkness after BL irradiation reverts the whole process resulting in reassociation of NPH3 to the PM. This cycling of NPH3 seems to be essential for the proper function of NPH3 mediating hypocotyl bending.

3.8 14-3-3 association is essential for the “general” dephosphorylation of NPH3 upon blue light irradiation

It has been assumed that the BL-induced “general” dephosphorylation of NPH3 is responsible for PM detachment (Haga *et al.*, 2015; Sullivan *et al.*, 2019; Legris and Boccaccini, 2020). In other words, “general” dephosphorylation might be a prerequisite for or a consequence of condensate formation. To investigate this in more detail, we again made use of the genetic tool SAC1 (see chapter 3.2) that alters the phospholipid composition of the PM by depleting Pi4P (Simon *et al.*, 2016). SAC1 was co-expressed with the permanently PM localizing and “general” phosphorylated 35S::GFP:NPH3-S744A, WT NPH3 served as control. The plants were dark adapted and as already displayed in chapters 3.2 and 3.4 both, NPH3 and NPH3-S744A already localize to condensates in darkness (Fig 3.7B and Fig 3.12A). The plants were in addition treated with BL (10 µmol/m^2/s) for 40 min, samples were collected and crude extracts were used for electrophoretic mobility/phosphoshift assays.

The WT protein when coexpressed with SAC1 shows the characteristic shift of “general” dephosphorylation only upon BL irradiation and also the phosphorylation of S744 only occurs after BL treatment (Fig 3.21A). Although NPH3 is already localizing to condensates in darkness when coexpressed with SAC1, NPH3 is “generally” phosphorylated and “general” dephosphorylation could exclusively be detected upon BL treatment (Fig 3.21A). Hence, these posttranslantional modifications are neither a prerequisite for nor a consequence of condensate formation but depend on BL irradiation. Remarkably, NPH3-S744A, the mutant incapable of 14-3-3 interaction, still displays a permanent “generally” phosphorylated status although localizing to condensates after co-expression with SAC1 (Fig 3.21A), suggesting that both BL-triggered S744 phosphorylation and 14-3-3 binding are required for “general” dephosphorylation of NPH3.

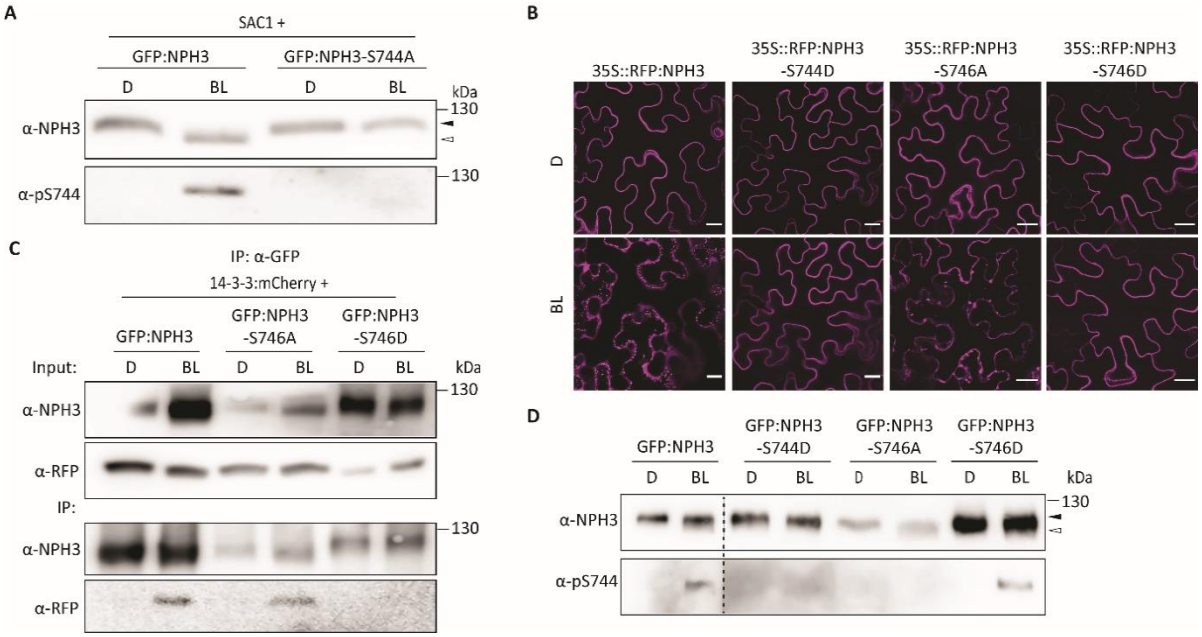

Figure 3. 21: 14-3-3 interaction with NPH3 is essential for “general” dephosphorylation upon blue light irradiation. A Immunoblot analysis of crude extracts from transiently transformed *N. benthamiana* leaves co-expressing 35S::GFP:NPH3 variants with 35S::MAP:mCherry:SAC1 separated on a 7.5 % SDS-PAGE gel. Plants were dark adapted (D) and irradiated with blue light (10 µmol/m^2/s) for 40 min (BL). **B** Representative confocal images of epidermal cells from *N. benthamiana* leaves expressing 35S::RFP:NPH3 variants. Plants were dark adapted (D) and treated with 20 % GFP-Laser for ~11 min (BL). Maximum projection of a z-stack is shown for 35S:RFP:NPH3 and 35S::RFP:NPH3-S744D (BL). Scale bar 25 µm. **C** *In vivo* interaction of 35S::GFP:NPH3 variants and 35S::RFP:14-3-3omega transiently expressed in *N.benthamiana* leaves. Plants were dark adapted (D) and irradiated with blue light (10 µmol/m^2/s) for 30 min (BL). Crude extract was immunoprecipitated by using GFP beads. Input and IP were separated on 7.5 % SDS-PAGE gels followed by α-RFP or α-GFP immunodetection. **D** Immunoblot analysis of crude extracts from transiently transformed *N. bethamiana* leaves expressing 35S::RFP:NPH3 variants separated on a 7.5 % SDS-PAGE gel. Plants were dark adapted (D) and irradiated with blue light (10 µmol/m^2/s) for 30 min (BL). GFP:NPH3 was incubated in the respective antibodies separately (dashed line). Experiments were repeated at least three times. Black arrowheads indicate the phosphorylated state of NPH3 whereas white arrowheads indicate the dephosphorylated state of NPH3.

A collaboration with the group of John Christie from the university of Glasgow revealed that exchange of the last serine residue to alanine or aspartate (S764A, S746D) prevents or reduces BL-induced relocalization of NPH3 (Sullivan *et al.*, 2021). Yet, an Y2H assay performed by Andrea Bock demonstrated NPH3-S746A to still be able to interact with 14-3-3, while NPH3-S746D – like NPH3-S744A – is not (Reuter *et al.*, 2021) (Andrea Bock, unpublished). Therefore, we investigated these two NPH3 mutant variants together with the phosphomimic version of the 14-3-3 binding site (NPH3-S744D) which is similar to NPH3-S744A incapable of association to 14-3-3 proteins (Reuter *et al.*, 2021).

To examine the subcellular localization of these NPH3 variants (N-terminally tagged with RFP), we performed transient overexpression in *N. benthamiana*. The plants were dark adapted and in addition treated with 20 % GFP laser for ~ 11 min. NPH3-S744D permanently localizes to the PM (Fig 3.21B) (Reuter *et al.*, 2021; Sullivan *et al.*, 2021). The subcellular localization of the mutant version NPH3-S746A – still able to interact with 14-3-3 in Y2H – reflects the localization of the WT protein in that it localizes to the PM in darkness and forms condensates upon BL treatment (Fig 3.21B). The subcellular localization for NPH3-S746A was already described before as a greatly reduced translocation upon BL in *N. benthamiana* but not in *A. thaliana* (Sullivan *et al.*, 2021). Comparable to NPH3-S744D, NPH3-S746D localizes permanently to the PM confirming previous published results from Sullivan et al. (Fig 3.21B) (Sullivan *et al.*, 2021).

Since the NPH3-S746 mutant variants displayed different subcellular localization upon BL treatment we were further interested to check whether they are still able to interact with 14-3-3 proteins upon BL. Therefore, N-terminally GFP tagged NPH3, NPH3-S746A or NPH3-S746D variants were transiently co-expressed in *N. benthamiana* with 14-3-3 proteins C-terminally tagged with mCherry. The plants were dark adapted and treated with BL (10 µmol/m^2/s) for 30 min followed by CoIP. As expected, NPH3-S746A is still capable of 14-3-3 binding upon BL irradiation whereas NPH3-S746D is not (Fig 3.21C). Sullivan et al. were also able to show that NPH3-S746A is able to bind 14-3-3 proteins in a far western analysis (Sullivan *et al.*, 2021). To support the results of the *in vivo* interaction between 14-3-3 proteins and the NPH3 variants, we also examined their respective phosphorylation status. NPH3-S746A is showing the characteristic shift upon BL irradiation indicative of “general” dephosphorylation (Fig 3.21D), however, phosphorylation of S744 is not detectable after BL treatment. This could be due to the low expression of NPH3-S746A, which we faced repeatedly, while Sullivan et al. were able to show that NPH3-S746A is still phosphorylated at S744 in BL (Sullivan *et al.*, 2021). Hence, NPH3-S746A displays the same subcellular localization, phosphorylation status and 14-3-3 interaction capability as the WT protein.

NPH3-S744D and NPH-S746D are permanently present in the “generally” phosphorylated state (Fig 3.21D). Most surprisingly NPH3-S746D is still phosphorylated at S744 in BL (Fig 3.21D). Hence, phosphorylation of S744 is not sufficient for PM detachment, since NPH3-S746D is permanently localizing to the PM. Taken together, this indicates that 14-3-3 association mediated by phosphorylation of S744 is essential for “general” dephosphorylation of NPH3. Furthermore, phosphorylation of S746 could interfere with 14-3-3 binding to NPH3 *in vivo*.

3.9 Condensate formation is not required for “general” dephosphorylation of NPH3

Examination of the transgenic Arabidopsis lines revealed a permanent “general” dephosphorylation of the condensate forming NPH3 variant NPH3-4K/A (Fig 3.20). To further investigate the role of condensates in the phosphorylation status of NPH3, the variant NPH3ΔN155 was examined in more detail. As already presented before, NPH3ΔN155 - when transiently overexpressed in *N. benthamiana* - is associated to the PM in darkness, detaches from the PM upon BL treatment, but is not able to form condensates (Fig 3.14B). Interestingly NPH3ΔN155 is able to reassociate to the PM when retransferred to darkness (Fig 3.22A). To monitor the retransfer to darkness in *N. benthamiana* the sample was first treated with 20 % GFP-laser for ~ 11 min followed by treatment with the RFP-laser only.

To monitor the phosphorylation status, the WT protein or NPH3ΔN155 N-terminally tagged with GFP were transiently overexpressed in *N. benthamiana*. The plants were dark adapted, treated with BL and retransferred to darkness after BL treatment followed by an IP. As expected, the WT protein shows the characteristic increased electrophoretic mobility described as “general” dephosphorylation upon BL treatment as well as a phosphorylation of S744 (Fig 3.22B). This whole process is reversible after retransfer to darkness (Fig 3.22B). NPH3ΔN155 is also showing a slight “general” dephosphorylation upon BL treatment accompanied by a phosphorylation of S744 and also here this process is reversible after retransfer to darkness (Fig 3.22B). For both proteins a far western analysis revealed that 14-3-3 proteins bind to the BL irradiated protein (Fig 3.22B). To confirm this finding, a CoIP was performed with transiently co-expressed GFP:NPH3 variants and 14-3-3:mCherry in *N. benthamiana*. Indeed, 14-3-3 proteins interact with the WT protein and NPH3ΔN155 exclusively upon BL irradiation (Fig 3.22C).

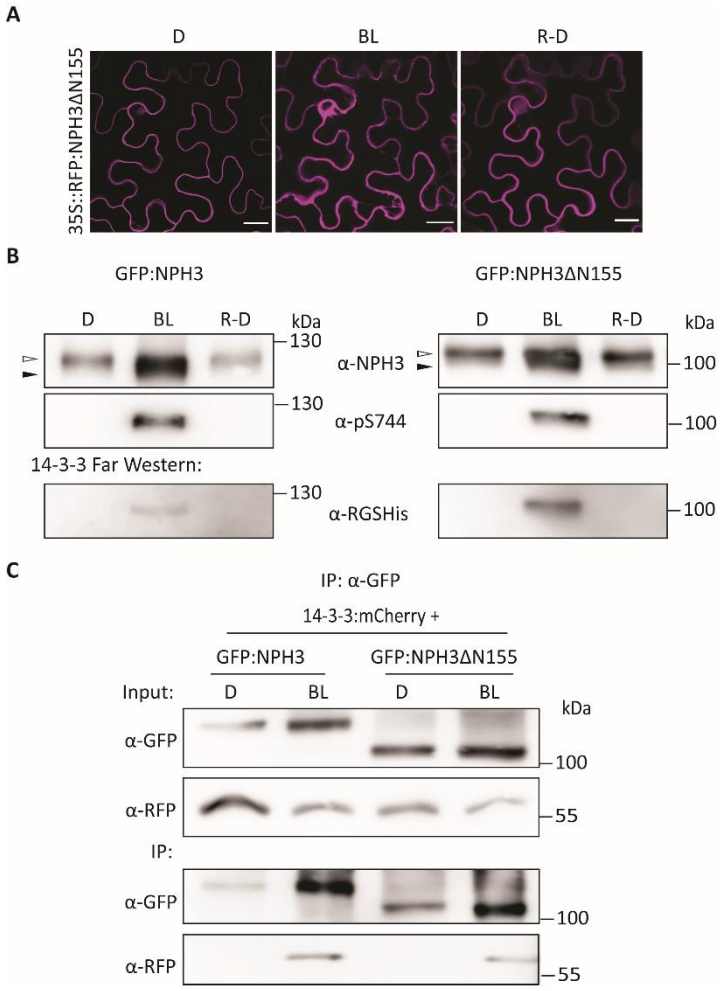

Figure 3. 22: Condensate formation is not required for "general" dephosphorylation of NPH3 upon blue light irradiation. A Representative confocal images of epidermal cells from *N. benthamiana* leaves expressing 35S::RFP:NPH3ΔN155. Construct was co-infiltrated with p19. Plants were dark adapted (D), treated with 20 % GFP-Laser for ~11 min (BL) and treated with RFP-Laser for ~11 min after GFP-Laser treatment (R-D). D and BL are already shown in figure 3.14. Maximum projection of a z-stack is shown for BL and R-D. Scale bar 25 µm. **B** Immunoblot analysis and 14-3-3 far western of immunoprecipitated proteins (IP α-GFP) from transiently transformed *N. benthamiana* leaves expressing 35S::GFP:NPH3 variants separated on a 7.5 % SDS-PAGE gel. Plants were dark adapted (D), irradiated with blue light (10 µmol/m^2/s) for 40 min (BL) or transferred back to darkness for 1 h after blue light irradiation (R-D). **C** *In vivo* interaction of 35S::GFP:NPH3 variants and 35S::RFP:14-3-3omega transiently expressed in *N.benthamiana* leaves. Plants were dark adapted (D) or irradiated with blue light (10 µmol/m^2/s) for 40 min (BL). Crude extract was immunoprecipitated by using GFP beads. Input and IP were separated on 7.5 % SDS-PAGE gels followed by α-RFP or α-GFP immunodetection. Experiments were repeated at least three times. Black arrowheads indicate the phosphorylated state of NPH3 whereas white arrowheads indicate the dephosphorylated state of NPH3.

Thus, the condensate formation is not required for the "general" dephosphorylation of NPH3 upon BL irradiation. In addition, the ability of NPH3ΔN155 to reassociate to the PM shows that the condensates are not essential for the process of reassociation. The biochemical function of the condensate formation still remains elusive.

3.10 “General” phosphorylation of NPH3 in darkness takes place at the plasma membrane

Another question arose in regard of the phosphorylation status of NPH3: where is the phot1-independent “general” phosphorylation of NPH3 in darkness taking place? In chapter 3.7 it became evident that NPH3-4K/A, a variant that is permanently localizing to condensates, is always present in the “generally” dephosphorylated state (Fig 3.20). Suggesting that cytosolic localization is sufficient for dephosphorylation. We, however, could show that “general” dephosphorylation is neither a prerequisite for nor a consequence of condensate formation (see chapter 3.8).

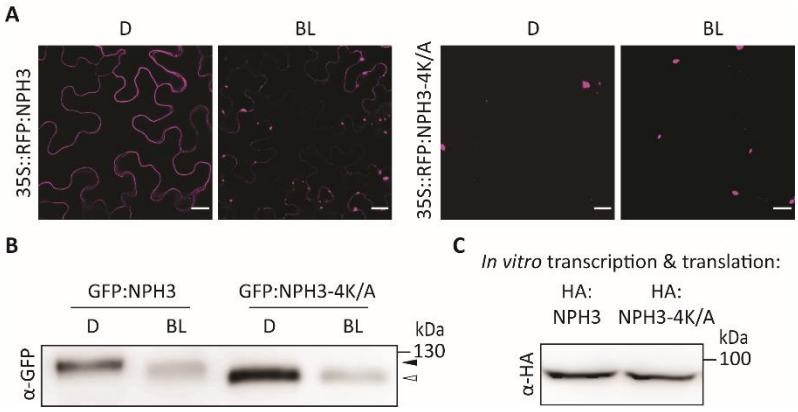

Figure 3. 23: The electrophoretic mobility of NPH3-4K/A is unmodified compared to NPH3. **A** Representative confocal images of epidermal cells from *N. benthamiana* leaves expressing 35S::RFP:NPH3 variants. Plants were dark adapted (D) and irradiated with blue light (10 µmol/m^2/s) for 40 min (BL). Scale bar 25 µm. **B** Immunoblot analysis of crude extracts from transiently transformed *N. benthamiana* expressing 35S::GFP:NPH3 variants separated on a 7.5 % SDS-PAGE gel. Plants were dark adapted (D) and irradiated with blue light (10 µmol/m^2/s) for 40 min (BL). **C** Immunoblot analysis of *in vitro* transcribed and translated HA:NPH3 and HA:NPH3-4K/A separated on a 7.5 % SDS-PAGE gel.

To confirm that NPH3-4K/A displays the “generally” dephosphorylated state of NPH3, GFP:NPH3-4K/A and GFP:NPH3 were transiently overexpressed in *N. benthamiana* (Fig 3.23A) followed by preparation of crude extract. Interestingly, NPH3-4K/A is again showing an increased electrophoretic mobility referred to as the “generally” dephosphorylated state of NPH3 (Fig 3.23B). To ensure that the exchange of four lysine’s to alanine in NPH3-4K/A is not causing a shift *per se*, we performed an *in vitro* transcription and translation and compared the molecular size of NPH3-4K/A and the WT protein. As Fig 3.23C illustrates, the electrophoretic mobility of NPH3-4K/A is unmodified.

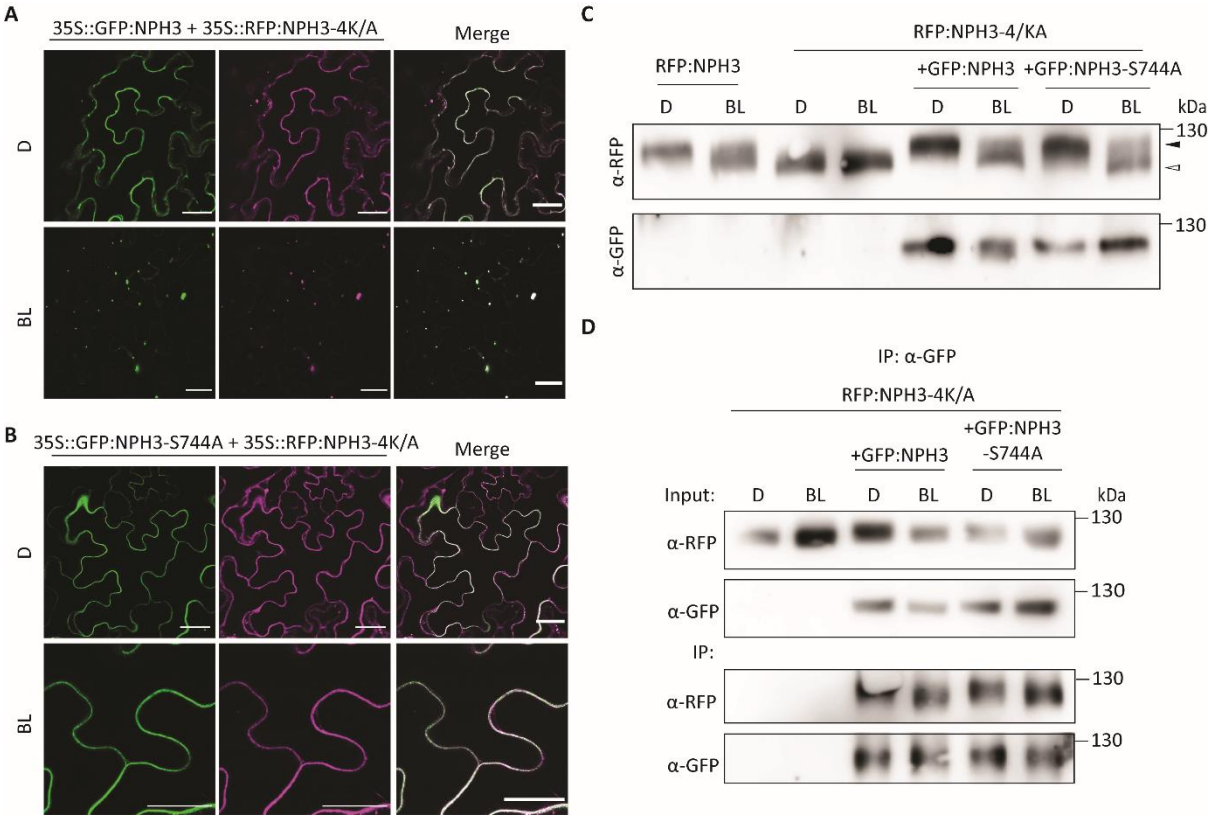

Figure 3. 24: "General" phosphorylation of NPH3 in darkness takes place at the plasma membrane. A Representative confocal images of epidermal cells from *N. benthamiana* leaves co-expressing 35S::GFP:NPH3 with 35S::RFP:NPH3-4K/. Plants were dark adapted (D) and irradiated with blue light (10 µmol/m^2/s) for 40 min (BL). Scale bar 25 µm. **B** Representative confocal images of epidermal cells from *N. benthamiana* leaves co-expressing 35S::GFP:NPH3-S744A with 35S::RFP:NPH3-4K/A. Plants were dark adapted (D) and irradiated with blue light (10 µmol/m^2/s) for 40 min (BL). Scale bar 25 µm. **C** Immunoblot analysis of crude extracts from transiently transformed *N. benthamiana* co-expressing 35S::RFP:NPH3 variants with 35S::GFP:NPH3 variants separated on a 7.5 % SDS-PAGE gel. **D** *In vivo* interaction of 35S::RFP:NPH3-4K/A and 35S::GFP:NPH3 variants transiently expressed in *N.benthamiana* leaves. Plants were dark adapted (D) and irradiated with blue light (10 µmol/m^2/s) for 40 min (BL). Crude extract was immunoprecipitated by using GFP beads. Input and IP were separated on 7.5 % SDS-PAGE gels followed by α-RFP or α-GFP immunodetection. Experiments were repeated at least three times. Black arrowheads indicate the phosphorylated state of NPH3 whereas white arrowheads indicate the dephosphorylated state of NPH3.

To address the question why NPH3-4K/A is only present in a "generally" dephosphorylated state we made use of an observation from Prabha Manishankar: co-expression of the NPH3 WT protein with a NPH3 variant permanently localizing to condensates results in an attraction of the condensate-forming variant to the PM in darkness suggesting homo-oligomerization (Prabha Manishankar, unpublished). BL treatment, however, still induces PM detachment of both NPH3 variants. Indeed, transient co-expression of GFP:NPH3 with RFP:NPH3-4K/A in *N. benthamiana* results in PM localization of both proteins in darkness (Fig 3.24A) and upon BL treatment both proteins localize to condensates (Fig 3.24A). Interestingly, co-expression

of NPH3-4K/A with NPH3-S744A, a permanently PM localizing mutant, causes permanent PM association of both proteins (Fig 3.24B).

Next, we examined whether the co-expression of NPH3-4K/A with the WT protein is changing the phosphorylation status of NPH3-4K/A besides altering the subcellular localization. In fact, co-expression of GFP:NPH3 with RFP:NPH3-4K/A resulted in a decreased electrophoretic mobility for NPH3-4K/A in darkness (Fig 3.24C) with a band corresponding to the “generally” phosphorylated state of the WT protein. Thus, attraction to the PM shifts NPH3-4K/A to the “generally” phosphorylated state in the dark, and the protein is still able to become “generally” dephosphorylated upon BL irradiation comparable to the WT (Fig 3.24C). Also, co-expression with NPH3-S744A, resulting in permanent PM localization, caused a “general” phosphorylation of NPH3-4K/A (Fig 3.24C). Surprisingly, NPH3-4K/A is still able to become “generally” dephosphorylated, suggesting that PM dissociation is not required for “general” dephosphorylation (Fig 3.24C). To ensure that NPH3-4K/A is able to interact with NPH3 or NPH3-S744A *in vivo,* a CoIP was performed, demonstrating that NPH3-4K/A is able to interact with NPH3 and NPH3-S744A both in darkness as well as upon BL irradiation (Fig 3.24D).

These findings indicate that the “general” phosphorylation of NPH3 in darkness takes place at the PM. Thus, NPH3-4K/A – due to missing interaction with phospholipids – is not associating to the PM, but permanently localizes to condensates and displays a permanent “generally” dephosphorylated state.

4 Discussion

NPH3 was shown to interact with 14-3-3 proteins of the epsilon and the non-epsilon group in an Y2H assay (Throm, 2017). In search for the 14-3-3 binding motif serial deletion constructs of NPH3 were generated and the following Y2H assays revealed that the C-terminal region of NPH3 is essential for 14-3-3 association (Throm, 2017; Reuter *et al.*, 2021). More specifically, exchange of the serine at position 744 (S744) for alanine - the third last amino acid residue in NPH3 - abolished interaction between 14-3-3 proteins and NPH3 (Throm, 2017; Reuter *et al.*, 2021). This binding motif is belonging to the mode III binding motifs allowing phosphorylation-dependent 14-3-3 association (Coblitz *et al.*, 2006).

4.1 NPH3 associates to the PM via a C-terminal amphipathic helix

PM association of the hydrophilic NPH3 in darkness is known since 1999 (Motchoulski and Liscum, 1999), yet the molecular mechanisms remained elusive. Association to the PM can be caused by different mechanisms like protein-protein interactions, protein-lipid interactions, lipid anchoring, electrostatic or hydrophobic interactions. Remorins for example are embedded into the inner leaflet of the PM via a C-terminal anchor (Gronnier *et al.*, 2017). The C-terminal helix of Remorins interacts with the negatively charged head groups of phospholipids whereas the hydrophobic anchor is inserted into the inner leaflet of the bilayer (Perraki *et al.*, 2012; Gronnier *et al.*, 2017). Thus, Remorins associate to the PM via hydrophobic and electrostatic interactions. Another example are AGCVIII kinases such as D6PK and PINOID (PID) that interact with the PM via a BH motif (Barbosa *et al.*, 2016; Simon *et al.*, 2016). BH motifs are regions enriched in hydrophobic and basic amino acids which can interact with negatively charged phospholipids at the PM. More specifically D6PK and PID bind to polyacidic phospholipids via such a BH motif – an insertion between kinase subdomains (Barbosa *et al.*, 2016; Simon *et al.*, 2016). Phot1 also belongs to the protein family of AGCVIII kinases but does not contain a BH motif in the middle domain of the kinase that mediates PM attachment (Barbosa *et al.*, 2016).

To obtain first insights into the molecular characteristics required for PM association of NPH3, the genetic tool SAC1 was used for coexpression experiments with NPH3. This genetic tool is comprised of the catalytic domain of the yeast Pi4P-phosphatase SAC1 fused to a mCherry-fluorophore as well as a myristoylation and palmitylation sequence (MAP) allowing for PM localization in plants (Simon *et al.*, 2016). Expression of the catalytically active SAC1 alters the phospholipid composition of the PM by depleting the pool of Pi4P (Simon *et al.*, 2016; Platre *et al.*, 2018). Since accumulation of Pi4P at the PM controls the electrostatic signature, a depletion of the Pi4P pool also changes the electronegativity of the PM (Simon *et al.*, 2016).

The drug phenylarsine oxide (PAO) displays a comparable effect to SAC1 by reducing the Pi4P pool in the cell (Simon *et al.*, 2016). PAO treatment of seedlings led to dissociation of usually membrane associated proteins, including PID, D6PK or the MEMBRANE ASSOCIATED KINASE REGULATOR 2 (MAKR2) (Barbosa *et al.*, 2016; Simon *et al.*, 2016). Co-expression of SAC1 with PM-associated proteins, including Remorin1.3 or the nucleotide-binding leucine-rich repeat receptors (NLRs) ACTIVATED DISEASE RESISTANCE 1 (ADR1), ADR1-LIKE1 (ADR1-L1) or ADR1-L2 also affected their PM association and in case of ADR1-L1 and ADR1-L2, their stability (Gronnier *et al.*, 2017; Saile *et al.*, 2021).

Transient co-expression of SAC1 with NPH3 in *N. benthamiana* led to NPH3 PM dissociation and particle formation already in darkness (Fig 3.7B). Hence, phospholipid interaction or the electronegativity of the PM could be causal of PM association of NPH3 in darkness. Lipid overlay and liposome binding assays performed by Tanja Schmidt revealed that NPH3 binds to polyacidic phospholipids, indicating that interaction with phospholipids is essential for PM association of NPH3 (Reuter *et al.*, 2021; Schmidt, 2022). The NLRs ADR1-L1 and ADR1-L2 are thought to be degraded after co-expression with SAC1, since they are not detectable in microscopic or western blot analyses anymore, unless the activity of the proteasome is inhibited (Saile *et al.*, 2021). Different from that, NPH3 is present in particle-like structures and seems not be degraded upon co-expression with SAC1 (Fig 3.7B, 3.21A).

MAB4/MEL proteins, another NRL protein family member, also displays an altered localization upon changed phospholipid composition of the PM. Here, treatment of seedlings expressing MEL1 with PAO led to a dissociation from the PM (Glanc *et al.*, 2021). Yet, different from NPH3, MEL1 is not forming particle-like structures in the cytosol after dissociation. PM association of MAB4/MEL proteins was described as a recruitment to the PM by PIN proteins and PID. Phosphorylation of PIN proteins by PID enhances the recruitment of MAB4/MELs to the PM resulting in a decreased lateral diffusion of PIN proteins thereby maintaining PIN polarity (Glanc *et al.*, 2021). However, co-expression experiments with SAC1, lipid overlay and liposome binding assays suggest that NPH3 directly interacts with polyacidic phospholipids at the PM (Reuter *et al.*, 2021; Schmidt, 2022). Hence, the mechanism of PM association for these two NRL proteins is different.

In search for the domain required for PM association of NPH3, deletion constructs were generated that either lack the N-terminal 54 amino acids (NPH3ΔN54) or the C-terminal 51 amino acids (NPH3ΔC51). While deletion of the N-terminal 54 amino acid residues did not alter the light-modulated subcellular localization of the protein (Fig 3.8B, 4.1), truncation of the region downstream of the CC domain resulted in PM dissociation in darkness, hence resembling the subcellular localization of NPH3 upon co-expression of SAC1 (Fig 3.8B, 4.1).

In vitro analyses of Tanja Schmidt confirmed that NPH3ΔC51 is incapable of binding polyacidic phospholipids (PIP Strips) or liposomes, while the C-terminal 51 amino acids (NPH3-C51) turned out to be sufficient to interact with phospholipids (Reuter *et al.*, 2021; Schmidt, 2022). These data indicate that the C-terminal region of NPH3 is essential for PM association in darkness.

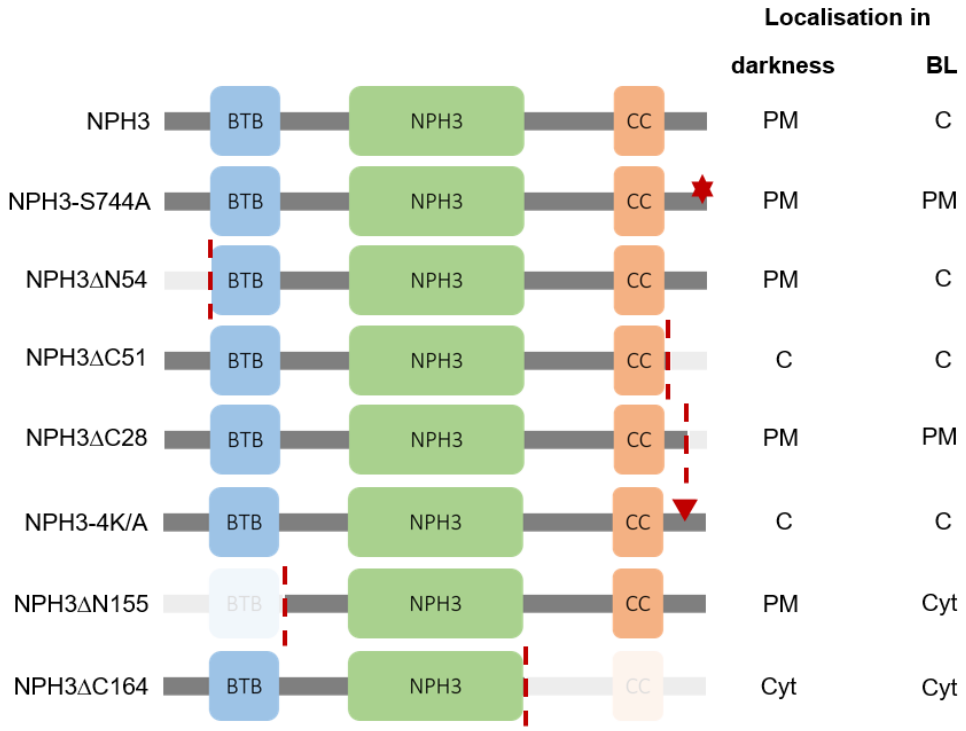

Figure 4. 1: Overview of constructs described in this study and their subcellular localization. Schematic illustration of the most important constructs described in this thesis. Subcellular localization of the constructs in darkness and after BL irradiation. PM = Plasma membrane, C = Condensates, Cyt = Cytosol. Red star represents exchange of S744 to alanine. Red triangle represents exchange of four lysine in the amphipathic helix to alanine.

Further in-depth analysis of the C-terminal region by Claudia Oecking revealed the presence of two putative BH motifs (Reuter *et al.*, 2021): (i) an R-rich motif adjacent to the 14-3-3 binding site and (ii) a predicted amphipathic helix downstream of the CC domain. Exchange of five basic amino acid residues in the R-rich motif for alanine (NPH3-5KR/A) abolished binding to phospholipids *in vitro* (Reuter *et al.*, 2021; Schmidt, 2022). This variant, however, exhibited permanent PM localization following transient expression in *N. benthamiana* (Fig 3.9B, 3.10). To ensure that the R-rich motif is not involved in PM association, the C-terminal 28 amino acid residues encompassing the R-rich motif were deleted. Indeed, NPH3ΔC28 permanently localized to the PM (Fig 3.9B, 3.10, 4.1). Consequently, the R-rich motif is not required for PM association in darkness. Remarkably, both NPH3-5KR/A and NPH3ΔC28 do not dissociate

from the PM upon BL treatment (Fig 3.9B, 3.10). Interference with the 14-3-3 interaction could be causal of this permanent PM association. While NPH3ΔC28 is devoid of the 14-3-3 binding site, site-directed mutagenesis of the R-rich motif could interfere with 14-3-3 association. On the one hand, destruction of a consensus sequence (RxS) could abolish potential phosphorylation of the 14-3-3 binding site by the AGVIII kinase phot1 and with that 14-3-3 interaction (Sullivan *et al.*, 2021), while, on the other hand, conformational changes could cause an inhibition of 14-3-3 binding *per se*. Y2H assays performed by Andrea Bock in our lab showed no interaction between 14-3-3 proteins and NPH3-5KR/A (Andrea Bock, unpublished), however we cannot differentiate between these two scenarios.

In contrast to the modification of the R-rich motif, reduction of either the positive charge (NPH3-4K/A) or the hydrophobicity (NPH3-4WLM/A) of the predicted amphipathic helix resulted in permanent localization to particles (Fig 3.9B, 3.10, 4.1). Thus, the amphipathic helix in the C-terminal region of NPH3 is essential for PM anchoring *in vivo*, suggesting a model where the basic amino acid residues of the amphipathic helix interact electrostatically with polyacidic phospholipids, while the hydrophobic residues are embedded into the inner leaflet establishing contacts to the hydrocarbon region of the bilayer. A similar molecular mechanism has been described for the Pi4P 5 kinase (PIP5K), PM association of which is also established via an amphipathic helix (Fairn *et al.*, 2009; Liu *et al.*, 2016; Nishimura *et al.*, 2019).

BL triggered 14-3-3 binding might result in a conformational change which “extracts” the amphipathic helix out of the PM followed by dissociation into the cytosol.

It is noteworthy to mention that the C-terminal 51 amino acid residues (NPH3-C51) N-terminally tagged with RFP are insufficient to mediate PM association in *N. benthamiana* (Fig 3.11B) despite the fact that this region binds to phospholipids *in vitro* (Reuter *et al.*, 2021; Schmidt, 2022). However, the C-terminal 164 amino acid residues (NPH3-C164) are capable to associate with the PM in *N. benthamiana* (Fig 3.11B), suggesting that, in addition to the amphipathic helix, a region downstream of the NPH3 domain contributes to PM association *in vivo.* CoIP experiments performed by Prabha Manishankar demonstrated that NPH3 is able to form homo-oligomers *in vivo*. Hence, it is possible that formation of homo-oligomers, in addition to the amphipathic helix, is required for PM association.

4.2 BL triggers 14-3-3 binding to NPH3 leading to changes in the subcellular localization of NPH3

Tanja Schmidt confirmed the interaction between 14-3-3 and NPH3 *in vivo* via CoIP. Furthermore, the S744A mutation abolished complex formation (Reuter *et al.*, 2021; Schmidt, 2022). Using an IP/MS approach Tanja Schmidt moreover discovered a strict BL-dependent complex formation between NPH3 and 14-3-3 proteins (Reuter *et al.*, 2021; Schmidt, 2022). Prabha Manishankar later confirmed these results in a CoIP experiment (Reuter *et al.*, 2021).

14-3-3 proteins are known to interact with several target proteins in a phosphorylation-dependent and sequence-specific manner and alter for example their activity state or their subcellular localization (Oecking *et al.*, 1997; Kinoshita and Shimazaki, 1999; Gampala *et al.*, 2007; Wang *et al.*, 2011). Also, the AGCVIII kinase phot1 is an identified interaction partner of 14-3-3 proteins (Kinoshita *et al.*, 2003; Inoue *et al.*, 2008a). Here a phosphorylation- and light-dependent association of 14-3-3s with phot1 was described (Inoue *et al.*, 2008a). However, the functional significance of this interaction remains unknown, since mutation of two 14-3-3 binding sites in phot1 did not impair the phot1-function during the phototropic response (Inoue *et al.*, 2008a).

Changes in the subcellular localization through 14-3-3 binding have been described for two proteins involved in brassinosteroid signaling, BZR1 and BRI1 KINASE INHIBITOR 1 (BKI1) (Gampala *et al.*, 2007; Wang *et al.*, 2011). 14-3-3 association with the phosphorylated transcription factor BZR1 leads to a retention of BZR1 in the cytosol (Gampala *et al.*, 2007). The presence of brassinosteroids causes a dephosphorylation of BZR1 and interrupts the interaction with 14-3-3 proteins followed by localization of BZR1 to the nucleus (Gampala *et al.*, 2007). BKI1 is present at the PM and associated to the receptor BRASSINOSTEROID INSENSITIVE 1 (BRI1) in the absence of brassinosteroids (Wang *et al.*, 2011). In the presence of brassinosteroids BKI1 becomes phosphorylated, interacts with 14-3-3 proteins followed by dissociation from BRI1 and the PM and localization to the cytosol (Wang *et al.*, 2011).

Microscopic analysis of NPH3 or NPH3-S744A transiently expressed in *N. benthamiana* or in transgenic *A. thaliana nph3-7* lines, revealed that inhibition of the NPH3 14-3-3 interaction affects the subcellular localization of NPH3 (Fig 3.1, 3.2, 3.4, 3.5). While NPH3 localized to the PM in darkness and forms particle-like structures in the cytosol upon BL irradiation, NPH3-S744A remained PM-associated upon BL treatment (Fig 4.1), whether expression was driven by the 35S or the endogenous promoter (Fig 3.1, 3.2, 3.4, 3.5). Transient co-expression with 14-3-3 proteins in *N. benthamiana* illustrated strict colocalization of 14-3-3 and NPH3 but not NPH3-S744A in particles upon BL treatment (Fig 3.3). Furthermore, microscopic analysis of transgenic *nph3-7* lines expressing GFP:NPH3 under control of the 35S promoter showed

cycling of NPH3 between the PM and cytosolic particles in a BL-dependent manner (Fig 3.4, 3.6). Hence, the altered subcellular localization of NPH3 upon BL irradiation and 14-3-3 association from the PM to the cytosol is reminiscent of BKI1, which is also localizing from the PM into the cytosol upon 14-3-3 binding. The findings of this study unraveled that 14-3-3 interaction with NPH3 is essential for dynamic changes in the subcellular localization of NPH3 upon BL treatment.

Inhibition of 14-3-3 binding to NPH3 causes permanent PM association (NPH3-S744A), further Sullivan et al. created a NPH3 variant permanently binding 14-3-3 proteins (Sullivan *et al.*, 2021). Here the last three amino acid residues of NPH3 were replaced with a R18 peptide sequence, a synthetic peptide that enables 14-3-3 binding in a phosphorylation-independent manner (Sullivan *et al.*, 2021). Interestingly, this NPH3 variant was permanently present in particle-like structures, suggesting that permanent 14-3-3 binding as well as inhibition of 14-3-3 association with NPH3 interfere with the dynamic changes in subcellular localization of NPH3 upon BL treatment.

Phot1 is present at the PM in darkness like NPH3 and is partially internalized via endocytosis upon BL irradiation (Sakamoto and Briggs, 2002; Wan *et al.*, 2008; Kaiserli *et al.*, 2009). BL-triggered changes in subcellular localization, however, seem to be dispensable for the function of phot1 in the phototropic response (Preuten *et al.*, 2015). Preuten et al. prevented phot1 internalization and permanently attached it to the PM through myristoylation or farnesylation. Although constitutively attached to the PM, these phot1 variants were still functional and thus, able to fully restore the phototropic response. These data suggest that the subcellular relocalization of phot1 is not required for its function during phototropism (Preuten *et al.*, 2015). For NPH3 it has been suggested that it is not internalized via endocytosis, since it is not sensitive to BFA treatment (Haga *et al.*, 2015). Our findings illustrate, PM detachment and formation of particle-like structures in the cytosol are two separate and consecutive processes (Supplementary Movie 1). Furthermore, physiological studies performed by Tanja Schmidt and Jutta Keicher displayed that the WT protein expressed in transgenic *nph3-7* lines but not NPH3-S744A was able to restore the phototropic response (Reuter *et al.*, 2021; Sullivan *et al.*, 2021; Schmidt, 2022). These data indicate that 14-3-3 interaction with NPH3 and changes in the subcellular localization upon BL irradiation are required for NPH3 function in the phototropic response.

It has been previously reported that dissociation of NPH3 from the PM is phot1-dependent (Haga *et al.*, 2015) and furthermore, phot1 is able to interact with NPH3 directly (Lariguet *et al.*, 2006; de Carbonnel *et al.*, 2010). In an Y2H assay this interaction is mediated by the LOV domains of phot1 and the C-terminal region (162 amino acid residues) of NPH3 (Motchoulski

and Liscum, 1999). It is hence conceivable that 14-3-3 proteins could function as a scaffold protein between NPH3 and phot1 at the PM. However, Tanja Schmidt could show that NPH3ΔC28, a NPH3 variant permanently associating to the PM, is still able to interact with phot1, although it is lacking the 14-3-3 binding site (Reuter *et al.*, 2021; Schmidt, 2022).

Interestingly, other NRL protein family members, namely RPT2, DOT3 and ENP, also display interaction with 14-3-3 proteins in a Y2H assay via a C-terminal binding site (Reuter *et al.*, 2021), suggesting that there might exist a conserved motif for 14-3-3 binding among the NRL protein family members. Furthermore, Sullivan et al. identified the phot1 phosphorylation consensus sequence (RxS) - found in NPH3 - to be conserved in several other NRL proteins (Sullivan *et al.*, 2021). Lukas Dittiger performed an *in silico* analysis to find 14-3-3 binding motifs in the NRL protein family (Lukas Dittiger, unpublished). In 19 out of 20 members of the NPH3, the RPT2 and the NPY subclade a putative 14-3-3binding site was found. Here further experiments like Y2H, CoIP or colocalization studies have to be performed to confirm these findings.

4.3 NPH3 shows characteristics of biomolecular and membraneless condensates upon BL irradiation

In 2015 Haga et al. described an altered subcellular localization of YFP:NPH3 in response to light treatment. In darkness NPH3 localizes to the PM and upon BL irradiation is released from the PM and forms aggregates in the cytosol (Haga *et al.*, 2015). Thus, NPH3 was thought to be internalized rapidly from the PM into aggregates (Haga *et al.*, 2015; Sullivan *et al.*, 2019). Yet, the identity of the aggregates remained elusive.

Supplementary Movie1 displays that in darkness NPH3 is attached to the PM and detaches from the PM upon BL treatment (Supplementary Movie 1). After dissociation from the PM NPH3 first becomes cytoplasmic followed by formation of particles after 4-5 min of BL irradiation (Supplementary Movie 1). Thus, PM dissociation and particle-like structure formation of NPH3 are two consecutive and separate processes.

A possible causal process that could be involved in generation of such particles is liquid liquid phase separation (LLPS) (Cuevas-Velazquez and Dinneny, 2018; Jaillais and Ott, 2020). Here, two liquids demix and form two separate phases as soon as a certain critical concentration is reached (Alberti, 2017; Banani *et al.*, 2017). The dense phase is referred to as membraneless compartment, which can be involved in several cellular processes like mRNA processing, DNA damage response or stress response (Emenecker, Holehouse and Strader, 2021). Cellular compartments that are known to be membraneless are for example

the nucleolus, processing bodies or stress granules (Alberti, 2017; Cuevas-Velazquez and Dinneny, 2018; Emenecker, Holehouse and Strader, 2021). Membraneless compartments are also known as biomolecular condensates referring to their ability to concentrate biomolecules (Emenecker, Holehouse and Strader, 2021). Also, in plants several examples for the formation of such condensates are known. Localization of the auxin response factor (ARF) 7 and ARF19 to cytoplasmic, biomolecular condensates decreases the response to auxin in the upper root (Powers *et al.*, 2019). Thus, ARF7 and ARF19 undergo phase separation into condensates to regulate the auxin response in a tissue-specific manner (Powers *et al.*, 2019). Another protein that forms condensates in the cytosol is NONEXPRESSER OF PATHOGENESIS-RELATED GENES 1 (NPR1), which is involved in plant immunity. In response to salicylic acid (SA) NPR1 localizes in so called SA-induced NPR1 condensates (Zavaliev *et al.*, 2020). In these condensates NPR1 targets substrates for degradation and with that restricts cell death during plant immunity (Zavaliev *et al.*, 2020). NPR1 undergoes phase separation mediated by intrinsically disordered regions (IDRs) which are known to promote phase separation (Zavaliev *et al.*, 2020). IDRs lack a well-defined three-dimensional structure and therefore display a high conformational flexibility (Alberti, 2017; Banani *et al.*, 2017; Cuevas-Velazquez and Dinneny, 2018). NPH3 contains IDRs and protein-protein interaction domains and is, thus, likely to undergo LLPS in a BL-dependent manner (see chapter 4.4).

We therefore performed a single-cell time-lapse imaging where a Z-stack, covering the entire thickness of an epidermal cell is analyzed in darkness followed by prolonged GFP laser treatment (Fig 3.13). As described earlier, NPH3 is attached to the PM in darkness and forms particles upon GFP laser treatment (Fig 3.13A). NPH3 first becomes cytosolic after detachment from the PM followed by particle formation (Fig 3.13A). The fluorescence intensity per body increases with prolonged GFP laser treatment (Fig 3.13B). Interestingly, the number of bodies first increases until it reaches a maximum after approximately 10.5 min and after decreases (Fig 3.13C). This might be due fusion of the bodies. Formation of the NPH3 bodies upon BL irradiation is reminiscent of the formation of condensates for NPR1 upon SA treatment. Taken together, these analyses indicate that NPH3 undergoes a dynamic transition from a PM associated state to membraneless, biomolecular condensates in the cytosol in a BL-dependent manner.

Furthermore, subcellular fractionation of NPH3 variants verified that the WT protein is membrane-associated in darkness, thus confirming previous results (Fig 3.12B). Remarkably, deletion of the C-terminal 51 amino acid residues shifts the protein from the microsomal to the soluble fraction (Fig 3.12B), indicating a non-membrane attached state of NPH3 in condensates.

After dissociation from the PM upon BL irradiation NPH3 first becomes cytosolic. As the concentration of NPH3 in the cytosol continuously increases, NPH3 could undergo LLPS as soon as a critical concentration is reached resulting in condensate formation. When retransferred to darkness after BL treatment NPH3 relocalizes from the cytosolic condensates to the PM (Fig 3.6). Thus, the formation of biomolecular, membraneless condensates is reversible for NPH3.

14-3-3 interaction with NPH3 is essential for PM dissociation (see chapter 4.2). To examine, whether 14-3-3 interaction with NPH3 might be required for condensate formation again the genetic tool SAC1 was used for co-expression with NPH3-S744A, the mutant variant incapable of 14-3-3 interaction. SAC1 is a phosphatase from yeast that depletes Pi4P from the PM and with that changes the phospholipid composition of the PM (Simon et al., 2016). Interestingly, co-expression of SAC1 with NPH3-S744A led to formation of condensates in darkness (Fig 3.12A). This indicates that 14-3-3 interaction is dispensable for condensate formation. It rather suggests that interference with the PM association of NPH3 is responsible for the formation of condensates.

4.4 Condensate formation of NPH3 requires the BTB domain and conserved motifs in the C-terminal region

It has already been described that PM dissociation and condensate formation of NPH3 are two consecutive and separate processes (Supplementary Movie 1). To uncover which domains or motifs in NPH3 are involved in condensate formation the domain structure of NPH3 was studied in a more detailed manner. NPH3 comprises two protein-protein interaction domains, a C-terminal CC domain and a N-terminal BTB/POZ domain (Motchoulski and Liscum, 1999). Both of these domains have been described to be involved in oligomerization (Albagli *et al.*, 1995; Lupas, 1996; Lupas and Bassler, 2017). For Remorins for example trimerization via a CC domain is required for membrane recruitment and could promote clustering into nanodomains (Martinez *et al.*, 2019). The BTB domain has been described to for example mediate oligomerization of the BTB-BACK-Kelch (BBK) proteins consistent with their role in the organization of actin filaments (Stogios *et al.*, 2005). In general, BTB/POZ domains are characterized by a minimum of five conserved α-helices and three β-sheets, whereas CC domains consist of up to seven bundled helices (Lupas, 1996; Stogios *et al.*, 2005). CC domains can be characterized by heptad repeats, meaning that seven amino acid residues show a repeated pattern with the first and the fourth amino acid being hydrophobic and forming the core of the helix (Lupas and Bassler, 2017). Besides BTB/POZ or CC domains, also IDRs can be involved in condensate formation (Banani *et al.*, 2017). NPH3

comprises five IDRs that are located in the N-terminal region, the NPH3 domain and the C-terminal region as shown by a MobiDB plot of IDRs in NPH3 (Reuter *et al.*, 2021).

Inada et al. showed that the N-terminal region of NPH3, including the BTB/POZ domain, is able to interact with the N-terminal region of RPT2, also including a BTB/POZ domain, in an Y2H assay (Inada *et al.*, 2004). Furthermore, NPH3 interacts with a CUL3a ubiquitin ligase via the N-terminal BTB/POZ domain (Roberts *et al.*, 2011). The C-terminal region of NPH3, including the CC domain interacts with a fragment of phot1 including both LOV domains in an Y2H assay and *in vitro* (Motchoulski and Liscum, 1999).

Yet, nothing is known about the role of these two domains or IDRs in condensate formation of NPH3. Transient overexpression of a NPH3 version truncated by the N-terminal 155 amino acid residues including the BTB/POZ domain (NPH3ΔN155) in *N. benthamiana* shows a PM localization in darkness similar to the WT protein (Fig 3.14B). Upon BL treatment NPH3ΔN155 dissociates from the PM also comparable to the WT protein (Fig 3.14B). However, the truncated NPH3 variant does not form condensates (Fig 3.14B), indicating that the BTB/POZ domain is required for condensate formation after BL treatment (Fig 4.1).

An interesting aspect is that other family members of the NRL protein family namely RPT2, DOT3 and ENP also comprise of a BTB/POZ domain while others like NRL4 and NRL12 do not (Lukas Dittiger, unpublished). Hence, it would be interesting to study whether these proteins also show condensate formation similar to NPH3 and to check whether the BTB/POZ domain is involved.

Transient expression of serial truncations of the C-terminal region in *N. benthamiana* confirmed that a NPH3 variant lacking the C-terminal 93 amino acid residues including the CC domain is still able to form condensates (Fig 3.15B), indicating that the CC domain is not involved in condensate formation. However, deletion of the C-terminal 164 amino acid residues - the C-terminal region downstream of the NPH3 domain - resulted in permanent cytosolic and nuclear localization (Fig 3.15B, 4.1). Hence, in addition to the BTB domain a motif in the C-terminal region contributes to condensate formation. It is known since 1999, that a highly conserved motif II (^{583}HAAQNERLPL^{592}) is present within the above-described C-terminal region (Moutchoulski and Liscum, 1999). Furthermore, a linear interacting peptide (LIP) or short linear motif (SLiM) is located in close proximity to this conserved motif (Fig 3.16, Suppl. Fig 1). LIPs are often located within IDRs and only build their three-dimensional structure upon binding to another molecule (van der Lee *et al.*, 2014).

Protein structure prediction of NPH3 using the program AlhpaFold revealed that this conserved region II and the LIP could possibly mediate inter- and intramolecular interactions leading to condensate formation (Fig 3.16, Suppl. Fig 1). AlphaFold is an AI system that is

able to predict 3D protein structures based on the amino acid sequence and commonly achieves comparable results to experiments (AlQuraishi, 2021; Jumper *et al.*, 2021; Varadi *et al.*, 2022). To examine whether the conserved region II or the LIP are involved in condensate formation three mutant versions were generated - exchanged amino acid residues highlighted in grey: (i) mutation of the conserved region by exchanging the highly conserved amino acid residues QNE within motif II to alanine (^{583}HAAQNERLPL^{592}) (NPH3-CON), (ii) mutation of the LIP by exchanging three valines for alanine (^{594}VVVQVLF^{600}) (NPH3-LIP), (iii) mutation of two arginine's within and between the conserved motif II and the LIP (^{583}HAAQNERLPLRVVVQVLF^{600}) (NPH3-RR/A). All these three mutations aim to disrupt inter- or intramolecular interactions. The amino acids Q586, E588 and R593 could be surface exposed and with that contribute to intermolecular interactions (Fig 3.16D, Suppl. Fig 1F,H+J). Protein structure prediction displays that N587, R589, V595, V596 and V598 might be involved in intramolecular interactions (Fig 3.16D, Suppl. Fig 1G,I,K-M). The exchange for alanine aims to interrupt these possible intra- or intermolecular interactions. All amino acid residues were exchanged for alanine - comprising only a methyl group as a side chain - to interrupt the abovementioned interactions of the investigated amino acids. Yet, an exchange to the nonpolar amino acid residue alanine is thought to affect the structure of the protein as little as possible.

Indeed, all mutant variants of NPH3 lost the ability to form condensates upon BL irradiation (Fig 3.17A). Yet, combination of a mutation of the conserved region II with a deletion of the amphipathic helix (NPH3ΔC51-CON) resulted in cytosolic condensates (Fig 3.17B), suggesting that two or three motifs might act together and not a single motif alone is required for condensate formation.

In addition to the conserved region II a conserved region I is located upstream in the NPH3 domain (^{545}LYRAID^{550}) (Fig 3.16, Suppl. Fig 1) also with unknown function (Motchoulski and Liscum, 1999). However, deletion of Y546 in the *nph3-2* mutant results in a loss of the phototropic response (Moutchoulski and Liscum 1999). To examine whether this conserved motif I is involved in condensate formation, the tyrosine and arginine residues were exchanged to alanine (^{545}LYRAID^{550}). Y546 possibly contributes to intramolecular interactions, while R547 might be surface exposed and could be involved in intermolecular interactions (Fig 3.16D, Suppl. Fig 1D+E). These mutations were introduced in NPH3ΔC51 (NPH3ΔC51-LYRA) to study the subcellular localization in a mutant incapable of PM association. This mutant variant indeed displays permanent cytosolic localization without condensate formation (Fig 3.17C). However, due to lack of time the subcellular localization of this NPH3 variant was only analysed twice. Further investigation of this mutant by Prabha Manishankar revealed that it

partially localizes to both the cytosol and condensates, indicating that this region by itself is not essential for condensate formation.

A possible scenario is involvement of both conserved regions and the LIP in condensate formation. To test this, higher-order mutants comprising two or more of the above-mentioned mutants need to be generated and tested for their subcellular localization.

Taken together, the BTB/POZ domain and conserved motifs in the C-terminal region are required for condensate formation of NPH3 upon BL irradiation.

4.5 BL irradiation and 14-3-3 interaction alter the phosphorylation status of NPH3

Phot1-dependent “general” dephosphorylation of NPH3 upon BL irradiation is known since 2007 (Pedmale and Liscum, 2007). This “general” dephosphorylation is visible by an increased electrophoretic mobility of the protein in an SDS-PAGE after BL treatment which is reversible after transfer to darkness or prolonged irradiation with BL (Pedmale and Liscum, 2007; Haga *et al.*, 2015; Sullivan *et al.*, 2019). Tanja Schmidt, however, demonstrated a strictly BL-triggered interaction of 14-3-3 and NPH3 (Reuter *et al.*, 2021; Schmidt, 2022). Since 14-3-3 proteins mostly interact in a phosphorylation dependent manner with their targets (Mackintosh, 2004), the question arose whether NPH3 becomes also phosphorylated at S744 - the 14-3-3 binding site - upon BL irradiation (Reuter *et al.*, 2021).

To test this, a phosphosite-specific peptide antibody was generated that was assumed to specifically recognize the phosphorylated serine at position 744 (α-pS744). As control an antibody raised against the unmodified peptide (α-NPH3) was used. Investigation of the phosphorylation status of GFP:NPH3 after transient expression in *N. benthamiana* or in transgenic *nph3-7 A. thaliana* lines displayed the characteristic “general” dephosphorylation of the WT protein (Fig 3.18). Interestingly, NPH3-S744A did not display an increased electrophoretic mobility upon BL irradiation meaning that the protein is not “generally” dephosphorylated (Fig 3.18). Furthermore, the phosphosite-specific peptide antibody specifically recognizes BL-treated NPH3 but not NPH3-S744A (Fig 3.18), thereby confirming the specificity of the antibody. Altogether, BL triggers two posttranslational modifications for NPH3: (i) phosphorylation of the 14-3-3 binding site (S744) and (ii) a “general” dephosphorylation (Fig 3.18).

Far Western analyses in both *N. benthamiana* and *A. thaliana* confirmed that phosphorylation of S744 mediates 14-3-3 association to NPH3 only after BL treatment supporting Tanja Schmidt’s results (Fig 3.18) (Reuter *et al.*, 2021; Schmidt, 2022). These findings confirm that

NPH3 and 14-3-3 interact in a strict BL-dependent manner and suggest that BL-triggered phosphorylation of S744 might be required for the “general” dephosphorylation of NPH3.

Confocal microscopy revealed that NPH3 relocalizes to the PM when retransferred to darkness after BL irradiation (Fig 3.18C), supporting previous findings that prolonged BL irradiation leads to reassociation of NPH3 to the PM (Haga *et al.*, 2015). After transfer back to darkness NPH3 not only relocalizes to the PM, but also becomes dephosphorylated at S744 and “generally” rephosphorylated (Fig 3.18C) confirming results obtained by Pedmale and Liscum in 2007 (Pedmale and Liscum, 2007). Thus, a retransfer to darkness after BL irradiation results in a relocalization of the protein to the PM and a “general” rephosphorylation (Fig 3.18C).

To summarize, there are two post-translational and light-dependent modifications: (i) upon BL irradiation NPH3 becomes “generally” dephosphorylated, but phosphorylated at S744, (ii) after retransfer to darkness NPH3 becomes “generally” rephosphorylated, but dephosphorylated at S744 (Reuter *et al.*, 2021). Interestingly, a recent study reported that phot1 is the kinase responsible for phosphorylating S744 upon BL irradiation (Sullivan *et al.*, 2021).

To examine the sequential order, a time course experiment was performed (Fig 3.19). Here it became evident that phosphorylation of S744 is already visible after 0.5 min of BL treatment (Fig 3.19A) allowing for 14-3-3 binding (Fig 3.19B). “General” dephosphorylation of NPH3, however, starts slightly after 2 min and a complete electrophoretic mobility shift is visible after 30 min of BL treatment (Fig 3.19A+B). In WT Col-0 seedlings the complete shift requires 15 min (Fig 3.19C). The faster dephosphorylation in Col-0 seedlings could be due to the fact, that NPH3 is not overexpressed. Taken together, this shows that phosphorylation of S744 and binding of 14-3-3 proteins precede the “general” dephosphorylation of NPH3.

A collaboration with the group of John Christie from the university of Glasgow revealed that exchange of the last serine residue to alanine or aspartate (S764A, S746D) prevents or reduces BL-induced relocalization of NPH3 (Sullivan *et al.*, 2021). Yet, an Y2H assay performed by Andrea Bock demonstrated NPH3-S746A to still be able to interact with 14-3-3, while NPH3-S746D – like NPH3-S744A – is not (Reuter *et al.*, 2021) (Andrea Bock, unpublished). Thus, to analyze whether 14-3-3 interaction is required for “general” dephosphorylation, three NPH3 mutants were investigated: (i) NPH3-S744D, (ii) NPH3-S746D both of which are incapable of 14-3-3 interaction in a Y2H, (iii) NPH3-S746A that is still able to interact with 14-3-3s in Y2H (Reuter *et al.*, 2021) (Andrea Bock, unpublished).

As expected, NPH3-S744D and NPH3-S746D are not able to dissociate from the PM upon BL irradiation, thus reflecting NPH3-S744A (Fig 3.21B) (Sullivan *et al.*, 2021). The NPH3-S746A mutant, however, still detached from the PM and formed condensates in BL (Fig 3.21B).

Sullivan et al. observed greatly reduced BL-triggered translocation of NPH3-S746A following transient expression in *N. benthamiana* (Sullivan *et al.*, 2021). Expression of NPH3-S746A in transgenic *nph3 A. thaliana* lines, however, resulted in aggregate formation after BL treatment (Sullivan *et al.*, 2021). Our observations after transient expression in *N. benthamiana* support the results obtained by Sullivan et al. in *A. thaliana* (Fig 3.21B) (Sullivan *et al.*, 2021). While NPH3-S746A interacted with 14-3-3 upon BL in CoIP experiments, NPH3-S746D does not (Fig 3.21C). Closer inspection revealed that NPH3-S746A shows the characteristic shift upon BL irradiation indicative of “general” dephosphorylation (Fig 3.21D), however, phosphorylation of S744 is not detectable after BL treatment. This could be due to the low expression of NPH3-S746A, which we faced repeatedly, while Sullivan et al. were able to show that NPH3-S746A is still phosphorylated at S744 in BL (Sullivan *et al.*, 2021). Hence, NPH3-S746A displays the same subcellular localization, phosphorylation status and 14-3-3 interaction capability as the WT protein. NPH3-S746D, nevertheless, is still phosphorylated at S744 upon BL treatment (Fig 3.21D). Most importantly, NPH3-S746D does not show the characteristic shift indicative of a “general” dephosphorylation upon BL irradiation (Fig 3.21D).

This demonstrates in fact that S744 phosphorylation-dependent 14-3-3 association is essential for “general” dephosphorylation of NPH3, while sole phosphorylation of S744 is not sufficient.

4.6 Phosphorylation status and condensate formation of NPH3

It has been assumed that condensate formation is a prerequisite for or a consequence of the “general” dephosphorylation of NPH3 (Haga *et al.*, 2015; Sullivan *et al.*, 2019; Legris and Boccaccini, 2020). To test this, we examined the phosphorylation status of NPH3 and NPH3-S744A after transient co-expression with SAC1 in *N. benthamiana*. The yeast phosphatase SAC1 depletes the pool of Pi4P at the PM thereby changing the phospholipid composition and the electronegativity of the PM (Simon *et al.*, 2016). This leads to permanent localization to condensates for NPH3 and NPH3-S744A already in darkness (Fig 3.7B + 3.12A). Interestingly, the phosphorylation status of both NPH3 variants remained unchanged by SAC1 co-expression (Fig 3.21A). The WT protein is “generally” phosphorylated in darkness and only shows an increased electrophoretic mobility upon BL irradiation accompanied by phosphorylation of S744 (Fig 3.21A), whereas NPH3-S744A is neither showing the characteristic shift nor S744 phosphorylation (Fig 3.21A).

Altogether, these results clearly demonstrate condensate formation to be neither the prerequisite for nor the consequence of “general” dephosphorylation of NPH3 as assumed before (Haga *et al.*, 2015; Sullivan *et al.*, 2019; Legris and Boccaccini, 2020). The findings indicate that phosphorylation of S744 is essential for “general“ dephosphorylation of NPH3 in BL and support the results obtained and discussed in chapters 3.8 and 4.5, that 14-3-3 interaction is required for “general” dephosphorylation. Furthermore, these results suggest that BL irradiation is crucial for the “general” dephosphorylation of NPH3.

Similar to NPH3 and NPH3-S744A upon co-expression with SAC1, NPH3-4K/A is permanently localized to condensates (Fig 3.23A). However, NPH3-4K/A displays a reduced electrophoretic shift corresponding to a “generally” dephosphorylated state already in darkness after transient expression in *N. benthamiana* and in transgenic *A. thaliana nph3-7* lines (Fig 3.20B + 3.23B). The difference in electrophoretic mobility of NPH3-4K/A is, however, not due to the site-directed mutations (Fig 3.23C). Sullivan et al. examined a comparable localization pattern to NPH3-4/KA for their NPH3 variant NPH3-R18, hence a permanent localization to condensates (Sullivan *et al.*, 2021). Here, the last three amino acids of NPH3 were replaced with the synthetic R18 peptide that enables phosphorylation-independent 14-3-3 association. However, NPH3-18 only displays a partially enhanced electrophoretic mobility in darkness and upon BL treatment (Sullivan *et al.*, 2021). The difference observed between NPH3-4K/A and NPH3-R18 could be due to the permanent 14-3-3 association observed for NPH3-R18 (Sullivan *et al.*, 2021).

A question that arose from the observations with NPH3-4K/A was: where is the phot1-independent “general” phosphorylation in darkness initially taking place? To investigate this further, we made use of an observation by Prabha Manishankar: Co-expression of NPH3-4K/A with the WT protein or NPH3-S744A leads to an attraction of NPH3-4K/A to the PM in darkness (Prabha Manishankar, unpublished data, Fig 3.24A+B). BL treatment, however, caused PM dissociation of NPH3 + NPH3-4K/A while NPH3-4K/A remained PM-associated upon co-expression with NPH3-S744A (Fig 3.24A+B). The phosphorylation status of NPH3-4K/A after co-expression with NPH3 or NPH3-S744A interestingly displays a decreased electrophoretic mobility in darkness indicative of a “general” phosphorylation (Fig 3.24C). Upon BL irradiation NPH3-4K/A shows an enhanced electrophoretic mobility indicative of a “general” dephosphorylation (Fig 3.24C). This clearly indicates that “general” phosphorylation of NPH3 takes place at the PM in darkness. NPH3-4K/A by itself – due to disturbed interaction with phospholipids – never reaches the PM but permanently localizes to condensates and therefore does not become “generally” phosphorylated in darkness.

The function of the condensates still remains elusive, phosphorylation studies of the NPH3 variant NPH3ΔN155 that is unable to form condensates illustrate that it is still able to bind 14-3-3 proteins and “generally” dephosphorylated upon BL irradiation, indicating that the body formation is not a prerequisite for the “general” dephosphorylation of NPH3 (Fig 3.22B+C). Consequently, phosphorylation of NPH3 at S744 and 14-3-3 binding upon BL irradiation seems to be accompanied by a “general” dephosphorylation in the cytosol independent of condensate formation (Fig 3.22). Furthermore, NPH3ΔN155 is able to reassociate to the PM when retransferred to darkness, indicating that PM reassociation does not require condensate formation (Fig 3.22A). Yet, the question whether the condensates are required for the phototropic response remains to be resolved. Therefore, the generation of transgenic *A. thaliana nph3-7* lines expressing NPH3ΔN155 is of utmost importance.

A possible mechanism to regulate granule formation via LLPS is phosphorylation as shown by Fang et al. (Fang *et al.*, 2022). Here, a phosphoprotein from the rhabdovirus *Barley yellow striate mosaic virus* undergoes LLPS promoting replication of the virus (Fang *et al.*, 2022). However, phosphorylation of the phosphoprotein by the host casein kinase 1 suppresses LLPS leading to reduction of virus replication (Fang *et al.*, 2022). The phosphorylated residues within the phosphoprotein localized to IDRs and mutant variants, mimicking constitutive phosphorylation, showed reduced condensate formation (Fang *et al.*, 2022). In this regard, Tanja Schmidt generated two NPH3 mutant variants where either two serine residues (S469/S474) or five serine residues (S213/S223/S237/S469/S474) were exchanged to aspartate to generate phosphomimetic mutant variants. In both cases the serine residues were located in IDRs and microscopic analyses showed reduced condensate formation (Schmidt, 2022). Thus, it could be possible that “general” dephosphorylation of NPH3 is required for LLPS and formation of condensates upon BL irradiation.

However, the co-expression of NPH3-S744A and SAC1 discussed above, illustrates that the permanently “generally” phosphorylated NPH3-S744A localizes to condensates when the phospholipid composition of the PM is altered (Fig 3.12A + 3.21A). Furthermore, a recent publication by Kimura et al. in 2021 identified several serine residues as phosphorylation sites in NPH3 via MS analysis that were exchanged to glutamate, to generate a phosphomimetic mutant variant (Kimura *et al.*, 2021). This included four of the five serine residues analyzed by Tanja Schmidt (Kimura *et al.*, 2021; Schmidt, 2022). Here, the NPH3 phosphomimic version still was able to form condensates and was only impaired in the ability to relocalize to the PM (Kimura *et al.*, 2021). Altogether, this suggests that the phosphorylation status of NPH3 is not impairing condensate formation in the cytosol.

4.7 Cycling of NPH3 between the PM and cytosolic condensates upon BL is required for its function in the phototropic response

In 2015 it has been suggested NPH3 being present in cytosolic aggregates and in the "generally" dephosphorylated state represents the inactive form of the protein and Sullivan et al. supported this by considering PM-localizing versions of NPH3 to promote hypocotyl bending (Haga *et al.*, 2015; Sullivan *et al.*, 2019). The results obtained by Tanja Schmidt and Jutta Keicher demonstrate, however, that GFP:NPH3-S744A and GFP:NPH3ΔC28 are not able to fully restore the phototropic response in transgenic *nph3-7* lines despite the fact that they are localizing permanently to the PM and display a permanent "generally" phosphorylated state (Fig 3.20) (Reuter *et al.*, 2021; Schmidt, 2022). These data indicate that localization to the PM and "general" phosphorylation of NPH3 are not sufficient for the phototropic response (Fig 4.2). Both NPH3 variants are, however, able to partially restore the phototropic response (Reuter *et al.*, 2021; Schmidt, 2022). This residual activity could be due to the permanent PM localization, that could allow for a partial relocalization of the protein within the PM upon BL irradiation.

In addition to permanently PM localizing NPH3 variants, mutants permanently localizing to condensates were examined in regard of the phototropic response, their subcellular localization and phosphorylation status in transgenic *nph3-7* lines. Here, GFP:NPH3-4K/A displayed permanent condensate localization and "general" dephosphorylation in transgenic lines comparable to the transient expression in *N. benthamiana* (Fig 3.9B, Fig 3.23B, Fig 3.20). Tanja Schmidt and Jutta Keicher were able to prove that this NPH3 variant is also not able to restore the phototropic response (Reuter *et al.*, 2021; Schmidt, 2022). In addition, Prabha Manishankar confirmed that GFP:NPH3ΔC51, another mutant variant permanently localizing to condensates, is also not able to restore the phototropic response (Reuter *et al.*, 2021).

This clearly indicates that neither a permanent PM localization nor a permanent condensate formation of NPH3 is able to restore the phototropic response in *nph3-7* (Fig 4.2). GFP:NPH3 as well as GFP:NPH3ΔN54 – the mutant variant that is capable of PM association and condensate formation comparable to the WT – are able to restore the phototropic response (Fig. 3.20) (Reuter *et al.*, 2021; Schmidt, 2022). Therefore, we suggest that cycling of NPH3 between the PM in darkness and the cytosolic condensates in BL is crucial for the hypocotyl bending during phototropism (Fig 4.2).

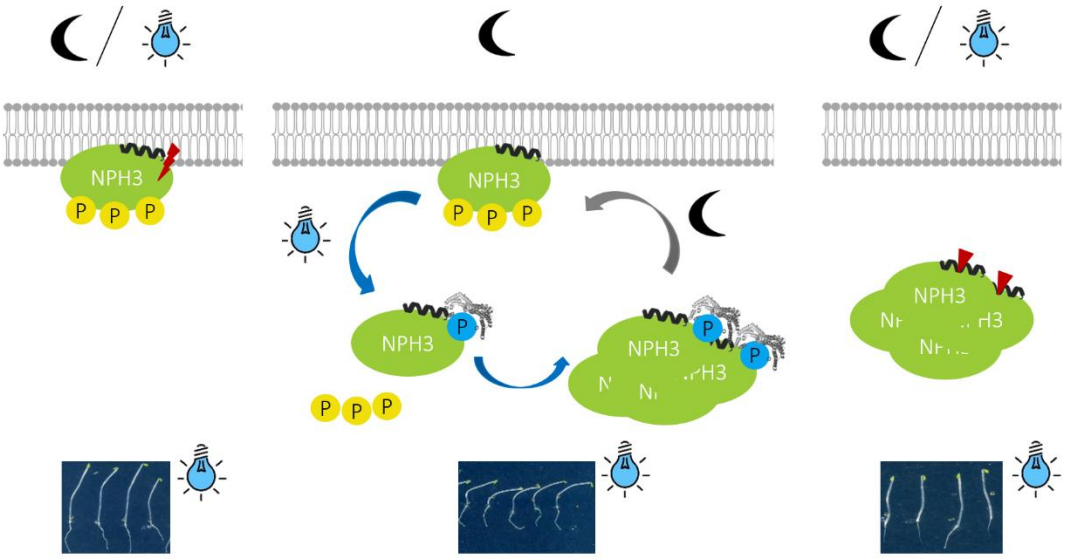

Figure 4. 2: Model of NPH3 subcellular localization, phosphorylation status and function under alternating light conditions. NPH3 attaches to the PM in darkness, upon BL irradiation it becomes phosphorylated at S744, 14-3-3 binding is initiated and NPH3 detaches from the PM. In the cytosol it forms membraneless condensates, the whole process is reversible in darkness. Cycling of NPH3 leads to a proper phototropic response (middle). Permanent PM association or permanent condensate localization is not restoring the phototropic response. Pictures of hypocotyl phototropism obtained from Tanja Schmidt. Schematic illustration modified from Reuter et al., 2021.

The photoreceptor phot1 is present at the PM in darkness and is partially internalized via endocytosis upon BL irradiation (Sakamoto and Briggs, 2002; Wan *et al.*, 2008; Kaiserli *et al.*, 2009). However, Preuten et al. prevented phot1 internalization and permanently attached it to the PM through myristoylation or farnesylation. These phot1 variants were still able to fully restore the phototropic response. Hence, BL-triggered changes in the subcellular localization of phot1 seem to be dispensable for the function of phot1 in the phototropic response (Preuten *et al.*, 2015). Cycling of NPH3 upon BL irradiation, however, is essential for its function during the phototropic response.

4.8 Perspectives of NPH3 and the NRL protein family contribution to PIN reallocation in the phototropic response

PIN-formed (PIN) proteins are auxin efflux carrier and PIN3, PIN4 and PIN7 are thought to be involved in the phototropic response (Willige *et al.*, 2013). The polar localization of PIN proteins is essential for the direction of auxin transport. PIN proteins display tissue-specific subcellular localization. PIN1 for example is basally localized in cells of the vasculature, whereas PIN2 shows an apical localization in epidermal cells (Grunewald and Friml, 2010; Christie and Murphy, 2013). PIN3 is mainly localizing lateral in endodermal cells, while PIN4 shows a polar localization in the root meristem (Grunewald and Friml, 2010; Ding *et al.*, 2011; Christie and Murphy, 2013).

Clustering of PIN proteins at the PM seems to be important for the maintenance of PIN polarity, since it is suggested to reduce the lateral diffusion of PIN proteins (Kleine-Vehn *et al.*, 2011; Marhava, 2022). PIN2 clusters for example are significantly reduced in a *pip5k1 pip5k2* double mutant and furthermore, PIN2 is able to directly interact with several phospholipids like Pi4P (Li *et al.*, 2021), suggesting that phospholipids contribute to the formation of PIN2 clusters (Li *et al.*, 2021).

However, clustering of PIN proteins at the PM is not sufficient to maintain PIN polarity, clathrin-mediated endocytosis is required as well (Kleine-Vehn *et al.*, 2011; Marhava, 2022). PIN proteins continuously cycle between the PM and endosomes via clathrin-dependent endocytosis (Dhonukshe *et al.*, 2007). Impairing the clathrin-dependent internalization of PIN2 by mutating a conserved tyrosine residue, partially caused a localization to the lateral side and not the apical side of epidermal cells, suggesting that clathrin-mediated endocytosis is required for maintaining PIN polarity (Kleine-Vehn *et al.*, 2011).

Besides recycling, clustering and endocytosis, PIN polarity and activity can be modulated by a molecular rheostat involving the AGC kinase PROTEIN KINASE ASSOCIATED WITH BRX (PAX) and BREVIS RADIX (BRX) (Marhava, 2022). At low auxin concentrations BRX is recruited to the PM by PAX and inhibits PIN-mediated auxin efflux (Marhava *et al.*, 2018; Marhava, 2022). With increasing auxin levels BRX dissociates from the PM and PAX can activate PIN proteins and thereby increase auxin efflux (Marhava *et al.*, 2018; Marhava, 2022). PAX activates PIN proteins via phosphorylation and thereby modulates local auxin transport and concentration in the protophloem (Marhava *et al.*, 2018).

In addition to PAX and BRX, also other members of the AGC kinase family like PID and D6PK are known to regulate PIN activity via phosphorylation (Sauer and Kleine-Vehn, 2019; Lanassa Bassukas, Xiao and Schwechheimer, 2022). Furthermore, AGC kinases like PID and D6PK

were suggested to act in a positive feedback loop together with PIN proteins and the NRL protein MAB4/MEL to maintain PIN polarity (Glanc *et al.*, 2021; Marhava, 2022). PIN proteins recruit MAB4/MEL proteins to the PM and this is enhanced by phosphorylation of PINs by PID and probably D6PK (Glanc *et al.*, 2021; Marhava, 2022). Recruitment of MAB4/MELs to the PM limits the lateral diffusion of PIN proteins and thereby maintains PIN polarity (Fig 4.3) (Glanc *et al.*, 2021; Sauer and Grebe, 2021). MAB4 was already shown to display a similar localization pattern as PIN proteins at the PM and it was suggested that members of the NPY subclade contribute to the regulation of PIN polarity at the PM and function as organizers of PIN polarity (Furutani *et al.*, 2011; Sauer and Grebe, 2021).

Establishment and maintenance of polarity in animal cells requires the partitioning-defective (PAR) proteins (Goldstein and Macara, 2007; Geldner, 2009; McCaffrey and Macara, 2009). The PAR proteins are highly conserved and therefore seem to play a crucial role in cell polarity in animal cells (Goldstein and Macara, 2007; McCaffrey and Macara, 2009). PAR proteins show an asymmetric localization at the PM and furthermore PAR proteins themselves are required to establish these defined domains they are localizing to (Goldstein and Macara, 2007; Geldner, 2009; McCaffrey and Macara, 2009). PAR1 for example phosphorylates PAR3, and drives the association of 14-3-3 proteins to PAR3 leading to a destabilization of PAR3 PM association. Thus, PAR3 is not able to localize to regions containing PAR1 and they are mutually excluding each other (Goldstein and Macara, 2007; McCaffrey and Macara, 2009). The small GTPase cellular division control protein 42 (CDC42) also plays an essential role in cell polarity in yeast and animal cells (Geldner, 2009; McCaffrey and Macara, 2009; Johnson, Jin and Lew, 2011). It interacts with PAR6 and seems to be essential for cell polarization (McCaffrey and Macara, 2009). CDC42 is thought to function in a feedback loop where activated CDC42 recruit actin filaments towards itself causing more activated CDC42 to be transported to the same region initiating a symmetry-breaking pathway (Geldner, 2009; Johnson, Jin and Lew, 2011).

PAR proteins and also CDC42 cannot be found in plants, therefore PIN proteins were discussed to represent the pendant of PAR proteins in plants (Geldner, 2009). Both PAR proteins and PIN proteins are required to induce polarity in their respective systems (Geldner, 2009). However, PIN proteins are not only functioning as polarity regulators, but are also auxin transporters and furthermore they are transmembrane proteins in contrast to PAR proteins (Geldner, 2009). Thus, differences exist between PIN proteins in plants and PAR proteins in the animal system (Geldner, 2009). Glanc et al. compared their findings about the NRL protein MAB4/MEL and its involvement in PIN polarity maintenance via a positive feedback loop with the symmetry breaking by CDC42 in yeast cells (Glanc *et al.*, 2021). This opens up the

question whether the NRL protein family in plants could function in a comparable way to PAR proteins and CDC42 in animal and yeast cells.

Lukas Dittiger was able to demonstrate that PIN proteins and NPH3 localize to distinct and diverse domains at the PM after co-expression in *N. benthamiana* (Lukas Dittiger, unpublished). They seem to mutually exclude each other at the PM (Lukas Dittiger, unpubslished). This could explain the residual activity of the permanently PM-localized NPH3 variants NPH3-S744A and NPH3ΔC28 (Reuter *et al.*, 2021; Schmidt, 2022), since it could allow for partial relocalization of the protein within the PM and thereby partially influencing the reallocation of PIN proteins. Cycling of NPH3 between the PM and cytosolic condensates and localization of NPH3 and PIN proteins to distinct and diverse domains upon BL irradiation, therefore, could be required for their specific functions during the phototropic response. Here, investigation of PIN polarity of different PINs expressed under the respective endogenous promoter in the loss-of-function mutant background of *nph3-7* would be very interesting to examine the impact of NPH3 on PIN polarity. Furthermore, it would be interesting to investigate the localization of PIN proteins in presence of a permanently PM-attached NPH3 variant like NPH3-S744A. These analyses should show whether the absence or permanent presence of NPH3 at the PM influence PIN polarity and their function in the phototropic response. Additionally, investigation of the protein dynamics at the PM via single particle tracking with photoactivated localization microscopy (sptPALM) could give new insights into the dynamic changes of NPH3 and PIN proteins localization upon BL irradiation.

The localization of NPH3 and PIN proteins to distinct domains is reminiscent of the localization pattern obtained for some of the PAR proteins. Interestingly,14-3-3 proteins are involved in the changes in subcellular polarity for PAR proteins and NPH3 and furthermore in PIN polarity. Changes in the subcellular localization of PAR proteins require interaction with 14-3-3 proteins (Goldstein and Macara, 2007; McCaffrey and Macara, 2009). The dynamic changes in subcellular localization of NPH3 as well depend on the association of 14-3-3 proteins with NPH3 upon BL treatment (Reuter *et al.*, 2021). Direct interaction between PIN proteins and 14-3-3 proteins could not be proven so far, however, 14-3-3 proteins are required to maintain PIN polarity (Keicher *et al.*, 2017).

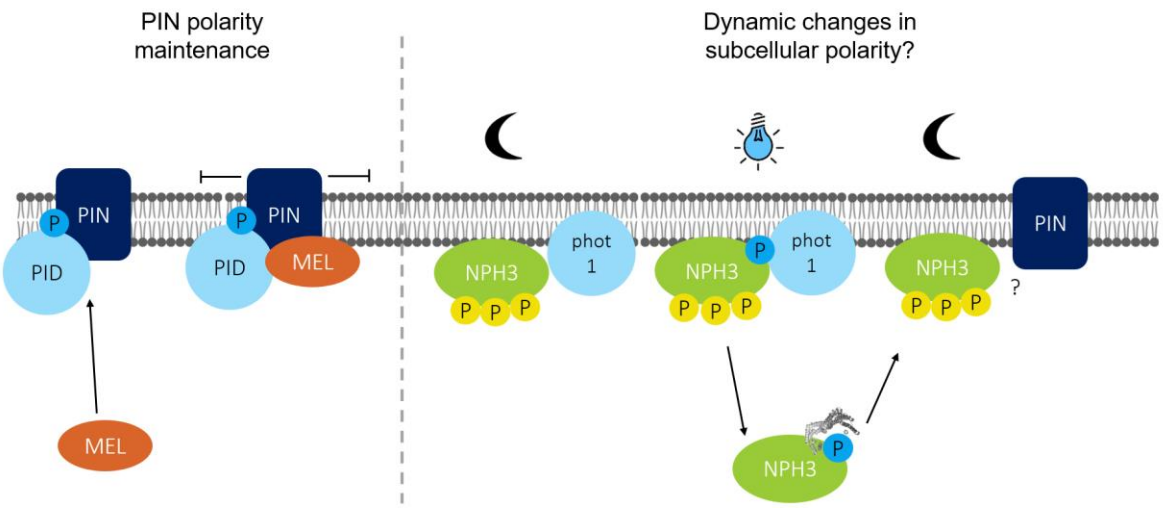

Figure 4. 3: Possible involvement of the NRL protein family in PIN reallocation at the PM. Left side: Modified schematic illustration of Glanc et al., 2021. MEL proteins are recruited to the PM by PIN proteins and PINOID (PID) in a PIN-phosphorylation enhanced manner. At the PM MEL proteins limit the lateral diffusion of PIN proteins. Right side: Cycling of NPH3 between the PM in darkness and membraneless condensates in cytosol upon BL treatment. The link between NPH3 and PINs remains elusive so far.

Hence, NRL proteins like NPH3 and MAB4/MEL in plants could fulfil a comparable function to PAR proteins in animal cells. However, NPH3 and MAB4/MEL seem to display different functions in localization of PIN proteins. MAB4/MEL is required to maintain PIN polarity (Glanc *et al.*, 2021; Sauer and Grebe, 2021) whereas the relocalization of NPH3 between the PM and cytosolic condensates could be involved in dynamic changes and PIN protein reallocation upon BL irradiation (Fig 4.3).

5 Summary

As sessile organisms, plants have to adapt to environmental changes such as varying light conditions. The ability to adapt their growth according to the direction of incoming light is called phototropic response. Perception of the light stimulus in *Arabidopsis thaliana* occurs via the BL photoreceptor phototropin 1 (phot1) followed by a reallocation of the PIN auxin efflux carriers at the PM. This causes a lateral auxin gradient associated with a higher auxin concentration on the shaded side of the shoot and resulting in a bending of the hypocotyl towards the light stimulus. So far, however, the link between light perception and reallocation of PIN proteins remains elusive.

NON PHOTOTROPIC HYPOCOTYL 3 (NPH3) is a plant specific protein that acts downstream of phot1 and is essential for the phototropic response. The hydrophilic NPH3 protein associates to the plasma membrane (PM) in darkness, but relocalizes to cytosolic particle-like structures upon BL irradiation. The molecular mechanism underlying the PM association of NPH3 and formation of particles, however, remains unknown. Former members of our group, furthermore, identified NPH3 as an interaction partner of 14-3-3 proteins that are known to interact in a sequence-specific and phosphorylation-dependent manner with their target proteins. Furthermore, they were able to identify the 14-3-3 binding site in the C-terminal region of NPH3. In darkness, NPH3 is present in its phosphorylated state and is dephosphorylated as a consequence of BL irradiation. Yet, Tanja Schmidt revealed that 14-3-3 and NPH3 interact in a strictly BL-dependent manner, suggesting a phosphorylation of the 14-3-3 binding site.

Modification of the phospholipid composition of the PM affected the PM association of NPH3 and led to particle-formation in the cytosol. Characterization of serial deletions of NPH3 furthermore demonstrated that the C-terminal region of NPH3 is required for PM association. Detailed examination of this region revealed that a C-terminal amphipathic helix causes PM association *in vivo* via electrostatic and hydrophobic interactions.

To analyze the functional significance of 14-3-3 association to NPH3, the subcellular localization of the NPH3 wild type (WT) protein and a mutant variant - incapable of 14-3-3 interaction (NPH3-S744A) - was examined via confocal laser scanning microscopy (CLSM). NPH3 localizes to the PM in darkness, upon BL irradiation it dissociates from the PM and forms cytosolic particle-like structures. Interestingly, NPH3-S744A is permanently associated to the PM. We propose that the interaction between NPH3 and 14-3-3 might cause a conformational change in the NPH3 C-terminal region preventing interaction of the amphipathic helix with the PM.

CLSM videos illustrate that detachment and formation of particle-like structures in the cytosol are separate and consecutive processes for NPH3. Results from our single-cell time-lapse approach and subcellular fractionation experiments, suggested that NPH3 forms membraneless, biomolecular condensates upon BL treatment. Microscopic analyses of N-terminal and C-terminal deletions moreover revealed that condensate formation of NPH3 requires two regions, the BTB domain and a region upstream of the CC domain. Furthermore, it showed that 14-3-3 interaction with NPH3 is not required for condensate formation in the cytosol.

The phosphorylation status of NPH3 was as well investigated in this thesis. The phosphorylation pattern of NPH3 and its light-induced changes are highly complex. The phot1-independent phosphorylation of NPH3 in darkness takes place at the PM. BL-irradiation first induces phosphorylation of the 14-3-3 binding site, followed by an association of 14-3-3 proteins. This interaction between NPH3 and 14-3-3 is essential for the PM dissociation and also for dephosphorylation of other amino acid residues. Formation of cytosolic condensates is, however not a consequence of the BL-induced dephosphorylation. Modification of the phosphorylation pattern as well as the altered subcellular localization of NPH3 upon BL treatment, are reversible after a retransfer to darkness. We propose, that light-dependent cycling of NPH3 between the PM and cytosolic condensates is essential for NPH3 function during the phototropic response.

Taken together this thesis gives novel insights into the highly dynamic process during the phototropic response and into the molecular determinants underlying NPH3 function.

6 Zusammenfassung

Als sessile Organismen müssen Pflanzen in der Lage sein, sich an biotische und abiotische Faktoren in ihrer Umgebung anzupassen. Die Fähigkeit, die Wachstumsrichtung gemäß dem einfallenden Licht auszurichten, wird als Phototropismus bezeichnet. Die Perzeption des Lichtreizes erfolgt in *Arabidopsis thaliana* durch den Blaulichtrezeptor Phototropin 1 (phot1). Letztendlich kommt es zu einer Umverteilung von PIN-Auxin-Efflux-Carriern in der Plasmamembran (PM). Dies führt zum Aufbau eines lateralen Auxingradienten mit einer höheren Auxinkonzentration auf der beschatteten Seite des Hypocotyls im Vergleich zu der belichteten Seite und resultiert in einer Krümmung des Hypocotyls in Richtung des Lichtreizes. Bisher sind die molekularen Mechanismen der Kopplung der Perzeption des Lichtreizes und der Umverteilung der PIN-Proteine jedoch unbekannt.

NON PHOTOTROPIC HYPOCOTYL 3 (NPH3) ist ein pflanzenspezifisches Protein das „downstream“ von phot1 agiert und essenziell für die phototrope Reaktion ist. In Dunkelheit

assoziiert das hydrophile NPH3 an die PM, lokalisiert nach Blaulicht (BL)-Belichtung aber in cytosolischen Partikeln. Die molekularen Mechanismen, die der PM-Assoziation von NPH3 und der Formation der Partikel zu Grunde liegen, konnten bisher nicht identifiziert werden. Ehemalige Mitglieder der Arbeitsgruppe haben NPH3 zudem als Interaktionspartner von 14-3-3 Proteinen und außerdem die 14-3-3 Bindestelle in der C-terminalen Region von NPH3 identifiziert. Diese interagieren meist sequenz-spezifisch und phosphorylierungs-abhängig mit ihren Interaktionspartnern. Des Weiteren war bekannt, dass NPH3 in Dunkelheit phosphoryliert vorliegt und als Folge einer BL-Bestrahlung dephosphoryliert wird. Die von Tanja Schmidt gezeigte strikt BL-abhängige Interaktion zwischen NPH3 und 14-3-3 weist jedoch auf eine Phosphorylierung der 14-3-3 Bindestelle hin.

Untersuchungen zur PM-Assoziation mittels Modifikationen der Phospholipid Zusammensetzung der PM führten zu einer Mislokalisierung von NPH3 in cytosolische Partikel. Des Weiteren zeigten serielle Deletionen von NPH3, dass die C-terminale Region von NPH3 essentiell für die PM-Assoziation ist. Detaillierte Untersuchungen dieser Region machten deutlich, dass eine amphipatische Helix durch elektrostatische und hydrophobe Interaktionen die PM-Assoziation von NPH3 *in vivo* bedingt.
Um den Effekt der Interaktion von 14-3-3 und NPH3 zu analysieren, wurde im Rahmen dieser Arbeit die subzelluläre Lokalisierung von NPH3 und NPH3-S744A - eine Variante, die nicht mit 14-3-3 Proteinen interagieren kann – mittels konfokaler Laser-Scanning-Mikroskopie (CLSM) untersucht. NPH3 lokalisiert in Dunkelheit an der PM, dissoziiert nach BL-Bestrahlung von der PM und formt cytosolische Partikel. NPH3-S744A hingegen zeigt eine permanente PM-Assoziation. Die Interaktion von NPH3 und 14-3-3 könnte also eine Konformationsänderung in der C-terminalen Region auslösen, die ein Interaktion der amphipatischen Helix mit der PM unterbindet.
CLSM-Videos im Rahmen dieser Arbeit zeigen, dass PM-Dissoziation und die Ausbildung der Partikel im Cytoplasma separate und aufeinander folgende Prozesse sind. Um die Partikel genauer zu untersuchen, wurde ein „Single-Cell Time-Lapse“ Experiment und des Weiteren eine subzelluläre Fraktionierung durchgeführt, die nahelegen, dass NPH3 nach BL biomolekulare, membranlose Kondensate im Cytosol ausbildet. Mikroskopische Analysen von Deletionen der N-terminalen oder C-terminalen Region von NPH3 ergaben überdies, dass die N-terminale BTB-Domäne und eine Region zwischen der NPH3-Domäne und der CC-Domäne für die Bildung der Kondensate notwendig sind. Des Weiteren erfolgt die Kondensatbildung im Cytosol unabhängig von der Interaktion mit 14-3-3 Proteinen.
Im Rahmen dieser Arbeit wurde auch der Phosphorylierungs-Status von NPH3 untersucht. Es konnte gezeigt werden, dass die Phosphorylierungsmuster von NPH3 und lichtinduzierte Veränderungen derselben, äußerst komplex sind. Die phot1-unabhängige Phosphorylierung

von NPH3 im Dunkeln findet ausschließlich an der PM statt. Die BL-Behandlung induziert primär eine Phosphorylierung der 14-3-3 Bindestelle, die nachfolgende Assoziation von 14-3-3 ist für eine die Dissoziation von der PM und Dephosphorylierung anderer Aminosäurereste essentiell. Die Ausbildung cytosolischer Kondensate ist jedoch keine Konsequenz der Dephosphorylierung. Sowohl die Modifikationen des Phosphorylierungsmusters als auch die veränderte subzelluläre Lokalisierung von NPH3 nach BL-Bestrahlung, sind durch einen Retransfer in Dunkelheit reversibel. Die lichtabhängige Zirkulation von NPH3 zwischen der PM und cytosolischen Kondensaten könnte essentiell sein für die Funktion von NPH3 während der phototropen Reaktion.

Alles in allem geben uns die Ergebnisse dieser Arbeit neue Einsichten in den hoch dynamischen Prozess während der phototropen Reaktion und in die molekularen Faktoren, die die Funktion von NPH3 bestimmen.

7 List of references

Albagli, O., Dhordain, P., Deweindt, C., Lecocq, G. and Leprince, D. (1995) 'The BTB/POZ domain: a new protein-protein interaction motif common to DNA- and actin-binding proteins', *Cell Growth Differ,* 6(9), pp. 1193-8.

Albert, I., Böhm, H., Albert, M., Feiler, C. E., Imkampe, J., Wallmeroth, N., Brancato, C., Raaymakers, T. M., Oome, S., Zhang, H., Krol, E., Grefen, C., Gust, A. A., Chai, J., Hedrich, R., Van den Ackerveken, G. and Nürnberger, T. (2015) 'An RLP23-SOBIR1-BAK1 complex mediates NLP-triggered immunity', *Nat Plants,* 1, pp. 15140.

Alberti, S. (2017) 'Phase separation in biology', *Curr Biol,* 27(20), pp. R1097-R1102.

AlQuraishi, M. (2021) 'Protein-structure prediction revolutionized', *Nature,* 596(7873), pp. 487-488.

Bachmann, M., Huber, J. L., Liao, P. C., Gage, D. A. and Huber, S. C. (1996) 'The inhibitor protein of phosphorylated nitrate reductase from spinach (Spinacia oleracea) leaves is a 14-3-3 protein', *FEBS Lett,* 387(2-3), pp. 127-31.

Banani, S. F., Lee, H. O., Hyman, A. A. and Rosen, M. K. (2017) 'Biomolecular condensates: organizers of cellular biochemistry', *Nat Rev Mol Cell Biol,* 18(5), pp. 285-298.

Barbosa, I. C., Shikata, H., Zourelidou, M., Heilmann, M., Heilmann, I. and Schwechheimer, C. (2016) 'Phospholipid composition and a polybasic motif determine D6 PROTEIN KINASE polar association with the plasma membrane and tropic responses', *Development,* 143(24), pp. 4687-4700.

Binder, A., Lambert, J., Morbitzer, R., Popp, C., Ott, T., Lahaye, T. and Parniske, M. (2014) 'A modular plasmid assembly kit for multigene expression, gene silencing and silencing rescue in plants', *PLoS One,* 9(2), pp. e88218.

Blakeslee, J. J., Bandyopadhyay, A., Lee, O. R., Mravec, J., Titapiwatanakun, B., Sauer, M., Makam, S. N., Cheng, Y., Bouchard, R., Adamec, J., Geisler, M., Nagashima, A., Sakai, T., Martinoia, E., Friml, J., Peer, W. A. and Murphy, A. S. (2007) 'Interactions among PIN-FORMED and P-glycoprotein auxin transporters in Arabidopsis', *Plant Cell,* 19(1), pp. 131-47.
Briggs, W. R. (2014) 'Phototropism: some history, some puzzles, and a look ahead', *Plant Physiol,* 164(1), pp. 13-23.

Brzeska, H., Guag, J., Remmert, K., Chacko, S. and Korn, E. D. (2010) 'An experimentally based computer search identifies unstructured membrane-binding sites in proteins: application to class I myosins, PAKS, and CARMIL', *J Biol Chem,* 285(8), pp. 5738-47.

Cashmore, A. R., Jarillo, J. A., Wu, Y. J. and Liu, D. (1999) 'Cryptochromes: blue light receptors for plants and animals', *Science,* 284(5415), pp. 760-5.

Chaves, I., Pokorny, R., Byrdin, M., Hoang, N., Ritz, T., Brettel, K., Essen, L. O., van der Horst, G. T., Batschauer, A. and Ahmad, M. (2011) 'The cryptochromes: blue light photoreceptors in plants and animals', *Annu Rev Plant Biol,* 62, pp. 335-64.

Chi, J. C., Roeper, J., Schwarz, G. and Fischer-Schrader, K. (2015) 'Dual binding of 14-3-3 protein regulates Arabidopsis nitrate reductase activity', *J Biol Inorg Chem,* 20(2), pp. 277-86.

Christie, J. M. (2007) 'Phototropin blue-light receptors', *Annu Rev Plant Biol,* 58, pp. 21-45.

Christie, J. M., Blackwood, L., Petersen, J. and Sullivan, S. (2015) 'Plant flavoprotein photoreceptors', *Plant Cell Physiol,* 56(3), pp. 401-13.

Christie, J. M. and Murphy, A. S. (2013) 'Shoot phototropism in higher plants: new light through old concepts', *Am J Bot,* 100(1), pp. 35-46.

Christie, J. M., Reymond, P., Powell, G. K., Bernasconi, P., Raibekas, A. A., Liscum, E. and Briggs, W. R. (1998) 'Arabidopsis NPH1: a flavoprotein with the properties of a photoreceptor for phototropism', *Science,* 282(5394), pp. 1698-701.

Christie, J. M., Salomon, M., Nozue, K., Wada, M. and Briggs, W. R. (1999) 'LOV (light, oxygen, or voltage) domains of the blue-light photoreceptor phototropin (nph1): binding sites for the chromophore flavin mononucleotide', *Proc Natl Acad Sci U S A,* 96(15), pp. 8779-83.

Christie, J. M., Suetsugu, N., Sullivan, S. and Wada, M. (2018) 'Shining Light on the Function of NPH3/RPT2-Like Proteins in Phototropin Signaling', *Plant Physiol,* 176(2), pp. 1015-1024.

Coblitz, B., Shikano, S., Wu, M., Gabelli, S. B., Cockrell, L. M., Spieker, M., Hanyu, Y., Fu, H., Amzel, L. M. and Li, M. (2005) 'C-terminal recognition by 14-3-3 proteins for surface expression of membrane receptors', *J Biol Chem,* 280(43), pp. 36263-72.

Coblitz, B., Wu, M., Shikano, S. and Li, M. (2006) 'C-terminal binding: an expanded repertoire and function of 14-3-3 proteins', *FEBS Lett,* 580(6), pp. 1531-5.

Cuevas-Velazquez, C. L. and Dinneny, J. R. (2018) 'Organization out of disorder: liquid-liquid phase separation in plants', *Curr Opin Plant Biol,* 45(Pt A), pp. 68-74.

Darwin, C. and Darwin, F. 1880. The Power of Movement in Plants.

de Carbonnel, M., Davis, P., Roelfsema, M. R., Inoue, S., Schepens, I., Lariguet, P., Geisler, M., Shimazaki, K., Hangarter, R. and Fankhauser, C. (2010) 'The Arabidopsis PHYTOCHROME KINASE SUBSTRATE2 protein is a phototropin signaling element that regulates leaf flattening and leaf positioning', *Plant Physiol,* 152(3), pp. 1391-405.

DeLille, J. M., Sehnke, P. C. and Ferl, R. J. (2001) 'The arabidopsis 14-3-3 family of signaling regulators', *Plant Physiol,* 126(1), pp. 35-8.

Demarsy, E., Schepens, I., Okajima, K., Hersch, M., Bergmann, S., Christie, J., Shimazaki, K., Tokutomi, S. and Fankhauser, C. (2012) 'Phytochrome Kinase Substrate 4 is phosphorylated by the phototropin 1 photoreceptor', *EMBO J,* 31(16), pp. 3457-67.

Dhonukshe, P., Aniento, F., Hwang, I., Robinson, D. G., Mravec, J., Stierhof, Y. D. and Friml, J. (2007) 'Clathrin-mediated constitutive endocytosis of PIN auxin efflux carriers in Arabidopsis', *Curr Biol,* 17(6), pp. 520-7.

Ding, Z., Galván-Ampudia, C. S., Demarsy, E., Łangowski, Ł., Kleine-Vehn, J., Fan, Y., Morita, M. T., Tasaka, M., Fankhauser, C., Offringa, R. and Friml, J. (2011) 'Light-mediated polarization of the PIN3 auxin transporter for the phototropic response in Arabidopsis', *Nat Cell Biol,* 13(4), pp. 447-52.

Emenecker, R. J., Holehouse, A. S. and Strader, L. C. (2021) 'Biological Phase Separation and Biomolecular Condensates in Plants', *Annu Rev Plant Biol,* 72, pp. 17-46.

ENNIS, H. L. and LUBIN, M. (1964) 'CYCLOHEXIMIDE: ASPECTS OF INHIBITION OF PROTEIN SYNTHESIS IN MAMMALIAN CELLS', *Science,* 146(3650), pp. 1474-6.

Fairn, G. D., Ogata, K., Botelho, R. J., Stahl, P. D., Anderson, R. A., De Camilli, P., Meyer, T., Wodak, S. and Grinstein, S. (2009) 'An electrostatic switch displaces phosphatidylinositol phosphate kinases from the membrane during phagocytosis', *J Cell Biol,* 187(5), pp. 701-14.

Fang, X. D., Gao, Q., Zang, Y., Qiao, J. H., Gao, D. M., Xu, W. Y., Wang, Y., Li, D. and Wang, X. B. (2022) 'Host casein kinase 1-mediated phosphorylation modulates phase separation of a rhabdovirus phosphoprotein and virus infection', *Elife,* 11.

Ferl, R. J. (1996) '14-3-3 PROTEINS AND SIGNAL TRANSDUCTION', *Annu Rev Plant Physiol Plant Mol Biol,* 47, pp. 49-73.

Ferl, R. J., Manak, M. S. and Reyes, M. F. (2002) 'The 14-3-3s', *Genome Biol,* 3(7), pp. REVIEWS3010.

Furutani, M., Kajiwara, T., Kato, T., Treml, B. S., Stockum, C., Torres-Ruiz, R. A. and Tasaka, M. (2007) 'The gene MACCHI-BOU 4/ENHANCER OF PINOID encodes a NPH3-like protein and reveals similarities between organogenesis and phototropism at the molecular level', *Development,* 134(21), pp. 3849-59.

Furutani, M., Sakamoto, N., Yoshida, S., Kajiwara, T., Robert, H. S., Friml, J. and Tasaka, M. (2011) 'Polar-localized NPH3-like proteins regulate polarity and endocytosis of PIN-FORMED auxin efflux carriers', *Development,* 138(10), pp. 2069-78.

Gampala, S. S., Kim, T. W., He, J. X., Tang, W., Deng, Z., Bai, M. Y., Guan, S., Lalonde, S., Sun, Y., Gendron, J. M., Chen, H., Shibagaki, N., Ferl, R. J., Ehrhardt, D., Chong, K., Burlingame, A. L. and Wang, Z. Y. (2007) 'An essential role for 14-3-3 proteins in brassinosteroid signal transduction in Arabidopsis', *Dev Cell,* 13(2), pp. 177-89.

Geisler, M., Blakeslee, J. J., Bouchard, R., Lee, O. R., Vincenzetti, V., Bandyopadhyay, A., Titapiwatanakun, B., Peer, W. A., Bailly, A., Richards, E. L., Ejendal, K. F., Smith, A. P., Baroux, C., Grossniklaus, U., Müller, A., Hrycyna, C. A., Dudler, R., Murphy, A. S. and Martinoia, E. (2005) 'Cellular efflux of auxin catalyzed by the Arabidopsis MDR/PGP transporter AtPGP1', *Plant J,* 44(2), pp. 179-94.

Geldner, N. (2009) 'Cell polarity in plants: a PARspective on PINs', *Curr Opin Plant Biol,* 12(1), pp. 42-8.

Glanc, M., Van Gelderen, K., Hoermayer, L., Tan, S., Naramoto, S., Zhang, X., Domjan, D., Včelařová, L., Hauschild, R., Johnson, A., de Koning, E., van Dop, M., Rademacher, E., Janson, S., Wei, X., Molnár, G., Fendrych, M., De Rybel, B., Offringa, R. and Friml, J. (2021) 'AGC kinases and MAB4/MEL proteins maintain PIN polarity by limiting lateral diffusion in plant cells', *Curr Biol,* 31(9), pp. 1918-1930.e5.

Goldstein, B. and Macara, I. G. (2007) 'The PAR proteins: fundamental players in animal cell polarization', *Dev Cell,* 13(5), pp. 609-622.

Grefen, C., Donald, N., Hashimoto, K., Kudla, J., Schumacher, K. and Blatt, M. R. (2010) 'A ubiquitin-10 promoter-based vector set for fluorescent protein tagging facilitates temporal stability and native protein distribution in transient and stable expression studies', *Plant J,* 64(2), pp. 355-65.

Gronnier, J., Crowet, J. M., Habenstein, B., Nasir, M. N., Bayle, V., Hosy, E., Platre, M. P., Gouguet, P., Raffaele, S., Martinez, D., Grelard, A., Loquet, A., Simon-Plas, F., Gerbeau-Pissot, P., Der, C., Bayer, E. M., Jaillais, Y., Deleu, M., Germain, V., Lins, L. and Mongrand, S. (2017) 'Structural basis for plant plasma membrane protein dynamics and organization into functional nanodomains', *Elife,* 6.

Grunewald, W. and Friml, J. (2010) 'The march of the PINs: developmental plasticity by dynamic polar targeting in plant cells', *EMBO J,* 29(16), pp. 2700-14.

Haga, K., Takano, M., Neumann, R. and Iino, M. (2005) 'The Rice COLEOPTILE PHOTOTROPISM1 gene encoding an ortholog of Arabidopsis NPH3 is required for phototropism of coleoptiles and lateral translocation of auxin', *Plant Cell,* 17(1), pp. 103-15.

Haga, K., Tsuchida-Mayama, T., Yamada, M. and Sakai, T. (2015) 'Arabidopsis ROOT PHOTOTROPISM2 Contributes to the Adaptation to High-Intensity Light in Phototropic Responses', *Plant Cell,* 27(4), pp. 1098-112.

Harper, R. M., Stowe-Evans, E. L., Luesse, D. R., Muto, H., Tatematsu, K., Watahiki, M. K., Yamamoto, K. and Liscum, E. (2000) 'The NPH4 locus encodes the auxin response factor ARF7, a conditional regulator of differential growth in aerial Arabidopsis tissue', *Plant Cell,* 12(5), pp. 757-70.

Hart, J. E., Sullivan, S., Hermanowicz, P., Petersen, J., Diaz-Ramos, L. A., Hoey, D. J., Łabuz, J. and Christie, J. M. (2019) 'Engineering the phototropin photocycle improves photoreceptor performance and plant biomass production', *Proc Natl Acad Sci U S A,* 116(25), pp. 12550-12557.

Hecker, A., Wallmeroth, N., Peter, S., Blatt, M. R., Harter, K. and Grefen, C. (2015) 'Binary 2in1 Vectors Improve in Planta (Co)localization and Dynamic Protein Interaction Studies', *Plant Physiol,* 168(3), pp. 776-87.

Hoang, N., Bouly, J. P. and Ahmad, M. (2008) 'Evidence of a light-sensing role for folate in Arabidopsis cryptochrome blue-light receptors', *Mol Plant,* 1(1), pp. 68-74.

Inada, S., Ohgishi, M., Mayama, T., Okada, K. and Sakai, T. (2004) 'RPT2 is a signal transducer involved in phototropic response and stomatal opening by association with phototropin 1 in Arabidopsis thaliana', *Plant Cell,* 16(4), pp. 887-96.

Inoue, S., Kinoshita, T., Matsumoto, M., Nakayama, K. I., Doi, M. and Shimazaki, K. (2008a) 'Blue light-induced autophosphorylation of phototropin is a primary step for signaling', *Proc Natl Acad Sci U S A,* 105(14), pp. 5626-31.

Inoue, S., Kinoshita, T., Takemiya, A., Doi, M. and Shimazaki, K. (2008b) 'Leaf positioning of Arabidopsis in response to blue light', *Mol Plant,* 1(1), pp. 15-26.

Jahn, T., Fuglsang, A. T., Olsson, A., Brüntrup, I. M., Collinge, D. B., Volkmann, D., Sommarin, M., Palmgren, M. G. and Larsson, C. (1997) 'The 14-3-3 protein interacts directly with the C-terminal region of the plant plasma membrane H(+)-ATPase', *Plant Cell,* 9(10), pp. 1805-14.

Jaillais, Y. and Ott, T. (2020) 'The Nanoscale Organization of the Plasma Membrane and Its Importance in Signaling: A Proteolipid Perspective', *Plant Physiol,* 182(4), pp. 1682-1696.

Jaspert, N., Throm, C. and Oecking, C. (2011) 'Arabidopsis 14-3-3 proteins: fascinating and less fascinating aspects', *Front Plant Sci,* 2, pp. 96.

Jenkins, G. I. (2014) 'The UV-B photoreceptor UVR8: from structure to physiology', *Plant Cell,* 26(1), pp. 21-37.

Johnson, J. M., Jin, M. and Lew, D. J. (2011) 'Symmetry breaking and the establishment of cell polarity in budding yeast', *Curr Opin Genet Dev,* 21(6), pp. 740-6.

Jumper, J., Evans, R., Pritzel, A., Green, T., Figurnov, M., Ronneberger, O., Tunyasuvunakool, K., Bates, R., Žídek, A., Potapenko, A., Bridgland, A., Meyer, C., Kohl, S. A. A., Ballard, A. J., Cowie, A., Romera-Paredes, B., Nikolov, S., Jain, R., Adler, J., Back, T., Petersen, S., Reiman, D., Clancy, E., Zielinski, M., Steinegger, M., Pacholska, M., Berghammer, T., Bodenstein, S., Silver, D., Vinyals, O., Senior, A. W., Kavukcuoglu, K., Kohli, P. and Hassabis, D. (2021) 'Highly accurate protein structure prediction with AlphaFold', *Nature,* 596(7873), pp. 583-589.

Kaiserli, E., Sullivan, S., Jones, M. A., Feeney, K. A. and Christie, J. M. (2009) 'Domain swapping to assess the mechanistic basis of Arabidopsis phototropin 1 receptor kinase activation and endocytosis by blue light', *Plant Cell,* 21(10), pp. 3226-44.

Kansup, J., Tsugama, D., Liu, S. and Takano, T. (2014) 'Arabidopsis G-protein β subunit AGB1 interacts with NPH3 and is involved in phototropism', *Biochem Biophys Res Commun,* 445(1), pp. 54-7.

Karimi, M., Depicker, A. and Hilson, P. (2007) 'Recombinational cloning with plant gateway vectors', *Plant Physiol,* 145(4), pp. 1144-54.

Keicher, J., Jaspert, N., Weckermann, K., Möller, C., Throm, C., Kintzi, A. and Oecking, C. (2017) '14-3-3 epsilon members contribute to polarity of PIN auxin carrier and auxin transport-related development', *Elife,* 6.

Kimura, T., Haga, K., Nomura, Y., Higaki, T., Nakagami, H. and Sakai, T. (2021) 'Phosphorylation of NONPHOTOTROPIC HYPOCOTYL3 affects photosensory adaptation during the phototropic response', *Plant Physiol,* 187(2), pp. 981-995.

Kimura, T., Tsuchida-Mayama, T., Imai, H., Okajima, K., Ito, K. and Sakai, T. (2020) 'Arabidopsis ROOT PHOTOTROPISM2 Is a Light-Dependent Dynamic Modulator of Phototropin1', *Plant Cell,* 32(6), pp. 2004-2019.

Kinoshita, T., Doi, M., Suetsugu, N., Kagawa, T., Wada, M. and Shimazaki, K. (2001) 'Phot1 and phot2 mediate blue light regulation of stomatal opening', *Nature,* 414(6864), pp. 656-60.
Kinoshita, T., Emi, T., Tominaga, M., Sakamoto, K., Shigenaga, A., Doi, M. and Shimazaki, K. (2003) 'Blue-light- and phosphorylation-dependent binding of a 14-3-3 protein to phototropins in stomatal guard cells of broad bean', *Plant Physiol,* 133(4), pp. 1453-63.

Kinoshita, T. and Shimazaki, K. (1999) 'Blue light activates the plasma membrane H(+)-ATPase by phosphorylation of the C-terminus in stomatal guard cells', *EMBO J,* 18(20), pp. 5548-58.

Kleine-Vehn, J., Wabnik, K., Martinière, A., Łangowski, Ł., Willig, K., Naramoto, S., Leitner, J., Tanaka, H., Jakobs, S., Robert, S., Luschnig, C., Govaerts, W., Hell, S. W., Runions, J. and Friml, J. (2011) 'Recycling, clustering, and endocytosis jointly maintain PIN auxin carrier polarity at the plasma membrane', *Mol Syst Biol,* 7, pp. 540.

Koncz, C. and Schell, J. 1986. The Promoter of TI-DNA Gene 5 Controls the Tissue-Specific Expression of Chimeric Genes Carried by a Novel Type of Agrobacterium Binary Vector. Molecular and General Genetics.

Kong, S. G., Suzuki, T., Tamura, K., Mochizuki, N., Hara-Nishimura, I. and Nagatani, A. (2006) 'Blue light-induced association of phototropin 2 with the Golgi apparatus', *Plant J,* 45(6), pp. 994-1005.

Krecek, P., Skupa, P., Libus, J., Naramoto, S., Tejos, R., Friml, J. and Zazímalová, E. (2009) 'The PIN-FORMED (PIN) protein family of auxin transporters', *Genome Biol,* 10(12), pp. 249.
Lanassa Bassukas, A. E., Xiao, Y. and Schwechheimer, C. (2022) 'Phosphorylation control of PIN auxin transporters', *Curr Opin Plant Biol,* 65, pp. 102146.

Lariguet, P., Schepens, I., Hodgson, D., Pedmale, U. V., Trevisan, M., Kami, C., de Carbonnel, M., Alonso, J. M., Ecker, J. R., Liscum, E. and Fankhauser, C. (2006) 'PHYTOCHROME KINASE SUBSTRATE 1 is a phototropin 1 binding protein required for phototropism', *Proc Natl Acad Sci U S A,* 103(26), pp. 10134-9.

Legris, M. and Boccaccini, A. (2020) 'Stem phototropism toward blue and ultraviolet light', *Physiol Plant,* 169(3), pp. 357-368.

Li, H., von Wangenheim, D., Zhang, X., Tan, S., Darwish-Miranda, N., Naramoto, S., Wabnik, K., De Rycke, R., Kaufmann, W. A., Gütl, D., Tejos, R., Grones, P., Ke, M., Chen, X., Dettmer, J. and Friml, J. (2021) 'Cellular requirements for PIN polar cargo clustering in Arabidopsis thaliana', *New Phytol,* 229(1), pp. 351-369.

Liscum, E. and Briggs, W. R. (1995) 'Mutations in the NPH1 locus of Arabidopsis disrupt the perception of phototropic stimuli', *Plant Cell,* 7(4), pp. 473-85.

Liu, A., Sui, D., Wu, D. and Hu, J. (2016) 'The activation loop of PIP5K functions as a membrane sensor essential for lipid substrate processing', *Sci Adv,* 2(11), pp. e1600925.

Liu, H., Liu, B., Zhao, C., Pepper, M. and Lin, C. (2011) 'The action mechanisms of plant cryptochromes', *Trends Plant Sci,* 16(12), pp. 684-91.

Lupas, A. (1996) 'Coiled coils: new structures and new functions', *Trends Biochem Sci,* 21(10), pp. 375-82.

Lupas, A. N. and Bassler, J. (2017) 'Coiled Coils - A Model System for the 21st Century', *Trends Biochem Sci,* 42(2), pp. 130-140.

Mackintosh, C. (2004) 'Dynamic interactions between 14-3-3 proteins and phosphoproteins regulate diverse cellular processes', *Biochem J,* 381(Pt 2), pp. 329-42.

Marhava, P. (2022) 'Recent developments in the understanding of PIN polarity', *New Phytol,* 233(2), pp. 624-630.

Marhava, P., Bassukas, A. E. L., Zourelidou, M., Kolb, M., Moret, B., Fastner, A., Schulze, W. X., Cattaneo, P., Hammes, U. Z., Schwechheimer, C. and Hardtke, C. S. (2018) 'A molecular rheostat adjusts auxin flux to promote root protophloem differentiation', *Nature,* 558(7709), pp. 297-300.

Martinez, D., Legrand, A., Gronnier, J., Decossas, M., Gouguet, P., Lambert, O., Berbon, M., Verron, L., Grélard, A., Germain, V., Loquet, A., Mongrand, S. and Habenstein, B. (2019) 'Coiled-coil oligomerization controls localization of the plasma membrane REMORINs', *J Struct Biol,* 206(1), pp. 12-19.

Matsuoka, D. and Tokutomi, S. (2005) 'Blue light-regulated molecular switch of Ser/Thr kinase in phototropin', *Proc Natl Acad Sci U S A,* 102(37), pp. 13337-42.

McCaffrey, L. M. and Macara, I. G. (2009) 'Widely conserved signaling pathways in the establishment of cell polarity', *Cold Spring Harb Perspect Biol,* 1(2), pp. a001370.

Mergner, J., Frejno, M., List, M., Papacek, M., Chen, X., Chaudhary, A., Samaras, P., Richter, S., Shikata, H., Messerer, M., Lang, D., Altmann, S., Cyprys, P., Zolg, D. P., Mathieson, T., Bantscheff, M., Hazarika, R. R., Schmidt, T., Dawid, C., Dunkel, A., Hofmann, T., Sprunck, S., Falter-Braun, P., Johannes, F., Mayer, K. F. X., Jürgens, G., Wilhelm, M., Baumbach, J., Grill, E., Schneitz, K., Schwechheimer, C. and Kuster, B. (2020) 'Mass-spectrometry-based draft of the Arabidopsis proteome', *Nature,* 579(7799), pp. 409-414.

Motchoulski, A. and Liscum, E. (1999) 'Arabidopsis NPH3: A NPH1 photoreceptor-interacting protein essential for phototropism', *Science,* 286(5441), pp. 961-4.

Nishimura, T., Gecht, M., Covino, R., Hummer, G., Surma, M. A., Klose, C., Arai, H., Kono, N. and Stefan, C. J. (2019) 'Osh Proteins Control Nanoscale Lipid Organization Necessary for PI(4,5)P', *Mol Cell,* 75(5), pp. 1043-1057.e8.

Oecking, C. and Jaspert, N. (2009) 'Plant 14-3-3 proteins catch up with their mammalian orthologs', *Curr Opin Plant Biol,* 12(6), pp. 760-5.

Oecking, C., Piotrowski, M., Hagemeier, J. and Hagemann, K. 1997. Topology and target interaction of the fusicoccin-binding 14-3-3 homologs of Commelina communis. The Plant Journal.

Okada, K., Ueda, J., Komaki, M. K., Bell, C. J. and Shimura, Y. (1991) 'Requirement of the Auxin Polar Transport System in Early Stages of Arabidopsis Floral Bud Formation', *Plant Cell,* 3(7), pp. 677-684.

Park, M., Touihri, S., Müller, I., Mayer, U. and Jürgens, G. (2012) 'Sec1/Munc18 protein stabilizes fusion-competent syntaxin for membrane fusion in Arabidopsis cytokinesis', *Dev Cell,* 22(5), pp. 989-1000.

Pedmale, U. V., Celaya, R. B. and Liscum, E. (2010) 'Phototropism: mechanism and outcomes', *Arabidopsis Book,* 8, pp. e0125.

Pedmale, U. V. and Liscum, E. (2007) 'Regulation of phototropic signaling in Arabidopsis via phosphorylation state changes in the phototropin 1-interacting protein NPH3', *J Biol Chem,* 282(27), pp. 19992-20001.

Perraki, A., Cacas, J. L., Crowet, J. M., Lins, L., Castroviejo, M., German-Retana, S., Mongrand, S. and Raffaele, S. (2012) 'Plasma membrane localization of Solanum tuberosum remorin from group 1, homolog 3 is mediated by conformational changes in a novel C-terminal anchor and required for the restriction of potato virus X movement]', *Plant Physiol,* 160(2), pp. 624-37.

Petricka, J. J., Clay, N. K. and Nelson, T. M. (2008) 'Vein patterning screens and the defectively organized tributaries mutants in Arabidopsis thaliana', *Plant J,* 56(2), pp. 251-263.

Platre, M. P., Noack, L. C., Doumane, M., Bayle, V., Simon, M. L. A., Maneta-Peyret, L., Fouillen, L., Stanislas, T., Armengot, L., Pejchar, P., Caillaud, M. C., Potocký, M., Čopič, A., Moreau, P. and Jaillais, Y. (2018) 'A Combinatorial Lipid Code Shapes the Electrostatic Landscape of Plant Endomembranes', *Dev Cell,* 45(4), pp. 465-480.e11.

Powers, S. K., Holehouse, A. S., Korasick, D. A., Schreiber, K. H., Clark, N. M., Jing, H., Emenecker, R., Han, S., Tycksen, E., Hwang, I., Sozzani, R., Jez, J. M., Pappu, R. V. and

Strader, L. C. (2019) 'Nucleo-cytoplasmic Partitioning of ARF Proteins Controls Auxin Responses in Arabidopsis thaliana', *Mol Cell,* 76(1), pp. 177-190.e5.

Preuten, T., Blackwood, L., Christie, J. M. and Fankhauser, C. (2015) 'Lipid anchoring of Arabidopsis phototropin 1 to assess the functional significance of receptor internalization: should I stay or should I go?', *New Phytol,* 206(3), pp. 1038-1050.

Péret, B., Swarup, K., Ferguson, A., Seth, M., Yang, Y., Dhondt, S., James, N., Casimiro, I., Perry, P., Syed, A., Yang, H., Reemmer, J., Venison, E., Howells, C., Perez-Amador, M. A., Yun, J., Alonso, J., Beemster, G. T., Laplaze, L., Murphy, A., Bennett, M. J., Nielsen, E. and Swarup, R. (2012) 'AUX/LAX genes encode a family of auxin influx transporters that perform distinct functions during Arabidopsis development', *Plant Cell,* 24(7), pp. 2874-85.

Rakusová, H., Fendrych, M. and Friml, J. (2015) 'Intracellular trafficking and PIN-mediated cell polarity during tropic responses in plants', *Curr Opin Plant Biol,* 23, pp. 116-23.

Reuter, L., Schmidt, T., Manishankar, P., Throm, C., Keicher, J., Bock, A., Droste-Borel, I. and Oecking, C. (2021) 'Light-triggered and phosphorylation-dependent 14-3-3 association with NON-PHOTOTROPIC HYPOCOTYL 3 is required for hypocotyl phototropism', *Nat Commun,* 12(1), pp. 6128.

Roberts, D., Pedmale, U. V., Morrow, J., Sachdev, S., Lechner, E., Tang, X., Zheng, N., Hannink, M., Genschik, P. and Liscum, E. (2011) 'Modulation of phototropic responsiveness in Arabidopsis through ubiquitination of phototropin 1 by the CUL3-Ring E3 ubiquitin ligase CRL3(NPH3)', *Plant Cell,* 23(10), pp. 3627-40.

Rosenquist, M., Alsterfjord, M., Larsson, C. and Sommarin, M. (2001) 'Data mining the Arabidopsis genome reveals fifteen 14-3-3 genes. Expression is demonstrated for two out of five novel genes', *Plant Physiol,* 127(1), pp. 142-9.

Saile, S. C., Ackermann, F. M., Sunil, S., Keicher, J., Bayless, A., Bonardi, V., Wan, L., Doumane, M., Stöbbe, E., Jaillais, Y., Caillaud, M. C., Dangl, J. L., Nishimura, M. T., Oecking, C. and El Kasmi, F. (2021) 'Arabidopsis ADR1 helper NLR immune receptors localize and function at the plasma membrane in a phospholipid dependent manner', *New Phytol,* 232(6), pp. 2440-2456.

Sakai, T., Kagawa, T., Kasahara, M., Swartz, T. E., Christie, J. M., Briggs, W. R., Wada, M. and Okada, K. (2001) 'Arabidopsis nph1 and npl1: blue light receptors that mediate both phototropism and chloroplast relocation', *Proc Natl Acad Sci U S A,* 98(12), pp. 6969-74.

Sakai, T., Wada, T., Ishiguro, S. and Okada, K. (2000) 'RPT2. A signal transducer of the phototropic response in Arabidopsis', *Plant Cell,* 12(2), pp. 225-36.

Sakamoto, K. and Briggs, W. R. (2002) 'Cellular and subcellular localization of phototropin 1', *Plant Cell,* 14(8), pp. 1723-35.

Sauer, M. and Grebe, M. (2021) 'Plant cell biology: PIN polarity maintained', *Curr Biol,* 31(9), pp. R449-R451.

Sauer, M. and Kleine-Vehn, J. (2019) 'PIN-FORMED and PIN-LIKES auxin transport facilitators', *Development,* 146(15).

Schindelin, J., Arganda-Carreras, I., Frise, E., Kaynig, V., Longair, M., Pietzsch, T., Preibisch, S., Rueden, C., Saalfeld, S., Schmid, B., Tinevez, J. Y., White, D. J., Hartenstein, V., Eliceiri,

K., Tomancak, P. and Cardona, A. (2012) 'Fiji: an open-source platform for biological-image analysis', *Nat Methods,* 9(7), pp. 676-82.

Schmidt, T. 2022. Die Interaktion von 14-3-3 Proteinen mit NON-PHOTOTROPIC HYPOCOTYL 3: Untersuchungen zur Komplexbildung und funktionellen Bedeutung.

Schumacher, P., Demarsy, E., Waridel, P., Petrolati, L. A., Trevisan, M. and Fankhauser, C. (2018) 'A phosphorylation switch turns a positive regulator of phototropism into an inhibitor of the process', *Nat Commun,* 9(1), pp. 2403.

Simon, M. L., Platre, M. P., Marquès-Bueno, M. M., Armengot, L., Stanislas, T., Bayle, V., Caillaud, M. C. and Jaillais, Y. (2016) 'A PtdIns(4)P-driven electrostatic field controls cell membrane identity and signalling in plants', *Nat Plants,* 2, pp. 16089.

Stogios, P. J., Downs, G. S., Jauhal, J. J., Nandra, S. K. and Privé, G. G. (2005) 'Sequence and structural analysis of BTB domain proteins', *Genome Biol,* 6(10), pp. R82.

Suetsugu, N., Takemiya, A., Kong, S. G., Higa, T., Komatsu, A., Shimazaki, K., Kohchi, T. and Wada, M. (2016) 'RPT2/NCH1 subfamily of NPH3-like proteins is essential for the chloroplast accumulation response in land plants', *Proc Natl Acad Sci U S A,* 113(37), pp. 10424-9.

Suetsugu, N. and Wada, M. (2013) 'Evolution of three LOV blue light receptor families in green plants and photosynthetic stramenopiles: phototropin, ZTL/FKF1/LKP2 and aureochrome', *Plant Cell Physiol,* 54(1), pp. 8-23.

Sullivan, S., Kharshiing, E., Laird, J., Sakai, T. and Christie, J. M. (2019) 'Deetiolation Enhances Phototropism by Modulating NON-PHOTOTROPIC HYPOCOTYL3 Phosphorylation Status', *Plant Physiol,* 180(2), pp. 1119-1131.

Sullivan, S., Waksman, T., Paliogianni, D., Henderson, L., Lütkemeyer, M., Suetsugu, N. and Christie, J. M. (2021) 'Regulation of plant phototropic growth by NPH3/RPT2-like substrate phosphorylation and 14-3-3 binding', *Nat Commun,* 12(1), pp. 6129.

Takase, T., Nishiyama, Y., Tanihigashi, H., Ogura, Y., Miyazaki, Y., Yamada, Y. and Kiyosue, T. (2011) 'LOV KELCH PROTEIN2 and ZEITLUPE repress Arabidopsis photoperiodic flowering under non-inductive conditions, dependent on FLAVIN-BINDING KELCH REPEAT F-BOX1', *Plant J,* 67(4), pp. 608-21.

Takemiya, A., Sugiyama, N., Fujimoto, H., Tsutsumi, T., Yamauchi, S., Hiyama, A., Tada, Y., Christie, J. M. and Shimazaki, K. (2013) 'Phosphorylation of BLUS1 kinase by phototropins is a primary step in stomatal opening', *Nat Commun,* 4, pp. 2094.

Taoka, K., Ohki, I., Tsuji, H., Furuita, K., Hayashi, K., Yanase, T., Yamaguchi, M., Nakashima, C., Purwestri, Y. A., Tamaki, S., Ogaki, Y., Shimada, C., Nakagawa, A., Kojima, C. and Shimamoto, K. (2011) '14-3-3 proteins act as intracellular receptors for rice Hd3a florigen', *Nature,* 476(7360), pp. 332-5.

Throm, C. R. 2017. Identifizierung und Charakterisierung von „NON-PHOTOTROPIC HYPOCOTYL 3“ als neuartiger Interaktionspartner pflanzlicher 14-3-3 Proteine.

Towbin, H., Staehelin, T. and Gordon, J. (1979) 'Electrophoretic transfer of proteins from polyacrylamide gels to nitrocellulose sheets: procedure and some applications', *Proc Natl Acad Sci U S A,* 76(9), pp. 4350-4.

Tsuchida-Mayama, T., Nakano, M., Uehara, Y., Sano, M., Fujisawa, N., Okada, K. and Sakai, T. 2008. Mapping of the phosphorylation sites on the phototropic signal transducer, NPH3. Plant Science.

Ueno, K., Kinoshita, T., Inoue, S., Emi, T. and Shimazaki, K. (2005) 'Biochemical characterization of plasma membrane H+-ATPase activation in guard cell protoplasts of Arabidopsis thaliana in response to blue light', *Plant Cell Physiol,* 46(6), pp. 955-63.

van der Lee, R., Buljan, M., Lang, B., Weatheritt, R. J., Daughdrill, G. W., Dunker, A. K., Fuxreiter, M., Gough, J., Gsponer, J., Jones, D. T., Kim, P. M., Kriwacki, R. W., Oldfield, C. J., Pappu, R. V., Tompa, P., Uversky, V. N., Wright, P. E. and Babu, M. M. (2014) 'Classification of intrinsically disordered regions and proteins', *Chem Rev,* 114(13), pp. 6589-631.

van Heusden, G. P. (2005) '14-3-3 proteins: regulators of numerous eukaryotic proteins', *IUBMB Life,* 57(9), pp. 623-9.

Varadi, M., Anyango, S., Deshpande, M., Nair, S., Natassia, C., Yordanova, G., Yuan, D., Stroe, O., Wood, G., Laydon, A., Žídek, A., Green, T., Tunyasuvunakool, K., Petersen, S., Jumper, J., Clancy, E., Green, R., Vora, A., Lutfi, M., Figurnov, M., Cowie, A., Hobbs, N., Kohli, P., Kleywegt, G., Birney, E., Hassabis, D. and Velankar, S. (2022) 'AlphaFold Protein Structure Database: massively expanding the structural coverage of protein-sequence space with high-accuracy models', *Nucleic Acids Res,* 50(D1), pp. D439-D444.

Wan, Y. L., Eisinger, W., Ehrhardt, D., Kubitscheck, U., Baluska, F. and Briggs, W. (2008) 'The subcellular localization and blue-light-induced movement of phototropin 1-GFP in etiolated seedlings of Arabidopsis thaliana', *Mol Plant,* 1(1), pp. 103-17.

Wang, H., Yang, C., Zhang, C., Wang, N., Lu, D., Wang, J., Zhang, S., Wang, Z. X., Ma, H. and Wang, X. (2011) 'Dual role of BKI1 and 14-3-3 s in brassinosteroid signaling to link receptor with transcription factors', *Dev Cell,* 21(5), pp. 825-34.

Wang, P., Hsu, C. C., Du, Y., Zhu, P., Zhao, C., Fu, X., Zhang, C., Paez, J. S., Macho, A. P., Tao, W. A. and Zhu, J. K. (2020) 'Mapping proteome-wide targets of protein kinases in plant stress responses', *Proc Natl Acad Sci U S A,* 117(6), pp. 3270-3280.

Went, F. W. and Thimann, K. V. 1937. Phytohormones. Macmillan, New York.
Willige, B. C., Ahlers, S., Zourelidou, M., Barbosa, I. C., Demarsy, E., Trevisan, M., Davis, P. A., Roelfsema, M. R., Hangarter, R., Fankhauser, C. and Schwechheimer, C. (2013) 'D6PK AGCVIII kinases are required for auxin transport and phototropic hypocotyl bending in Arabidopsis', *Plant Cell,* 25(5), pp. 1674-88.

Win, J. and Kamoun, S. 2004. pCB301-p19: A Binary Plasmid Vector to Enhance Transient Expression of Transgenes by Agroinfiltration.

Yaffe, M. B. (2002) 'How do 14-3-3 proteins work?-- Gatekeeper phosphorylation and the molecular anvil hypothesis', *FEBS Lett,* 513(1), pp. 53-7.

Yaffe, M. B., Rittinger, K., Volinia, S., Caron, P. R., Aitken, A., Leffers, H., Gamblin, S. J., Smerdon, S. J. and Cantley, L. C. (1997) 'The structural basis for 14-3-3:phosphopeptide binding specificity', *Cell,* 91(7), pp. 961-71.

Zavaliev, R. and Epel, B. L. (2015) 'Imaging callose at plasmodesmata using aniline blue: quantitative confocal microscopy', *Methods Mol Biol,* 1217, pp. 105-19.

Zavaliev, R., Mohan, R., Chen, T. and Dong, X. (2020) 'Formation of NPR1 Condensates Promotes Cell Survival during the Plant Immune Response', *Cell,* 182(5), pp. 1093-1108.e18.

Zourelidou, M., Absmanner, B., Weller, B., Barbosa, I. C., Willige, B. C., Fastner, A., Streit, V., Port, S. A., Colcombet, J., de la Fuente van Bentem, S., Hirt, H., Kuster, B., Schulze, W. X., Hammes, U. Z. and Schwechheimer, C. (2014) 'Auxin efflux by PIN-FORMED proteins is activated by two different protein kinases, D6 PROTEIN KINASE and PINOID', *Elife,* 3.

8 Appendix

Description of Supplementary Movies

All movies can be found on the CD attached to the printed version of this thesis.

Supplementary Movie 1: Subcellular localization of 35S::RFP:NPH3 transiently expressed in *N. benthamiana* leaves.

Supplementary Movie 2: Subcellular localization of 35S::RFP:NPH3-S744A transiently expressed in *N. benthamiana* leaves.

Supplementary Movie 3: Subcellular localization of 35S::GFP:NPH3 in stably transformed *A. thaliana nph3-7* hypocotyl cells.

Supplementary Movie 4: Subcellular localization of 35S::GFP:NPH3-S744A in stably transformed *A. thaliana nph3-7* hypocotyl cells.

Supplementary Movie 5: Subcellular localization of 35S::RFP:NPH3ΔN155 transiently expressed in *N. benthamiana* leaves.

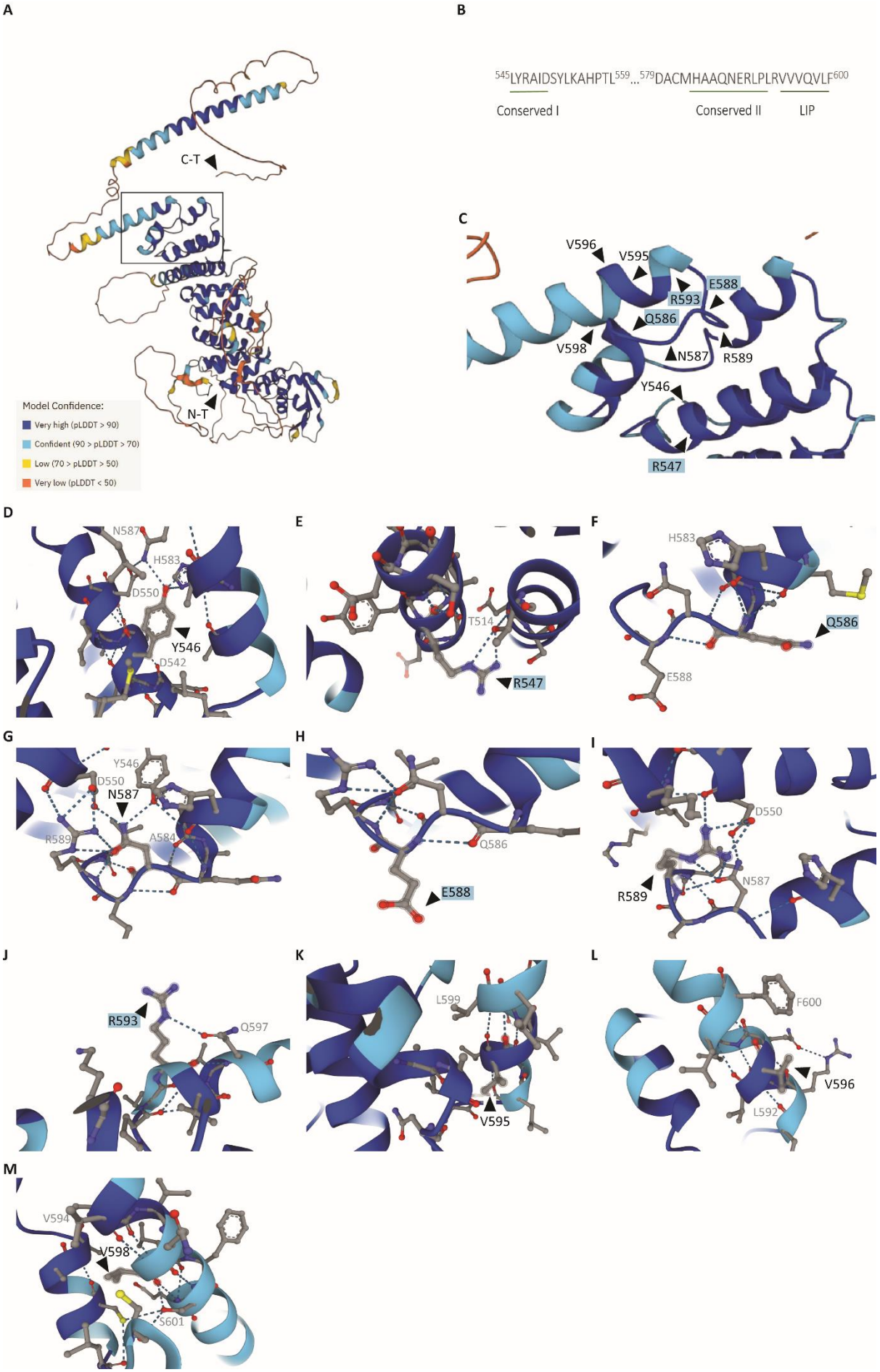
A
C-T
N-T
Model Confidence:
Very high (pLDDT > 90)
Confident (90 > pLDDT > 70)
Low (70 > pLDDT > 50)
Very low (pLDDT < 50)
B
545LYRAIDSYLKAHPTL559...579DACMHAAQNERLPLRVVVQVLF600
Conserved I
Conserved II
LIP
C
V596
V595
E588
R593
Q586
V598
N587
R589
Y546
R547
D
N587
H583
D550
Y546
D542
E
T514
R547
F
H583
Q586
E588
G
Y546
D550
N587
R589
A584
H
Q586
E588
I
D550
R589
N587
J
R593
Q597
K
L599
V595
L
F600
V596
L592
M
V594
V598
S601

Supplementary Figure 1: AlphaFold protein structure prediction of NPH3. A Predicted protein structure of NPH3 by AlphaFold (https://alphafold.ebi.ac.uk/entry/Q9FMF5, last checked: 2022-08-10, 13:03). The region that might be involved in condensate formation is highlighted. **B** Amino acid sequence of the conserved region I and II and the LIP. **C** Predicted protein structure of the region that might be involved in condensate formation of NPH3 by AlphaFold (https://alphafold.ebi.ac.uk/entry/Q9FMF5, last checked: 2022-08-10, 13:03). Amino acid residues that might be involved in condensate formation marked with arrowheads. Amino acid residues predicted to be surface exposed are in addition highlighted in blue. **D-M** Predicted protein structure and position of the single amino acid residues that might be involved in condensate formation of NPH3 by AlphaFold (https://alphafold.ebi.ac.uk/entry/Q9FMF5, last checked: 2022-08-10, 13:03). Amino acid residues predicted to be surface exposed are highlighted in blue. Dashed blue lines display hydrogen bonds. Possibly interacting amino acid residues are displayed in grey**.**

Danksagung

Zuerst möchte ich mich natürlich bei meiner Doktormutter Prof. Dr. Claudia Oecking bedanken. Vielen Dank, dass du mir dieses Thema zur Erstellung meiner Doktorarbeit überlassen hast. Ich möchte dir vor allem für deine Unterstützung in den letzten Jahren danken, für die zahlreichen Unterhaltungen und deinen Input im Labor und beim Schreiben dieser Arbeit. Ich habe unsere Unterhaltungen und deine Unterstützung immer sehr geschätzt und werde die Zeit in deiner Arbeitsgruppe immer in guter Erinnerung behalten.

Weiter möchte ich mich bei Prof. Dr. Klaus Harter bedanken für die Übernahme des Zweitgutachtens und für den Input und die Anregungen in den letzten Jahren. Auch bei Dr. Farid El Kasmi möchte ich mich für die zahlreichen Gespräche und die Anregungen in den letzten Jahren bedanken.

Besonders möchte ich mich bei Jutta und Andrea bedanken, den besten TAs die man sich nur vorstellen kann. Ich weiß nicht was ich ohne eure Hilfe im Labor gemacht hätte. Des Weiteren gilt mein Dank Tanja, die mich am Anfang mit sehr viel Geduld eingearbeitet hat und mir alles gezeigt hat. Auch bei Prabha möchte ich mich bedanken, für die gemeinsame Zeit und auch für die Anregungen und die Korrektur dieser Arbeit. Ich möchte mich auch bei Atiara bedanken, für die gemeinsame Zeit im Labor, aber auch gemeinsame Zeit beim Abendessen, Shoppen oder Kaffee trinken. Ein ganz besonderer Dank gilt Svenja, du warst immer für mich da, auch bei der Korrektur dieser Arbeit, und an unsere Zeit zusammen im Labor werde ich immer gerne zurückdenken. Bei Svenja und Jenny möchte ich mich außerdem für die tolle Zeit außerhalb der Arbeit bedanken, ob das nun beim Frühstück, bei Ausflügen, beim Abend essen oder im Urlaub war, die Zeit mit euch genieße ich immer sehr!

Auch bei allen anderen Arbeitsgruppen der Pflanzenphysiologie möchte ich mich bedanken, für die angenehme Atmosphäre und die gute Zusammenarbeit und natürlich die Retreats.

Meiner Familie und meinen Freunden gilt mein größter Dank, ohne euch wäre diese Arbeit nicht möglich gewesen! Die Unterstützung meiner Familie bedeutet mir unendlich viel und an den Wochenenden zu Hause konnte ich immer meine Energiereserven auftanken. Auch meinen Freunden, vor allem Jill, Katta, Ronja und Kadda möchte ich für alles danken. All die Gespräche, Telefonate, Abende in Mainz oder Bingen waren für mich immens wichtig!